

Stephen F. Austin State University

SFA ScholarWorks

Electronic Theses and Dissertations

12-2020

Aerial Mineral and Organic Particulate Deposition in East Texas

Sarah Caton

catonsa@jacks.sfasu.edu

Sarah Caton

Stephen F Austin State University, sa.caton@yahoo.com

Follow this and additional works at: <https://scholarworks.sfasu.edu/etds>



Part of the [Environmental Indicators and Impact Assessment Commons](#), [Environmental Monitoring Commons](#), and the [Other Environmental Sciences Commons](#)

[Tell us how this article helped you.](#)

Repository Citation

Caton, Sarah and Caton, Sarah, "Aerial Mineral and Organic Particulate Deposition in East Texas" (2020). *Electronic Theses and Dissertations*. 356.

<https://scholarworks.sfasu.edu/etds/356>

This Thesis is brought to you for free and open access by SFA ScholarWorks. It has been accepted for inclusion in Electronic Theses and Dissertations by an authorized administrator of SFA ScholarWorks. For more information, please contact cdsscholarworks@sfasu.edu.

Aerial Mineral and Organic Particulate Deposition in East Texas

Creative Commons License



This work is licensed under a [Creative Commons Attribution-Noncommercial-No Derivative Works 4.0 License](https://creativecommons.org/licenses/by-nc-nd/4.0/).

Aerial Mineral and Organic
Particulate Deposition in East Texas

By

SARAH CATON

Bachelor of Arts in Modern Languages

A Thesis

Presented to the Faculty of the Graduate School of
Stephen F. Austin State University

In Partial Fulfillment

Of the Requirements

For the Degree of

Master of Science in Environmental Science

DIVISION OF ENVIRONMENTAL SCIENCE

ARTHUR TEMPLE COLLEGE OF FORESTRY AND AGRICULTURE

STEPHEN F. AUSTIN STATE UNIVERSITY

December, 2020

Aerial Mineral and Organic

Particulate Deposition in East Texas

By

SARAH CATON, Bachelor of Arts in Modern Languages

APPROVED:

Dr. Kenneth Farrish, Thesis Director

Dr. Sheryl Jerez, Committee Member

Dr. Josephine Taylor, Committee Member

Pauline M. Sampson, Ph.D.
Dean of Research and Graduate Studies

ABSTRACT

This study determined the monthly amount, particle size distribution, and chemical composition of particulate deposition in East Texas over a one-year period. It also recognized the seasonal patterns of this deposition as well as its primary origins as either mineral or organic particulate deposition.

The study recorded the monthly mass of deposition, particle size distribution, and the chemical makeup of deposition throughout a period of twelve months at seven sampling locations. SEM-EDS technology was used in conjunction with PCI programming to measure the sizes of depositional particles throughout this time period and identify their chemical composition.

The total yearly deposition recorded in this study was 22.9865 kg/ha. Of this yearly deposition, 8.5582 kg/ha was Si deposition, 2.2923 kg/ha was C deposition, 1.4394 kg/ha was Ba deposition, 1.4679 kg/ha was Na deposition, 1.4679 kg/ha was Al deposition, 0.3146 kg/ha was Ca deposition, 0.7846 kg/ha was K deposition, and 1.4679 kg/ha was Fe deposition. Si deposition had a monthly range of 0.1939 kg/ha – 1.5393 kg/ha, C deposition had a monthly range of 0.0262 kg/ha – 0.6871 kg/ha, Ba had a monthly range of 0.0380 kg/ha – 0.2984 kg/ha, Na had a monthly range of 0.0330 kg/ha – 0.3619 kg/ha, Al had a monthly range of 0.0330 kg/ha – 0.3619 kg/ha, Ca had a monthly

range of 0.0022 kg/ha – 0.0958 kg/ha, K had a monthly range of 0.0190 kg/ha – 0.1714 kg/ha, and Fe had a monthly range of 0.0330 kg/ha – 0.3619 kg/ha. Mean particle size increased from January 2019-April 2019.

Particle size increased during high pollen months. Elements found in soils tended to make up a larger percentage of the deposition during drier months.

ACKNOWLEDGEMENTS

I'd like to thank Dr. Farrish for suggesting this thesis topic, helping me identify writing errors, and overseeing the construction of the samplers. I'd also like to thank him and the Division of Environmental Science for the acquisition of the materials in order to make this study possible. I'd like to thank the departments of biology and forestry for all of their contributions to this study. I would like to thank Stephen F. Austin State University and STMicroelectronics for allowing use of the properties for this study.

I would like to thank Jacalyn Jones, Hannah Bays, Sarah Hall, and Hadi Radnezhad for helping me collect samples as well as aiding in the setup, maintenance, driving, navigation, and dismantlement of my samplers. I would like to thank Jason Grogan for giving me keys and maps to the sampling properties. I want to thank Dr. Sheryll Jerez for allowing me use of her environmental measurements lab. I'd like to thank Dr. Yuhui Weng for helping me decide which statistical analysis to use and identifying errors in my program when I had trouble running it through SAS. I'd like to thank Dr. Taylor for allowing the use of her electron microscope, EDS technology, sputter coater, and for changing the filaments in the microscope for me. I would like to thank Twyla Caton for helping me input data for analysis.

TABLE OF CONTENTS

| | |
|---|-----|
| ABSTRACT | i |
| ACKNOWLEDGEMENTS | iii |
| INTRODUCTION | 1 |
| OBJECTIVES | 7 |
| LITERATURE REVIEW | 9 |
| Atmospheric Deposition | 9 |
| Particulate Mobilization and Transport | 10 |
| Particulate Deposition | 11 |
| Terrigenous Dry Deposition in Bodies of Water | 13 |
| Cloud Washout of Nutrients within Forested Areas | 14 |
| Sources of Particulate Matter | 14 |
| Mineral Sources | 15 |
| Organic Sources | 16 |
| Anthropogenic Sources | 17 |
| METHODS | 19 |
| Study Area | 19 |
| Samplers | 22 |
| Sample Analysis | 27 |
| Filtration Method | 27 |
| Electron Microscopy Analysis | 29 |
| Site Areas | 31 |

| | |
|---|-----------|
| STATISTICAL PROCEDURE | 33 |
| Overview | 33 |
| Mixed Model Repeated Measures..... | 35 |
| Weather Analysis..... | 38 |
| RESULTS AND DISCUSSION | 40 |
| Study Parameters | 40 |
| Summary Statistics for Particulate Weight | 41 |
| ANOVA for Particulate Weight..... | 41 |
| Yearly Results and Observations..... | 43 |
| Monthly Results and Observations..... | 50 |
| Mixed Model ANOVA for Particle Size Distribution | 59 |
| Elemental Composition of the Samples over Time | 62 |
| Summary Statistics for Si | 64 |
| Mixed Model for Si..... | 65 |
| Summary Statistics for O | 67 |
| Repeated Mixed Model for O..... | 67 |
| Summary Statistics for C..... | 69 |
| Repeated Mixed Model for C | 70 |
| Summary Statistics for Ba | 73 |
| Repeated Mixed Model for Ba | 74 |
| Summary Statistics for Na..... | 77 |
| Repeated Mixed Model for Na | 78 |
| Repeated Mixed Model for Al..... | 82 |
| Summary Statistics for K | 85 |
| Repeated Mixed Model for K..... | 86 |
| Summary Statistics for Ca..... | 88 |
| Repeated Mixed Model for Ca | 90 |
| Summary Statistics for Zn..... | 92 |

| | |
|--|-----|
| Repeated Mixed Model for Zn | 92 |
| Summary Statistics for Re | 94 |
| Repeated Mixed Model for Re | 94 |
| Summary Statistics for Ti | 96 |
| Repeated Mixed Model for Ti | 94 |
| Summary Statistics for Fe | 98 |
| Repeated Mixed Model for Fe | 99 |
| Summary Statistics for Ce | 101 |
| Repeated Mixed Model for Ce | 101 |
| Summary Statistics for Trace Elements | 102 |
| Repeated Mixed Model for Trace Elements | 103 |
| CONCLUSIONS | 107 |
| LITERATURE CITED | 112 |
| APPENDIX | 121 |
| VITA | 143 |

LIST OF FIGURES

| | |
|---|-----|
| Figure 1. Map of atmospheric aerosol suspension and transport on a global scale (NASA, 2018)..... | 13 |
| Figure 2. Map of sampling sites in relation to counties and populated cities with over 12,700 residents..... | 20 |
| Figure 3. Map of sampling points in relation to general elevation and 5m of surrounding topography..... | 211 |
| Figure 4. Diagram of Sampler at SFA Beef Farm. | 23 |
| Figure 5. Size and observation range of different nanostructures, colloids, and particulates using different lab techniques. Source: (Lower, 2018)..... | 30 |
| Figure 6. Map of weather stations used near sampling points. (NOAA, 2018)..... | 38 |
| Figure 7. Arithmetic means of samples collected from six sites in Stephen F. Austin University Real Estate Foundation’s STMicroelectronics carbon sequestration project and one site at the SFA Agriculture Center’s Beef Farm at monthly intervals over a twelve-month period. Units are in kg/ha per month. Error bars display standard errors. | 41 |
| Figure 8. Total yearly particulate weight recorded at each of the sampling sites between October 20 th , 2018 and October 19 th , 2019. Sites are displayed from westernmost to easternmost location. Particulate weight is recorded in kg/ha per year. Six of the sites used were in Stephen F. Austin University Real Estate Foundation’s STMicroelectronics carbon sequestration project and one site was located at Stephen F. Austin State University’s Beef Farm at the Agriculture Center. | 445 |

Figure 9. Average yearly particulate weight recorded at each of the counties between October 20th, 2018 and October 19th, 2019. Sites are displayed from westernmost to easternmost location as well as southernmost to northernmost location. Particulate weight is recorded in kg/ha per year. Six of the sites used were in Stephen F. Austin University Real Estate Foundation’s STMicroelectronics carbon sequestration project and one site was located at Stephen F. Austin State University’s Beef Farm at the Agriculture Center.446

Figure 10. Arithmetic monthly mean precipitation in cm depth collected during the sampling period of October 20th, 2018-October 19th, 2019 at each sampling location. Six of the properties used were in Stephen F. Austin University Real Estate Foundation’s STMicroelectronics carbon sequestration project and one site was located at the SFA Beef Farm.449

Figure 11. Arithmetic monthly mean size of sample particles across six sites in Stephen F. Austin University Real Estate Foundation’s STMicroelectronics carbon sequestration project and one site at the SFA Beef Farm. Units are in microns, and error bars are based on standard deviation of monthly mean particle sizes across sites.....660

Figure 12. Arithmetic mean of Si in kg/ha sampled across seven sites over a twelve-month period. Four subsamples were collected per sample. One sample was collected per site per month. Six of the seven sampling sites are in Stephen F. Austin University Real Estate Foundation’s STMicroelectronics carbon sequestration project and one sampling site is located at SFA’s Beef Farm.65

Figure 13. C in kg/ha sampled across seven sites over a twelve-month period. Four subsamples were collected per sample. One sample was collected per site per month. Six of the seven sampling sites are in Stephen F. Austin University Real Estate Foundation’s STMicroelectronics carbon sequestration project and one sampling site is located at SFA’s Beef Farm.70

Figure 14. Ba in kg/ha sampled across seven sites over a twelve-month period. Four subsamples were collected per sample. One sample was collected per site per month. Six of the seven sampling sites are in Stephen F. Austin University Real Estate Foundation’s STMicroelectronics carbon sequestration project and one sampling site is located at SFA’s Beef Farm.74

Figure 15. Arithmetic mean of Na in kg/ha sampled across seven sites over a twelve-month period. Four subsamples were collected per sample. One sample was collected per site per month. Six of the seven sampling sites are in Stephen F. Austin University Real Estate Foundation’s STMicroelectronics carbon sequestration project and one sampling site is located at SFA’s Beef Farm.....78

Figure 16. Arithmetic mean of Al in kg/ha sampled across seven sites over a twelve-month period. Four subsamples were collected per sample. One sample was collected per site per month. Six of the seven sampling sites are in Stephen F. Austin University Real Estate Foundation’s STMicroelectronics carbon sequestration project and one sampling site is located at SFA’s Beef Farm.....82

Figure 17. Arithmetic mean of K in kg/ha sampled across seven sites over a twelve-month period. Four subsamples were collected per sample. One sample was collected per site per month. Six of the seven sampling sites are in Stephen F. Austin University Real Estate Foundation’s STMicroelectronics carbon sequestration project and one sampling site is located at SFA’s Beef Farm.....86

Figure 18. Arithmetic mean of Ca in kg/ha sampled across seven sites over a twelve-month period. Four subsamples were collected per sample. One sample was collected per site per month. Six of the seven sampling sites are in Stephen F. Austin University Real Estate Foundation’s STMicroelectronics carbon sequestration project and one sampling site is located at SFA’s Beef Farm.....89

Figure 19. Arithmetic mean of Fe in kg/ha sampled across seven sites over a twelve-month period. Four subsamples were collected per sample. One sample was collected per site per month. Six of the seven sampling sites are in Stephen F. Austin University Real Estate Foundation’s STMicroelectronics carbon sequestration project and one sampling site is located at SFA’s Beef Farm.....99

Figure 20. Wind rose plot for all counties used in study (NOAA, 2018-2019). Freeware used was WRPLOT View from Lakes Environmental Software.....136

Figure 21. Wind rose plot for Cherokee county
(NOAA, 2018-2019). Freeware used was WRPLOT View
from Lakes Environmental Software.137

Figure 22. Wind rose plot for Houston county
(NOAA, 2018-2019). Freeware used was WRPLOT View
from Lakes Environmental Software.....138

Figure 23. Wind rose plot for Nacogdoches county
(NOAA, 2018-2019). Freeware used was WRPLOT View
from Lakes Environmental Software.139

Figure 24. Wind rose plot for Sabine Parish
(NOAA, 2018-2019). Freeware used was WRPLOT View
from Lakes Environmental Software.140

LIST OF TABLES

| | |
|--|----|
| Table 1. Latitude, longitude, clearing size in square ft, and clearing shape from aerial view of study site locations. Shape of clearing was used to determine which area formula to use when calculating after gathering the length and width of the clearing using a measuring wheel with an accuracy of 0.0001m per 1m..... | 22 |
| Table 2. Rainfall statistics near sampling locations (NOAA Weather stations, 2018). The start date refers to the first day of each county weather station’s rainfall collection period, and the end date refers to the last date of each county weather station’s rainfall collection period. | 25 |
| Table 3. Table of weather stations near sampling points (NOAA, 2018). Start Date refers to the day the weather station started collecting precipitation data, and End Date refers to the last date the weather station collected data used as a reference in this study..... | 39 |
| Table 4. Particulate weight in kg/ha per month for samples assessing monthly deposition between October 20 th , 2018 and October 19 th , 2019 at six of the sites in Stephen F. Austin University Real Estate Foundation’s STMicroelectronics carbon sequestration project and one site at the Stephen F. Austin Beef Farm..... | 50 |
| Table 5. Arithmetic mean, standard deviation, minimum and maximum of Si sampled across seven sites over a twelve-month period. Four subsamples were collected per sample. One sample was collected per site per month. Six of the seven sampling sites are in Stephen F. Austin University Real Estate Foundation’s STMicroelectronics carbon sequestration project and one sampling site is located at SFA’s Beef Farm. | 64 |

Table 6. Arithmetic mean, standard deviation, minimum and maximum of O sampled across seven sites over a twelve-month period. Four subsamples were collected per sample. One sample was collected per site per month. Six of the seven sampling sites are in Stephen F. Austin University Real Estate Foundation’s STMicronics carbon sequestration project and one sampling site is located at SFA’s Beef Farm.67

Table 7. Arithmetic mean, standard deviation, minimum and maximum of C sampled across seven sites over a twelve-month period. Four subsamples were collected per sample. One sample was collected per site per month. Six of the seven sampling sites are in Stephen F. Austin University Real Estate Foundation’s STMicronics carbon sequestration project and one sampling site is located at SFA’s Beef Farm.69

Table 8. Arithmetic mean, standard deviation, minimum and maximum of Ba sampled across seven sites over a twelve-month period. Four subsamples were collected per sample. One sample was collected per site per month. Six of the seven sampling sites are in Stephen F. Austin University Real Estate Foundation’s STMicronics carbon sequestration project and one sampling site is located at SFA’s Beef Farm.73

Table 9. Arithmetic mean, standard deviation, minimum and maximum of Na sampled across seven sites over a twelve-month period. Four subsamples were collected per sample. One sample was collected per site per month. Six of the seven sampling sites are in Stephen F. Austin University Real Estate Foundation’s STMicronics carbon sequestration project and one sampling site is located at SFA’s Beef Farm.77

Table 10. Arithmetic mean, standard deviation, minimum and maximum of Al sampled across seven sites over a twelve-month period. Four subsamples were collected per sample. One sample was collected per site per month. Six of the seven sampling sites are in Stephen F. Austin University Real Estate Foundation’s STMicronics carbon sequestration project and one sampling site is located at SFA’s Beef Farm.81

Table 11. Arithmetic mean, standard deviation, minimum and maximum of K sampled across seven sites over a twelve-month period. Four subsamples were collected per sample. One sample was collected per site per month. Six of the seven sampling sites are in Stephen F. Austin University Real Estate Foundation’s STMicroelectronics carbon sequestration project and one sampling site is located at SFA’s Beef Farm.85

Table 12. Arithmetic mean, standard deviation, minimum and maximum of Ca sampled across seven sites over a twelve-month period. Four subsamples were collected per sample. One sample was collected per site per month. Six of the seven sampling sites are in Stephen F. Austin University Real Estate Foundation’s STMicroelectronics carbon sequestration project and one sampling site is located at SFA’s Beef Farm.88

Table 13. Arithmetic mean, standard deviation, minimum and maximum of Zn sampled across seven sites over a twelve-month period. Four subsamples were collected per sample. One sample was collected per site per month. Six of the seven sampling sites are in Stephen F. Austin University Real Estate Foundation’s STMicroelectronics carbon sequestration project and one sampling site is located at SFA’s Beef Farm.92

Table 14. Arithmetic mean, standard deviation, minimum and maximum of Re sampled across seven sites over a twelve-month period. Four subsamples were collected per sample. One sample was collected per site per month. Six of the seven sampling sites are in Stephen F. Austin University Real Estate Foundation’s STMicroelectronics carbon sequestration project and one sampling site is located at SFA’s Beef Farm.94

Table 15. Arithmetic mean, standard deviation, minimum and maximum of Ti sampled across seven sites over a twelve-month period. Four subsamples were collected per sample. One sample was collected per site per month. Six of the seven sampling sites are in Stephen F. Austin University Real Estate Foundation’s STMicroelectronics carbon sequestration project and one sampling site is located at SFA’s Beef Farm.96

Table 16. Arithmetic mean, standard deviation, minimum and maximum of Fe sampled across seven sites over a twelve-month period. Four subsamples were collected per sample. One sample was collected per site per month. Six of the seven sampling sites are in Stephen F. Austin University Real Estate Foundation’s STMicroelectronics carbon sequestration project and one sampling site is located at SFA’s Beef Farm.98

Table 17. Arithmetic mean, standard deviation, minimum and maximum of Ce sampled across seven sites over a twelve-month period. Four subsamples were collected per sample. One sample was collected per site per month. Six of the seven sampling sites are in Stephen F. Austin University Real Estate Foundation’s STMicroelectronics carbon sequestration project and one sampling site is located at SFA’s Beef Farm.101

Table 18. Arithmetic monthly mean, maximum and minimum size with standard deviation of sample particles from six sites outlined in Stephen F. Austin State University Real Estate Foundation’s STMicroelectronics carbon sequestration project and one site at the SFA Beef Farm. Units are in Microns.....122

Table 19. Arithmetic monthly mean, maximum and minimum mass percentage of Si with standard deviation of sample particles from six sites outlined in Stephen F. Austin State University Real Estate Foundation’s STMicroelectronics carbon sequestration project and one site at the SFA Beef Farm.123

Table 20. Arithmetic monthly mean, maximum and minimum mass percentage of O with standard deviation of sample particles from six sites outlined in Stephen F. Austin State University Real Estate Foundation’s STMicroelectronics carbon sequestration project and one site at the SFA Beef Farm.124

Table 21. Arithmetic monthly mean, maximum and minimum mass percentage of C with standard deviation of sample particles from six sites outlined in Stephen F. Austin State University Real Estate Foundation’s STMicroelectronics carbon sequestration project and one site at the SFA Beef Farm.125

Table 22. Arithmetic monthly mean, maximum and minimum mass percentage of Ba with standard deviation of sample particles from six sites outlined in Stephen F. Austin State University Real Estate Foundation’s STMICROELECTRONICS carbon sequestration project and one site at the SFA Beef Farm.126

Table 23. Arithmetic monthly mean, maximum and minimum mass percentage of Na with standard deviation of sample particles from six sites outlined in Stephen F. Austin State University Real Estate Foundation’s STMICROELECTRONICS carbon sequestration project and one site at the SFA Beef Farm.127

Table 24. Arithmetic monthly mean, maximum and minimum mass percentage of Al with standard deviation of sample particles from six sites outlined in Stephen F. Austin State University Real Estate Foundation’s STMICROELECTRONICS carbon sequestration project and one site at the SFA Beef Farm.128

Table 25. Arithmetic monthly mean, maximum and minimum mass percentage of K with standard deviation of sample particles from six sites outlined in Stephen F. Austin State University Real Estate Foundation’s STMICROELECTRONICS carbon sequestration project and one site at the SFA Beef Farm.129

Table 26. Arithmetic monthly mean, maximum and minimum mass percentage of Ca with standard deviation of sample particles from six sites outlined in Stephen F. Austin State University Real Estate Foundation’s STMICROELECTRONICS carbon sequestration project and one site at the SFA Beef Farm.130

Table 27. Arithmetic monthly mean, maximum and minimum mass percentage of Zn with standard deviation of sample particles from six sites outlined in Stephen F. Austin State University Real Estate Foundation’s STMICROELECTRONICS carbon sequestration project and one site at the SFA Beef Farm.131

Table 28. Arithmetic monthly mean, maximum and minimum mass percentage of Re with standard deviation of sample particles from six sites outlined in Stephen F. Austin State University Real Estate Foundation’s STMicroelectronics carbon sequestration project and one site at the SFA Beef Farm.132

Table 29. Arithmetic monthly mean, maximum and minimum mass percentage of Ti with standard deviation of sample particles from six sites outlined in Stephen F. Austin State University Real Estate Foundation’s STMicroelectronics carbon sequestration project and one site at the SFA Beef Farm.133

Table 30. Arithmetic monthly mean, maximum and minimum mass percentage of Fe with standard deviation of sample particles from six sites outlined in Stephen F. Austin State University Real Estate Foundation’s STMicroelectronics carbon sequestration project and one site at the SFA Beef Farm.134

Table 31. Arithmetic monthly mean, maximum and minimum mass percentage of Ce with standard deviation of sample particles from six sites outlined in Stephen F. Austin State University Real Estate Foundation’s STMicroelectronics carbon sequestration project and one site at the SFA Beef Farm.135

Table 32. Summary of wind data during sampling period including monthly resultant vector direction, average wind speed, and percentage of calm winds for each county. The resultant vector direction was used to determine the mean wind direction. Data was obtained from NOAA (2019). Freeware used for calculations was WRPLOT View by Lakes Environmental Software.141

Table 33. Arithmetic mean of Si, C, Ba, Na, Al, Ca, K, and Fe in kg/ha sampled across seven sites over a twelve-month period. Four subsamples were collected per sample. One sample was collected per site per month. Six of the seven sampling sites are in Stephen F. Austin University Real Estate Foundation’s STMicroelectronics carbon sequestration project and one sampling site is located at SFA’s Beef Farm.142

INTRODUCTION

Atmospheric deposition refers to the process in which airborne particulate matter descends to Earth in either wet, dry, cloud, or fog deposition (Li et al., 2013). It is also a way in which nutrients enter forested ecosystems (the other way being soil weathering) (Lequy, 2013; Phillips and Watmough, 2012). As wind and clouds move through the trees, they begin to decrease in velocity, and the airborne particles are deposited on tree leaves, understory plants, and soils. In some studies, this deposition correlated to low concentrations of exchangeable base cations such as Mg, K, and Ca (Phillips and Watmough, 2012).

On a very broad scale, atmospheric deposition has two sources: marine and terrigenous (Lequy, 2013). Terrigenous sources are land based and generally include geologically sourced particulates and soil matter. Particulates with notable dissolved salts based on Cl, Na, and Mg are generally of marine sources, while particulates containing dissolved K, Ca, HCO, and mineral particulates are of terrigenous sources (Leguy, 2013).

In order to differentiate between anthropogenic particulates and natural organic particulates, their size must be taken into account. Fungal spores and pollen are naturally

bigger and can often be observed with a compound light microscope or a scanning electron microscope. In contrast, anthropogenic particulates like soot and smoke are often smaller than the range of particulates that the scanning electron microscope can observe. Additionally, natural organic particulates can be identified by their carbon-based compounds and by-products, while anthropogenic particles can be identified by NO_x , SO_x , and composite airborne ions such as nitrate, sulfate, and black carbon (Leguy, 2013).

Despite these general trends, it is important to note that deposition becomes much more complex once it reaches the forested environment. One of the greatest challenges of measuring atmospheric deposition in forested areas is that deposition concentrations and compositions are altered by particulate removal through mechanical means like wash-off events, which remove the dry accumulated deposition on leaves through precipitation, and the uptake and release of ions and plant nutrients by the canopy itself (Arisci et al., 2010; Li et al., 2013). Different species of trees within different canopies raise the potential for variation due to their differing surface areas and shapes, which provide varied amounts of nutrient uptake (Arisci et al., 2010). There is an additional source of nutrients supplied by the deposition that has landed on the ground. In fact, as airborne N and P values increased during one study, it was suggested that the uptake of nutrients such as N and P by the roots increased as well (Živkovic et al., 2017).

Many studies have used combination methods of measuring this deposition by recording the throughfall and using the canopy budget model to identify ion exchange fluctuations between rainfall and the forest canopy (Adriaenssens et al., 2012). This model is a continuously evolving tool used to calculate atmospheric deposition within forested regions. Many assumptions of this model have not been thoroughly evaluated, so its application is currently limited and nonuniform among different studies (Draaijers and Erisman, 1995; Adriaenssens et al., 2012).

N, an essential plant nutrient, becomes more biologically available through human activities while nutrients such as Mg, K, and Ca become less available due to the increasing acidity of the soil and lack of negatively charged ions retaining them in the soil (Zak et al., 2006; Phillips and Watmough, 2012). This biologically available nitrogen influences different tree species in different ways (Thomas et al., 2010). In a study measuring the carbon storage of trees in response to nitrogen deposition, the results demonstrate that there is a potential correlation among tree mycorrhizal associations and their reactions to nitrogen deposition (Thomas et al., 2009).

One of the drawbacks to nitrogen deposition is its potential to alter competitive relationships among plants, making the environment less sustainable for nitrogen efficient plant species and more sustainable for nitrophilous species (McDonnell et al., 2018). This, in turn, reduces plant species diversity, allows rare plants to be outcompeted, and increases the potential for plant diseases to spread across large areas

with little natural immunity (McDonnell et al., 2018). Nitrogen deposition has been observed in remote wilderness areas as well as national parks, which indicates this is not a strictly urbanized problem and could extend throughout much of the United States and other regions of the globe (McDonnell et al., 2018). That is why it is important to not only record the nitrogen deposition, but also other plant nutrients such as Ca, K, and Mg. When these are analyzed in conjunction with nitrogen deposition, it could help identify variances in tree species diversity among forested regions.

The study characterized airborne particulate matter within East Texas forests to possibly explain why soils in East Texas are less acidic than soils further east (NRCS, 2019). It examined deposition comprised of both mineral matter and organic particulates (such as pollen and fungal spores). However, anthropogenic particulates (such as soot and smoke) were not included in this study due to their small size and vulnerability to confounding variables such as forest fires.

In many previous studies, trees intercepted particulate matter that was primarily acidic in nature, and the resulting chemical processes reduced photosynthesis rates on the leaves (Radnor, 1986). However, the hypothesis of this study is that particles from soils in Oklahoma and Central Texas are potential sources for airborne mineral particulates that are high in basic cations (Ca and K) while areas south of East Texas in the Houston area are potential sources for mineral particulates that are high in anions (TCEQ, 2019; NRCS, 2003).

Naturally occurring organic deposition could also comprise a substantial portion of deposition (TCEQ, 2019). Since this deposition contains a lot of N, N deposition could fuel aquatic algal blooms in some areas. However, algal blooms do not appear to be present in East Texas freshwater ecosystems in significant amounts, with the most recent report of an algal bloom occurring in the Sabine lake at a very low concentration of 1 to 10 cells/ml on September 17, 2018 (TPWD, 2019).

Since precipitation in East Texas is prevalent throughout the year, the water could dilute the nutrient concentrations more than it contains them, and unlike areas with intemperate seasonal variations, such as those observed in the Zhang and Liv's study of the Yellow and East China Seas, it is unknown whether East Texas experiences similar seasonal variations (with high values during the dry season and low values during the rainy season) (Zhang and Liv, 2007). Since methods of utilizing the canopy budget model have differed from study to study, this study will eliminate the potential for variance by reporting the amount of atmospheric deposition collected as throughfall and dustfall within small clearings (Adriaenssens et al., 2012).

The information in this study is useful because East Texas forests may be acting as deposition zones that provide a unique research opportunity into how forests capture airborne particulates that may have a positive or negative impact on ecosystems. While this is a pilot study, it could lead to larger studies being done over more expansive areas such as in Oklahoma, Central Texas, Arkansas, and Louisiana, and it could lead to

research into the origins of incoming particulate matter, which would indicate which regions are losing nutrients and which ones are gaining nutrients on a regular basis.

OBJECTIVES

The overarching question addressed in this study is: ‘Is there a significant input of atmospheric particulate deposition and nutrients in East Texas forested regions?’.

The null hypothesis of this study was:

- H_0 : There is not a significant input of particulate deposition and nutrients in East Texas forested regions.

The alternative hypothesis was:

- H_A : There is a significant input of particulate deposition and nutrients in East Texas forested regions.

The specific objectives of this study were:

1. Determine the monthly amount of particulate deposition in East Texas over a one year period.
2. Determine the seasonal patterns, if any, of atmospheric particulate deposition in East Texas.
3. Determine the particle size distribution and chemical composition of the particulate deposition in East Texas.

4. Determine the amount of mineral and organic particulate deposition in East Texas.

LITERATURE REVIEW

Atmospheric Deposition

In the nutrient cycle, Aeolian deposition is a broad phase of atmospheric circulation in which nutrients such as N and P are returned to the soil as either wet or dry deposition (Zhang and Liu, 2007). In general, atmospheric deposition increases moving from West to East in the United States of America and is impacted by prevailing winds, precipitation, and the location of major source areas (Ruddy et al., 2006). Wet deposition involves the deposition of particulate matter with precipitation, and dry deposition involves the deposition of particulate matter being transported by wind and deposited by gravity. Particle size, particle density, and wind velocity impact the transport of both wet and dry deposition because fine grained particles are easier to transport than coarse grained particles, less dense particles are easier to transport than denser particles, and wind velocities impact both the speed and direction of dust transport.

Particulate Mobilization and Transport

It has been noted that different elements experience different transport rates based on their environmental conditions and structure, which produces varied chemical compositions of particulate matter throughout the year (Hartmann et. al, 2008). For example, total N in one study peaked in April and September/October, but dissolved Si (DSi) peaked in November and September/October (Hartmann et. al, 2008).

However, the two main ways that particles become mobile are 1) atmospheric turbulence and direct wind sheer stress as well as 2) abrasion and deflation (Lancaster, 2009). Deflation refers to the removal of particles from the earth's surface through wind turbulence, and abrasion occurs when airborne particulates grind against rock surfaces (Lancaster, 2009). Atmospheric turbulence and direct wind sheer stress can be generalized as transport by wind (Lancaster, 2009). When wind transports particles, it will pick up the finer particles first (for example, silt and clay) since they are the lightest and most readily airborne (Lancaster, 2009). Generally speaking, the smaller the particles, the longer they will remain airborne (Lancaster, 2009). However, the transport of particles ultimately depends on the wind sheer stress, turbulence intensity, particle density, vegetation cover, soil moisture, and the particle settling velocity (which depends on particle size and density) (Lancaster, 2009).

Particulate Deposition

Particle deposition depends on four factors: 1) wind velocity, 2) particle density, 3) vegetation cover, and 4) particle size. Low wind velocities will cause particles to settle faster than high wind velocities, and denser particles have a higher gravitational potential, which allows them to fall faster than less dense particles. Vegetation cover (as well as geographic barriers) often intercepts airborne particles and significantly decreases the wind velocity, which causes the particles to settle much faster than they would in flat, barren landscapes.

Extreme cases of dry aeolian deposition were extensively recorded in the 1930s in the United States. When there was sparse vegetation in the Southern Great Plains during the dust bowl era, the soil dried out and wind erosion created large dust storms. In order to prevent a future dust bowl, people were advised to start planting tree shelterbelts to reduce wind velocity and catch the dustfall, thereby lessening the impact of wind erosion.

Generally, the larger particles will reach the ground before the smaller particles once they become airborne (Lancaster, 2009). This is due in part to larger particles having greater surface area and greater weight, which makes them more likely to strike objects above the soil such as plants, decreasing their velocities and cause them to eventually drop faster than their smaller counter parts. For instance, particles under 20 microns are often transported tens of km or more due to turbulent eddies keeping them

aloft, while particles 20-70 microns are transported in temporary suspension for tens to hundreds of m (Lancaster, 2009).

In Northern China, the deterioration of vegetation cover in recent decades has led to not only increasing frequency of dust storms, but also increasing intensity of dust storms (Hartmann et al., 2008). Soil C and N losses in these areas have been documented as high as 66% and 73%, respectively (Hartmann et al., 2008). In order to ameliorate the impact of these storms on rural and urban populations, it is important to understand how natural barriers such as trees slow the transport rate of deposition and conserve soil productivity.

In Figure 1, Joshua Stevens (2018) has provided a visual representation of the dust, black carbon, and sea salt aerosols in the Earth's atmosphere. In the desert region, the dust production is very high due to the arid environment, lack of vegetative cover, as well as a lack of natural interceptors such as trees or geologic barriers (NASA et al., 2018). This could be why the desert-borne dust and the black carbon from Africa extended across a larger area than the wildfire smoke in the Western United States during the summer of 2018 (NASA et al., 2018).

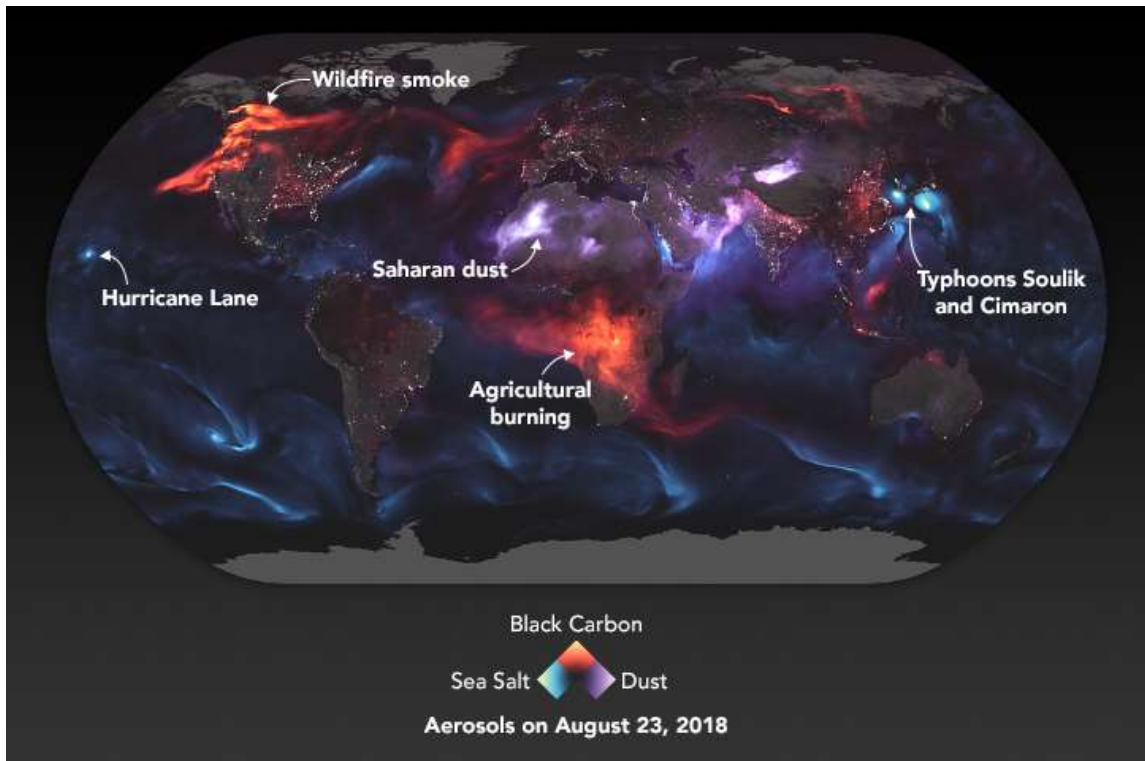


Figure 1. Map of atmospheric aerosol suspension and transport on a global scale (NASA, 2018).

Terrigenous Dry Deposition in Bodies of Water

Terrigenous deposition provides an input of essential nutrients to oceanic and freshwater ecosystems that many species utilize (Al-Tanni et al., 2014). In excess, N present in deposition could fuel algal blooms and influence the productivity and biodiversity of existing species within bodies of water (Al-Tanni et al., 2014).

Cloud Washout of Nutrients within Forested Areas

Normally the nutrients found in atmospheric deposition are washed out below the cloud base during high precipitation events, but forests and other topographic barriers such as mountains often catch airborne particulate matter and break up storms by decreasing the wind speed traveling through the trees (Zhang and Liu, 2007). This has been documented in cases such as in the Wieder et al. (2016) study describing the ‘Effects of Altered Atmospheric Nutrient Deposition from Alberta Oil Sands Development on Sphagnum Fuscum Growth and C, N, and S Accumulation in Peat’. It showed that the throughfall of daily -S, Ca^{2+} , SO_4^{2-} , ortho-P, and Mg^{2+} deposition was higher under wooded areas than it was in open areas (Wieder et al., 2016).

Sources of Particulate Matter

Sources of particulate matter can be divided into primarily three categories: 1) Anthropogenic sources such as industrial, urban, and agricultural areas, 2) Organic Sources, such as pollen, and 3) Mineral Sources such as geologic and soil particle deposition. These sources can further be classified by their origins as either marine or terrigenous particulates (Lequy, 2013). The following sections will discuss these three sources in greater detail.

Mineral Sources

Mineral dust has the unique characteristic of behaving as both a source of weatherable nutrients and a sink of trace metals and therefore performs a critical task in biogeochemical elemental cycling (Desboeufs et al., 2014). It generally refers to dust aerosols that originate as soil particles that become airborne and cycle through the atmosphere, impacting both cloud processes and the radiation budget (Scanza et al., 2014).

In a study of the input of dry deposition over the Gulf of Aqaba, it was recorded that the Gulf received a significant amount (averaging $34.68 \text{ g/m}^2/\text{year}$) of mineral dust from desert regions that border the Gulf (Al-Taani, Rashdan, and Khashashneh, 2014). This indicates that mineral dust has the potential to travel across large, unobstructed, and arid regions. There are some areas like this in West Texas, particularly in the Texas Hill Country, the Chihuahuan Desert, and the Rio Grande Valley. If there is a high amount of mineral deposition in this study, it could lead to stronger evidence of particulate transport throughout mixed ecosystems.

The Gulf of Aqaba study also recorded seasonal fluctuations, with high amounts of deposition occurring in the summer and lower amounts of deposition in the winter (Al-Taani, Rashdan, and Khashashneh, 2014). Therefore, it is important to take monthly measurements of the precipitation and throughfall in this study in order to address seasonal changes in particulate deposition.

Organic Sources

In one study, pollen was concentrated primarily in the spring with pine pollen deposition alone being recorded at 17.7–27.5 kg ha⁻¹ year⁻¹ (Lee and Booth, 2003). Since macronutrients are at high concentrations in pine pollen, with pollen based litterfall (plant sourced material falling to the surface of the Earth) being 1/30 N, 1/5 P, and 1/9 K, this is a considerable contribution to atmospheric deposition and nutrient deposition in the spring (Lee and Booth, 2003).

Fungal spores are present in forested ecosystems as well and contribute to atmospheric deposition. Generally speaking, there are fewer fungal spores as the distance from the source increases (Gregory, 2009). However, there are many sources of fungal spores throughout forested regions. In one study with a sampler 2m above the ground, small hyaline spores were often captured, and the types and concentration of spores often varied throughout the day, with the highest concentrations occurring in the afternoon and the lowest concentrations occurring in the early morning (Hirst, 2009). Generally rain washed spores from the air column, but during dry periods, the fungal spores that were often found included *Erysiphe*, *Alternaria*, *Cladosporium*, rusts, and smuts (Hirst, 2009). *Polythrincium trifolii* and *Phytophthora infestans* were also found, but did not display this pattern (Hirst, 2009).

It has been observed that particulate deposition from pollen and fungal spores displays a pattern based on the sampler height and the circadian rhythm of the plant or

fungi it originated from (Aulirantio-Lehtimäki, Helander, Pessi, 1991). For instance, *Alnus* pollen has been observed to have higher concentrations of deposition when the sampler was placed at roof level instead of at a height adjacent to the ground (Aulirantio-Lehtimäki, Helander, Pessi, 1991). However, most other types of pollen and fungal spores did not display a significant difference between their concentrations collected at the rooftop sampler vs the ground sampler (Aulirantio-Lehtimäki, Helander, Pessi, 1991).

Anthropogenic Sources

Heavy metal input from industrial sources of atmospheric deposition has declined significantly over the past few decades (Türtscher et al., 2017). However air pollution from nearby sources, such as agricultural areas or large cities, may contribute to the acidity of the observed deposition and, in unregulated and unmonitored scenarios, this could make soils more subject to nutrient leaching with pH reduction of as much as 1 unit over 30 to 50 years (Radnor, 1986).

While industrial heavy metal deposition is one cause of soil acidification, N, a very important macronutrient, also occurs in atmospheric dry deposition and acidifies soils as well due to nitrification. Globally, N deposition has quadrupled since the mid-twentieth century, when anthropogenic activities releasing N began rapidly increasing (Dörr et al., 2010).

Nitrogen inputs from fertilizers, industrial areas, and agricultural processes provide varied influxes of atmospheric deposition that can acidify the soil. This acidity

reduces the levels of other plant macronutrients such as Ca, Mg, and K by leaching basic cations and decreasing nutrient availability for plant roots and microbes, which may eventually reduce the productivity of soils and overall plant growth (Radnor, 1986).

Contaminants in industrial air pollution may even reduce seedling development and seed germination (Radnor, 1986). However, East Texas is not an industrial area, and the agricultural areas that would normally contribute to acid deposition are typically bordered by trees which reduce their wet and dry deposition transport capabilities. However, these impacts don't consider other compensating soil factors, such as a high natural ability to buffer, pH, low nutrient availability and low exchangeable base content (Radnor, 1986).

METHODS

Study Area

From most westerly to most easterly, the study area within East Texas extended from the Stephen F. Austin State University Real Estate Foundation's STMicroelectronics carbon sequestration project property near Lovelady, Texas, where the pine forested region begins, to the project's property in Shelby County, near the Louisiana border. Figure 2 details site locations in reference to counties and populated cities that had over 12,700 residents at the time of the study, and Figure 3 describes the elevation and topography that surrounded each sampler.

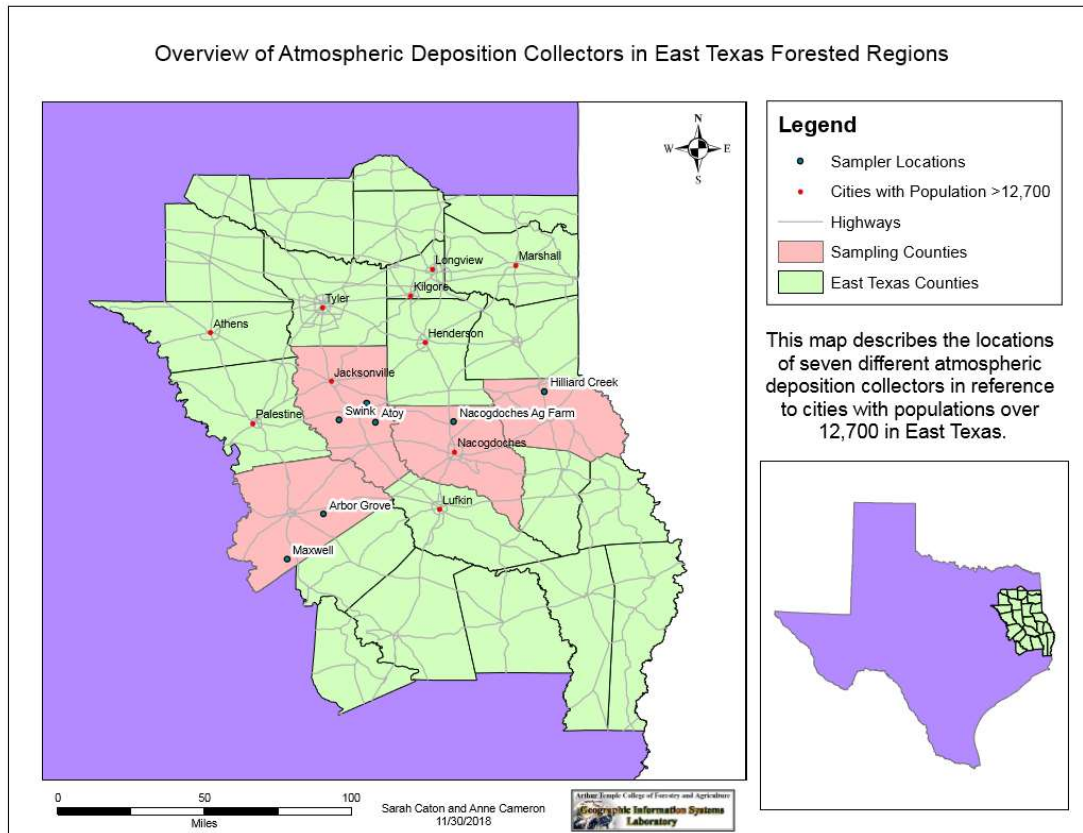


Figure 2. Map of sampling sites in relation to counties and populated cities with over 12,700 residents.

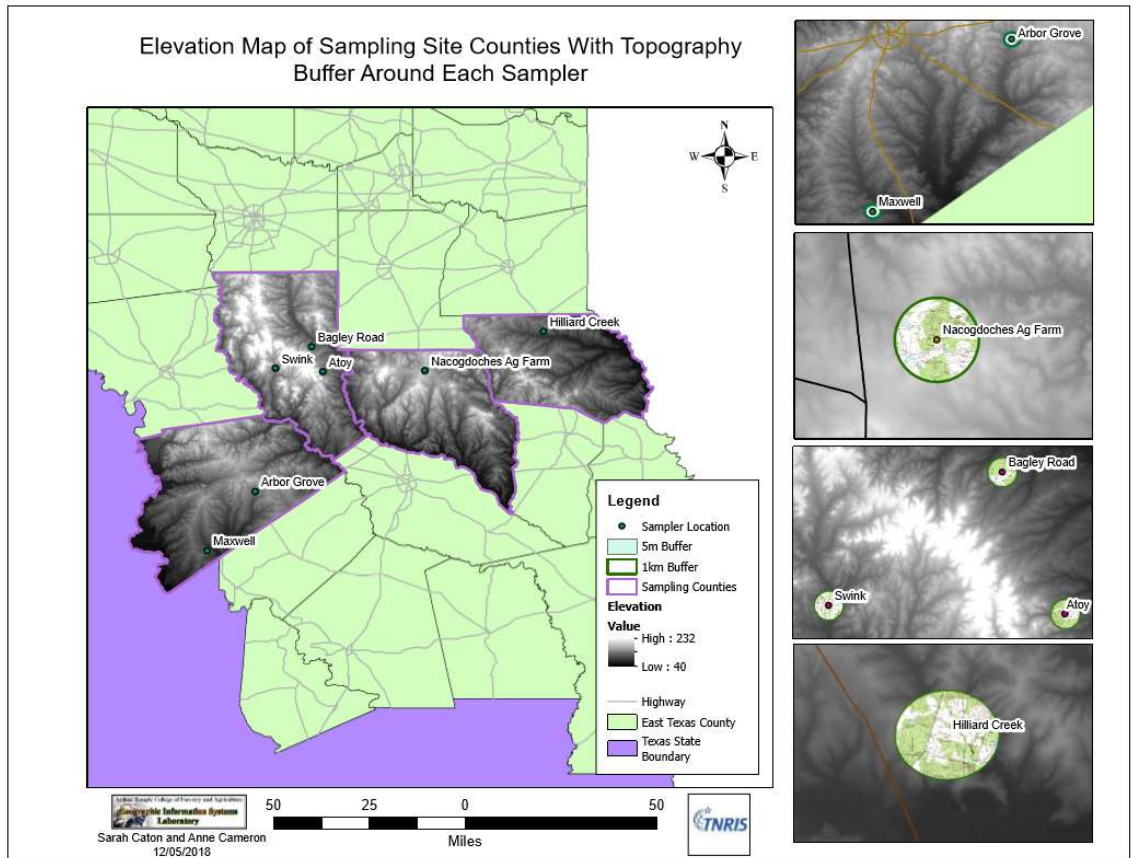


Figure 3. Map of sampling points in relation to general elevation and 5m of surrounding topography.

At the time of this project, the soils generally present in both East Texas and Western Louisiana were similar aside from fertility. They were located in ecoregion 35, which was the South Central Plains ecoregion according to the EPA’s level III ecoregions classification (EPA, 2016).

Table 1 provided the latitude and longitude of each sampler in decimal degrees. There were seven sites that were sampled monthly. Concerns about potential vandalism

were addressed by using only gated SFASU owned properties, and placing the sampling devices in clearings larger than 500m² within the forested areas. There was one sign placed close to each apparatus, and two SFASU Environmental Science stickers were placed on the poles and pails of the apparatus.

Table 1. Latitude, longitude, clearing size in square ft, and clearing shape from aerial view of study site locations. Shape of clearing was used to determine which area formula to use when calculating after gathering the length and width of the clearing using a measuring wheel with an accuracy of 0.0001m per 1m.

| Property | Location of sampler | Area of Clearing | Shape of Clearing |
|------------------------|------------------------|--------------------------|-------------------|
| Hilliard Creek | 31.911980, - 94.208220 | 105,739.24m ² | Rectangular |
| Bagley Road | 31.853823, -94.209266 | 5,031.31m ² | Oval |
| Atoy | 31.761080, -95.041823 | 9,770.24m ² | Oval |
| Swink | 31.773443, -95.221496 | 25,136.48m ² | Rectangular |
| Arbor Grove | 31.315130, -95.302230 | 148,609.31m ² | Triangular |
| Maxwell | 31.085440, -95.478244 | 960.36m ² | Oval |
| Stephen F. Austin Farm | 31.764415, -94.657070 | 7197.54m ² | Oval |

Samplers

There was one sampler at each site to collect particulate deposition. The sampler consisted of 3.05m of vertically oriented PVC pipe connected to a Hopkins FloTool funnel of 180mm diameter via a hose clamp of 33.3mm to 57.2mm. This airborne funnel was fastened to the PVC pipe at approximately 2.00m above the ground's surface and was connected to 305cm length of clear Tygon tubing with a 25.4mm outer diameter and 19.1mm inner diameter. This tubing drained into an 18.9L pail with a fitted hole at the top, which was caulked with outdoor/indoor silica caulking to ensure water and weatherproofing. To avoid algal growth in the hose, any slack present in the hose was

cut off with PVC pipe cutters. The hose was fastened to the PVC pipe via one additional hose clamp and zip ties. In addition to this, a T-post was fastened to the PVC pipe with a host clamp for stability, and a bird spike was fastened to the funnel via eight small zip ties that ran through eight small holes near the top edge of the funnel (Figure 4). In order to prevent particle loss, 147 acid washed glass marbles were placed within the funnel over a small section of rigid hardware cloth (Lancaster, 2009).

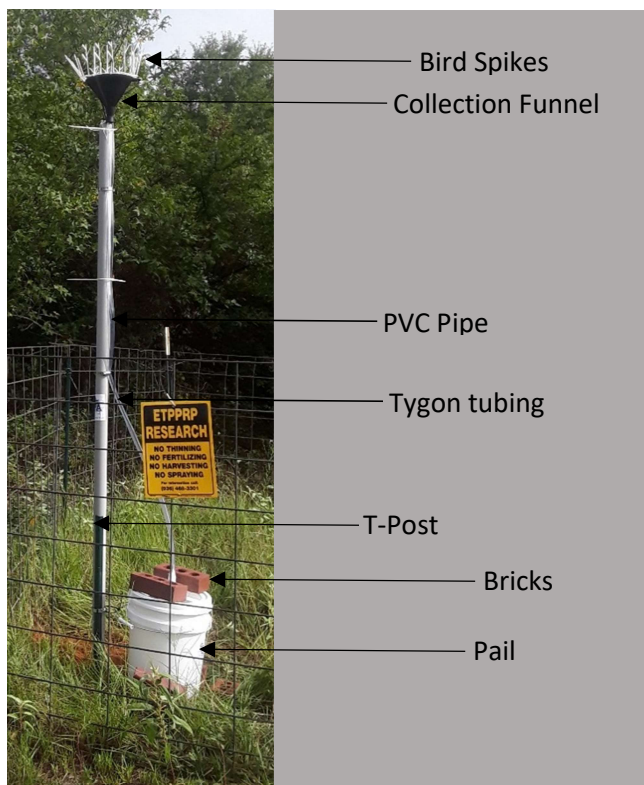


Figure 4. Diagram of Sampler at SFA Beef Farm.

These devices extended 2 m off the ground and were placed at least 5 m away from large objects to ensure that these objects did not block incoming air flow. Each PVC pipe was buried up to 0.89 m to increase stability. Plastic bird spikes were attached to the top of each sampler to deter avian interference in sample collection (Figure 4). The following table was created to calculate whether 18.93L would be large enough to hold the maximum and average precipitation in the sampling areas.

In **Table 2**, the average monthly rainfall in mm was calculated by dividing the average monthly volume of water collected in cm^3 by the area of the funnel in cm^2 . This value was then converted to mm. Maximum monthly rainfall in mm was calculated by dividing the maximum monthly volume of water collected in cm^3 by the area of the funnel in cm^2 . This value was then converted to mm. The monthly rainfall capacity of the pail in cm was calculated by dividing the water capacity of the pail in cm^3 by the area of the pail in cm^2 . The pail was large enough to hold the average monthly precipitation in these counties, but it could not hold the maximum monthly rainfalls documented for Cherokee county, Houston county, and San Augustine parish.

Table 2. Rainfall statistics near sampling locations (NOAA Weather stations, 2018). The start date refers to the first day of each county weather station’s rainfall collection period, and the end date refers to the last date of each county weather station’s rainfall collection period.

| Location (County/Parrish, State) | Average Monthly Rainfall (mm) | Maximum Monthly Rainfall (mm) | Area of funnel opening (cm ²) | Area of Pail (cm ²) | Water Capacity of Pail (L) | Monthly Rainfall Capacity of Pail (cm) | Start Date | End Date |
|--|--|--|--|------------------------------------|----------------------------------|---|------------|------------|
| Nacogdoches, TX | 6.40 | 103.07 | 254.47 | 77.62 | 18.93 | 243.88 | 10/1/1947 | 12/24/2013 |
| Cherokee, TX | 151.57 | 981.40 | 254.47 | 77.62 | 18.93 | 243.88 | 8/1/1962 | 9/27/1978 |
| Houston, TX | 14.58 | 328.98 | 254.47 | 77.62 | 18.93 | 243.88 | 9/1/1996 | 6/1/2013 |
| San Augustine, LA | 129.58 | 1472.20 | 254.47 | 77.62 | 18.93 | 243.88 | 7/5/1947 | 8/26/1947 |
| Sabine, TX | 19.33 | 25.77 | 254.47 | 77.62 | 18.93 | 243.88 | 10/1/1947 | 12/1/1957 |
| Sabine, LA | 11.59 | 57.97 | 254.47 | 77.62 | 18.93 | 243.88 | 1/11/1940 | 12/1/1986 |
| De Soto, LA | 2.88 | 38.65 | 254.47 | 77.62 | 18.93 | 243.88 | 5/21/1941 | 4/1/1972 |

The tygon tubing, funnel, and pail were placed in an acid wash of 5% HCl solution for 1 minute, and then rinsed with deionized water three times before being placed in the field. After that, only the pails were acid washed every month after the sample was collected. To prevent algal growth, 0.09g of CuSO₄ was added to each pail. Once the complete sampler was in its corresponding site location, the equipment was rinsed three times with deionized water to ensure there was little risk of contamination, and two bricks were placed on top of the pail to ensure stability while three more surrounded the pail to ensure that it stayed in place during high wind events.

In order to solve the issue of rainwater splashing out of the devices, the funnel was chosen to increase gravity flow into the device, and marbles were placed in the funnel to increase particle retention. This approach offered a sturdy, scientifically

reliable way of collecting data in these zones, and it was less likely to be targeted by wildlife and humans in these areas since the samplers were not immediately adjacent to any major metropolitan areas and they were too tall to be within reach of most wildlife. Additionally, since the funnel was significantly higher than ground level and had bird spikes, these measures not only aided in preventing animal interference, but likely produced a higher correlation of results between sites (Lehtimäki et al., 1991). This is because it focused on the airborne particulate matter instead of the particulate matter that was near the ground.

Sample Analysis

When collecting each sample, one liter of deionized water was used to rinse the dry deposition from the marbles within the funnel (This volume of water was later accounted for in calculations). The pail was then removed and covered before a new acid washed pail was placed in its stead for the following month. The covered sample was then transported to the environmental measurements lab within an enclosed vehicle to prevent contamination. In the lab, the contents of the pails were vigorously agitated using a mechanical stirrer to re-suspend particles, and a 400mL subsample was extracted from each sample. The subsample was then vacuum filtered through a glass microfiber filter to collect the particulate deposition. The electron microscope was used to identify particle size distribution of the dry sample, and the x-ray spectrometer was used to identify the elemental mass composition of the dry sample.

Filtration Method

The lab equipment used for initial measurement of the collected wet and dry deposition included a drying oven set at 60°C, a büchner funnel with 2L filtering flask, Si glass microfiber filter paper, evaporating dishes, a desiccator, an analytical balance, a sample container carrier, and a 1L graduated cylinder.

Initial measurement was modeled after ASTM standard D1739-98, which is the standard test method for collection and measurement of dustfall (ASTM, 2017). To

measure the dust from the sample collected in the 18927.1cm³ pail, a microfiber glass filter with a 9-cm diameter was pre-weighed after drying on a glass petri dish in the oven at 60°C for twelve hours and was then placed in a desiccator for two hours to cool (ASTM, 2017). Tweezers were used to prevent finger oil contamination and the filters were not allowed on any contaminated surfaces. The pore size of the filters was 2.5 microns.

An automatic mixer suspended the particulates in the liquid sample at a speed of 663 r/min for a minimum of two minutes. After two minutes, a subsample of 400mL was taken in 100mL increments using a metal reusable syringe while the mixer was running. The contents of the subsample were then filtered under vacuum through a büchner funnel, and the filter was dried at 60°C for twelve hours or until weight remained constant to the fourth significant digit on the analytical balance. The Calculation Formula for the general deposition rate was as follows:

$$D = W/A \text{ g/m}^2$$

In which A = Cross sectional area of the sampling container and W = Total Soluble Matter and Insoluble Matter normalized to a 30-day period in grams (ASTM, 2017). After the total deposition was calculated, the samples underwent two types of analysis each. For the elemental mass percentage, an x-ray spectrometer was used to identify macronutrients (N, P, K, Ca, and Mg) and to identify the micronutrients (Fe, B, Cl, Mn, Mo, and Zn). For particle size distribution, the scanning electron microscope was used to identify PM_{2.5}, PM₁₀, and TSP.

Electron Microscopy Analysis

The size and shape of particulates has been a widely discussed topic in the study of particulate matter because these properties, along with chemical makeup, could help identify the origin of the particulates, their behavior, and their potential effects on human health (Ličbinský, Frýbort, Huzlík, et al., 2010). An efficient way of measuring the size, shape, and chemical makeup was with a scanning electron microscope (SEM), which not only provided this data, but also provided a visual micrograph of the particulates.

For scanning electron microscopes, the procedure for preparing the sample as well as analyzing it varied with the type of sample under observation. The standard operating procedure this study used was the EPA's standard operating procedure for sample preparation and analysis of PM₁₀ and PM_{2.5} samples by scanning electron microscopy (EPA, 2008). Since there was not a practical method for removing the particulates from the filters without removing the organic matter for examination, four circular subsamples (1cm diameter) were cut from each filter with a bore and analyzed under the microscope after coating with Au₃Pd. Aggregates were ignored unless the space between the particles was 1 micron or larger.

While the scanning electron microscope was not the only mechanism used to identify particulates, it was the most accessible and practical for this study. As shown in Figure 5, mineral dust deposition generally ranges from 1-1000nm, which was within the

scanning electron microscope's range of observation, and larger organic particles like pollen and spores fell within both the scanning electron microscope and the optical microscope's observation range (Lower, 2018). Anthropogenic sourced deposition, like soot and smoke, were frequently out of observation range using this methodology so they were excluded from the analysis.

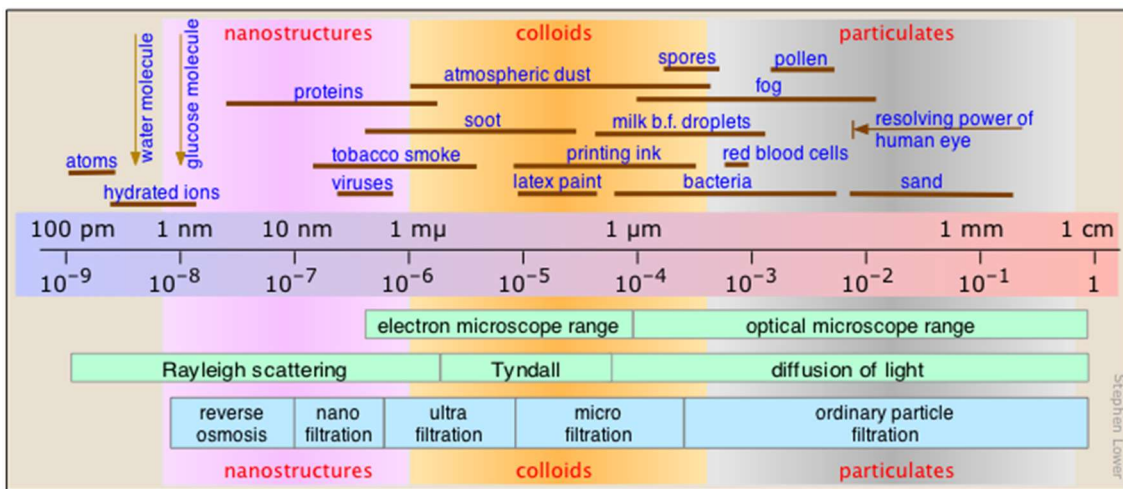


Figure 5. Size and observation range of different nanostructures, colloids and particulates using different lab techniques. Source: (Lower, 2018).

The program used to measure the particulates captured by the SEM was Quartz PCI. For each of the four subsamples cut from the original sample filter, eight micrograph images were captured at different x,y stage locations, and 40 particles were measured twice for each image. Measuring twice (vertically and horizontally) compensated for irregularly shaped particles, and eight uniform x,y stage locations on the scanning electron microscope were chosen to reduce bias when capturing the

micrographs used for measuring particulates. These stage locations remained constant throughout the data collection.

Attached to the SEM was an x-ray spectrometer, which could provide information about the elemental percent composition of subsamples placed within the SEM. This analysis was conducted before the sample was coated with Au₃Pd to obtain an accurate representation of the subsample.

Site Areas

Weather was observed closely to determine the correlation that monthly wind velocity and precipitation had on the particle sample collected at the end of every month. This data was taken to determine the consistency of the precipitation collected in the pail in comparison to the precipitation recorded by NOAA. Since there was no weather station within Shelby County, the weather data for this county was less reliable than the other locations.

The method used to measure atmospheric deposition in this study was relatively new, but it was chosen due to inapplicability and cost of previously used equipment in preceding studies. An ion exchange resin collector would have only measured the accumulated deposition over the year, which would have made seasonal differences difficult to quantify. Additionally, the dry Frisbee method would have had a higher potential for contamination due to the chemicals used in the materials of the collection zone and due to the relative frailty of the apparatus itself, which was left open to animal

interference. Also the frisbee was more likely to lose particulates through rainwater splashing them out of the devices in the event of a heavy storm. In order to solve the issue of rainwater splashing out of the devices, the funnel with marbles was chosen to increase retention into the device (Lancaster, 2009). This approach offered a sturdy, scientifically reliable, and inexpensive way of collecting particulate data, and it was less likely to be targeted by wildlife in these areas.

STATISTICAL PROCEDURE

Overview

The program used to perform the statistical analysis for this data was SAS 9.4 Software in the Arthur Temple College of Forestry's GIS lab. The independent variables were the time and location of the samplers. The dependent variables were the particulate concentrations, particle size distribution, and elemental composition of the samples. This data did not follow a normal distribution so a non-parametric test was used in its analysis (Ophthalmol, 2011). Since the samples were paired with a location, this data was considered non-independent. Summary statistics were calculated using the proc means mean std min max procedure.

The primary parameters observed in this study included the time, particle size distribution, elemental composition, and weight of the particulates. The formula used to calculate the monthly deposition rate in g/m^2 was $D = W/A$, in which A = Cross sectional area of the sampling container's inside diameter and W = Total Soluble Matter and Insoluble Matter normalized to a 30-day period in grams (ASTM, 2004). The particulate weight in g was calculated by taking the final dried weight of the filter minus the initial dried weight of the filter after running the 400mL monthly subsample through it.

$$D = \pi r^2 * (P_T/P_S)$$

The cross-sectional area of the sampling container in m^2 was calculated by taking the radius of the funnel (0.09m), squaring it, and then multiplying by Pi and the total precipitation collected (mL) divided by the subsample volume (400mL). The deposition rate in kg/ha per month was calculated by multiplying g/m^2 by 10.

For the second and third datasets (the particle size distribution and elemental compositions), four subsamples were collected from each sample filter that held the monthly deposition collected at one site for one month for all samples. Four subsamples were collected from each filter sample using a clean 1cm diameter cork bore.

These subsamples were mounted on a carbon stub and placed directly into the SEM without coating. Once an image of the lowest magnification (30X) was obtained, an X-Ray spectrum was collected from each randomly selected subsample using the SEM's EDS addition. This produced a table that recorded the elemental mass percentages for each subsample. After the X-Ray spectrum was taken, the carbon stubs were coated with a layer of Au_3Pd using a sputter coater for 4 minutes. The coated samples were placed back into the SEM, and eight stage locations were chosen to count particles at a magnification of 300X for the particle size distribution research. Eight additional locations on the SEM's sample stage were chosen using stratified random sampling to reduce bias in the particle measurements. During this analysis, the magnification of the subsamples remained constant.

Mixed Model Repeated Measures

The data was split into three smaller datasets: the particle weight measurements, the elemental mass percentages, and the particle size distribution. The procedure used was the proc mixed repeated analysis in SAS. Data was sorted and averaged using proc sort data=name; by location. The variation was observed to be different between months, locations and months*locations interactions so an analysis of covariance was used to further interpret the data within the mixed model. Three different covariance structures were compared using SAS, and the Autoregressive(1) (AR(1)) was chosen to be the best fit for this dataset over Compound Symmetry (CS) and UN (Unstructured) because it uses homogeneous variances, and its correlations decrease exponentially when the distance between the parameters increases (SAS, 2020). CS and AR(1) had similar fit test readings. Dataset three used this statistical procedure frequently.

The statistical model used for the first dataset was Particle Weight = μ + Location + Time where Time was the coded date range of the sample, Location was the property from which the sample was taken, and Particle Weight was weight of particulates for the month in $\text{kg ha}^{-1} \text{yr}^{-1}$. These samples were related (paired) using interval data. Two factor ANOVA was used for analysis.

The statistical model used for the second dataset was Element = μ + Location + Plot(Location) + Time where Time was the coded date range of the sample, Location was the property from which the sample was taken, sample was the filter, Element was the

element concentration in mass percent for each subsample, and Subsample was the sample taken from the filter to reduce the size of the sample so that it could be read by the Scanning Electron Microscope for Energy Dispersive Spectrometer (EDS) Analysis and Particle Size Distribution Analysis in the third dataset. The general detection limit for the EDS was 1000ppm, but since the detection limit per element varies based on how the element interacts with other elements (i.e. Carbon in CO₂ vs Carbon in CaCO₃), the non-detection values were recorded as zeros instead of halving the detection limit.

The statistical model used for the third dataset was Microns = m + Location + Sample(Location) + X + Y + Time where Time was the coded date range of the sample, Location was the property from which the sample was taken, Sample was the filter, Microns was the particle measurements for each subsample, X was the horizontal location on the stage, Y was the vertical location on the stage, and Subsample was the sample taken from the filter to reduce the size of the sample so that it could be read by the Scanning Electron Microscope for Energy Dispersive Spectrometer (EDS) Analysis and Particle Size Distribution Analysis in the third dataset. The third dataset included location, date, sample, subsample, X location on the SEM stage, Y location on the SEM stage, and measured particle diameter in microns. Particulate diameter was calculated by averaging the horizontal and vertical measurements. The X and Y locations were determined using stratified random sampling on the filter to prevent bias. After the summary statistics were calculated, the particulate matter was organized into size classifications of fine (≤ 2.5 microns), coarse (2.5-10 microns), and larger than 10

microns. This is in accordance with the EPA's size classifications of fine particulate matter, coarse particulate matter, and TSP.

Weather Analysis

Weather Analysis was performed at each of the sites to determine the impact of wind velocity as well as to track precipitation events throughout the sampling period at the locations listed in Figure 6 and Table 3. The precipitation recorded by NOAA was compared to the precipitation collected by the samplers to determine whether the samplers were collecting an amount of rainfall that accurately represented the typical conditions of the area.

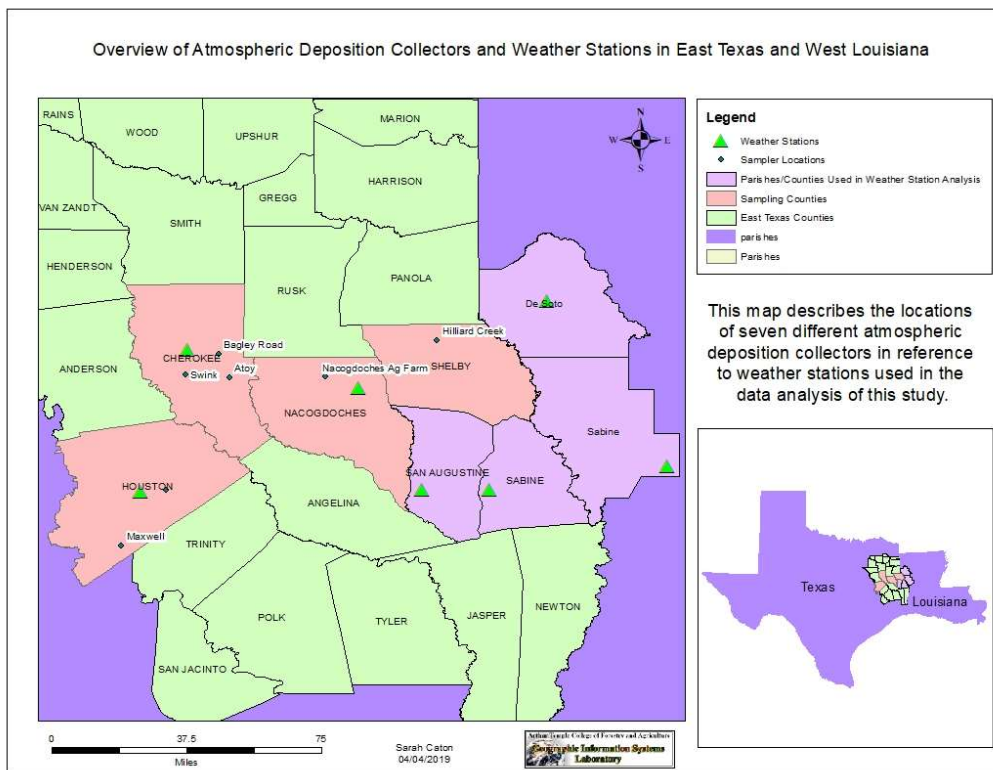


Figure 6. Map of weather stations used near sampling points. (NOAA, 2018).

Table 3. Table of weather stations near sampling points (NOAA, 2018). Start Date refers to the day the weather station started collecting precipitation data, and End Date refers to the last date the weather station collected data used as a reference in this study.

| Weather Station | County/Parrish | State | Elevation | Coordinates | Start Date | End Date |
|------------------------------|----------------|-------|-----------|-----------------------|------------|------------|
| Nacogdoches TX US | Nacogdoches | TX | 132.6 m | 31.6163°, -94.643° | 1947-10-01 | 2013-12-24 |
| San Augustine TX US | San Augustine | TX | 89.9 m | 31.51921°, -94.11866° | 1962-08-01 | 1978-09-27 |
| Mansfield 4 NW LA US | De Soto | LA | 98.1 m | 32.07119°, -93.75882° | 1996-09-01 | 2013-06-01 |
| Chambers Hill Guard TX US | Sabine | TX | 107 m | 31.46667°, -93.83333° | 1947-07-05 | 1947-08-26 |
| Many LA US | Sabine | LA | 70.1 m | 31.56667°, -93.48333° | 1947-10-01 | 1957-12-01 |
| Lovelady TX US | Houston | TX | 92 m | 31.13333°, -95.45° | 1940-01-11 | 1986-12-01 |
| Cherokee, TX US | Cherokee | TX | 454.2 m | 30.98333°, -98.71667° | 1941-05-21 | 1972-04-01 |

A Wind Rose Plot was obtained from each of the weather stations using publicly available wind data obtained throughout the sampling period. It was generated by first going to <http://www.ncdc.noaa.gov/>, then using their search tool to obtain the climate data online for each of the weather stations. WRPLOT was downloaded from www.weblakes.com, and the data was formatted to match the study.

Precipitation events were recorded and entered into an excel document. The daily and monthly total rainfall at each of the sampling locations as well as the prominent direction of wind that day was also recorded.

RESULTS AND DISCUSSION

Study Parameters

The results in this study were divided into three major sections: the weight of the monthly particulate deposition, the chemical composition of the monthly particulate deposition, and the particle size distribution of the monthly particulate deposition. The weight of the monthly deposition was displayed in chronological order by month. The chemical composition section was grouped by individual elements observed in the data. The particle size distribution section was sorted alphabetically by site name and then chronologically by sample collection date within site.

Summary Statistics for Particulate Weight

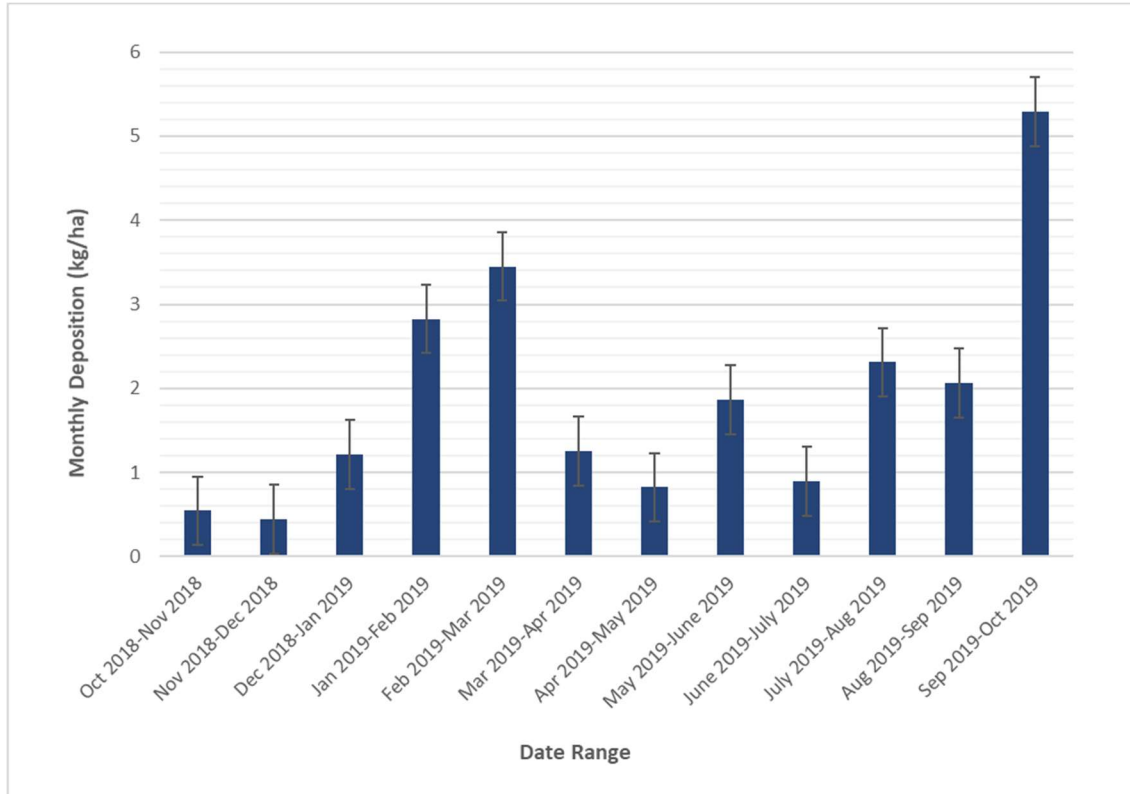


Figure 7. Arithmetic means of samples collected from six sites in Stephen F. Austin University Real Estate Foundation’s STMicroelectronics carbon sequestration project and one site at the SFA Agriculture Center’s Beef Farm at monthly intervals over a twelve-month period. Units are in kg/ha per month. Error bars display standard errors.

ANOVA for Particulate Weight

Mixed model ANOVA was the method used to determine the significance of each variable of particulate weight. The model for particulate weight is $PW = m + Location + Time$ where *Time* was the coded date range of the sample, *Location* was the property the sample was taken at, and *PW* was the particulate weight in grams. The dependent variable in this model is particulate weight in grams, and there were two independent variables,

location and time. Location had seven levels: one for each property in the study. Time had 12 values representing the dates each sample collected deposition. The significance level used for comparing P-values was 0.05. If $P \leq 0.05$, then the variable was statistically significant. If $P > 0.05$, then the variable was not statistically significant. Location was found to be significant at < 0.0001 Pr>F. Plot(Location) was found to be slightly significant at 0.0449. Time was found to be significant at 0.0003 Pr>F.

Yearly Results and Observations

Algae contamination was observed three times during this study: once from the Maxwell site sample analyzed on 07/24/2019, once from the Bagley Road site sample analyzed on 05/24/2019, and once from the SFA Agriculture Center site sample analyzed on 05/24/2019. This may have influenced the results of these three sites during this study by increasing the particulate weight of the samples somewhat, as well as influencing the particle morphology and chemical composition observed in later parts of this study. Future studies should account for this by utilizing more CuSO_4 in the pails.

Pollen deposition was observed at all seven sites, which were surrounded by trees and other flora. Since morphological pollen grain structures and larger particle sizes associated with pollen granules were observed throughout the sampling period, clearing size, wind, and surrounding trees may have influenced the total deposition. Mineral deposition was also likely influenced by wind direction and speed, since it had to be moved by wind or precipitation events to be deposited in the collection zones of the samplers.

From October 20th, 2018 to October 19th, 2019, high velocity winds over 7.00 knots primarily came from the South and Southeast (Figure 20 and NOAA, 2019). The sites furthest north recorded the lowest total deposition in kg/ha, and the sites furthest south recorded higher total deposition in kg/ha. Of the four counties, Nacogdoches County and Houston County experienced the highest amount of total yearly deposition as

well as the highest amount of winds coming from the Northwest (Figure 22, Figure 23 and NOAA, 2019). These are the two southernmost counties in this study and may have been influenced by the high velocity winds coming from the south as well as the slower winds coming from the north.

Louisiana's Sabine Parish (used for Shelby county's wind data) displayed the highest percentage of northerly winds but had very little western or eastern winds (Figure 24 and NOAA, 2019). Shelby county had the lowest total deposition of the four counties. Since Shelby county was in a densely forested area, the surrounding trees north and south of the sampler may have reduced incoming wind velocity as well as the amount of particulate matter deriving from distant sources.

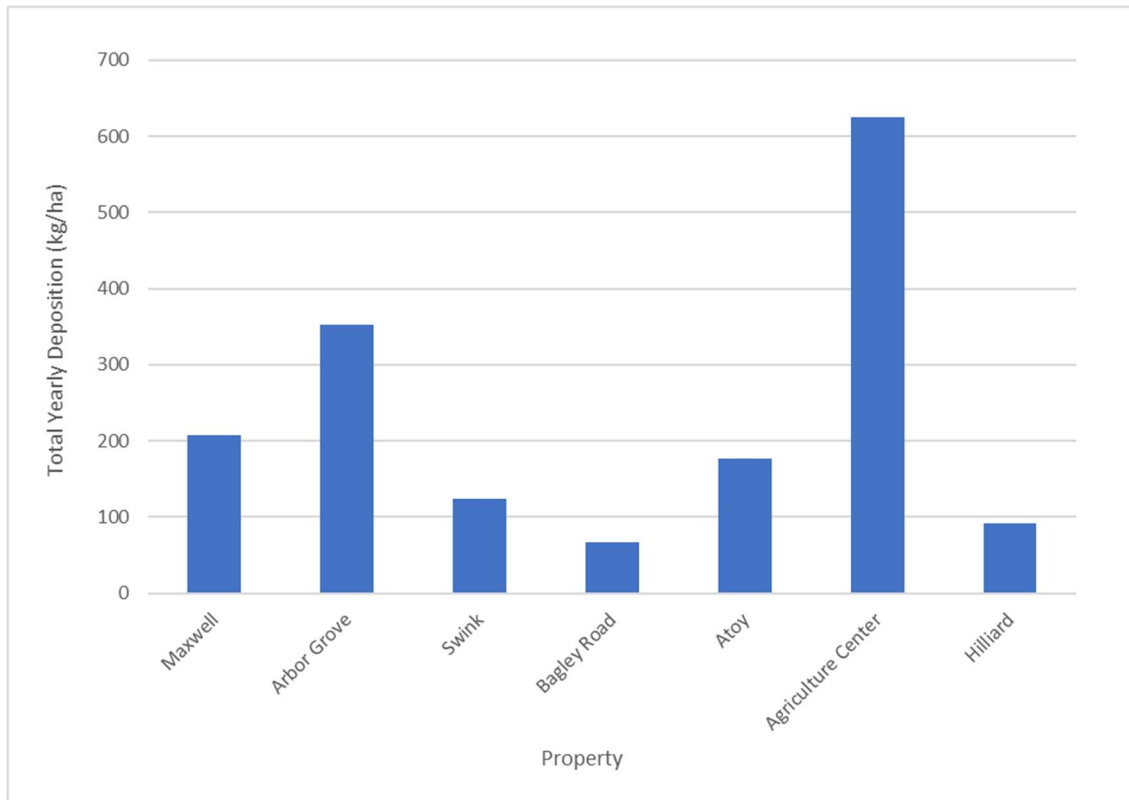


Figure 8. Total yearly particulate weight recorded at each of the sampling sites between October 20th, 2018 and October 19th, 2019. Sites are displayed from westernmost to easternmost location. Particulate weight is recorded in kg/ha per year. Six of the sites used were in Stephen F. Austin University Real Estate Foundation’s STMicroelectronics carbon sequestration project and one site was located at Stephen F. Austin State University’s Beef Farm at the Agriculture Center.

In the first four properties observed in Figure 8, the total deposition appeared to increase then rapidly decrease from west to east. Bagley Road’s sample had the lowest total deposition, and deposition generally increased east and south of this site (Figure 8). The SFA Agriculture Center experienced the highest amount of yearly deposition of the seven sites while Hilliard, the easternmost site, experienced the second lowest amount of yearly deposition.

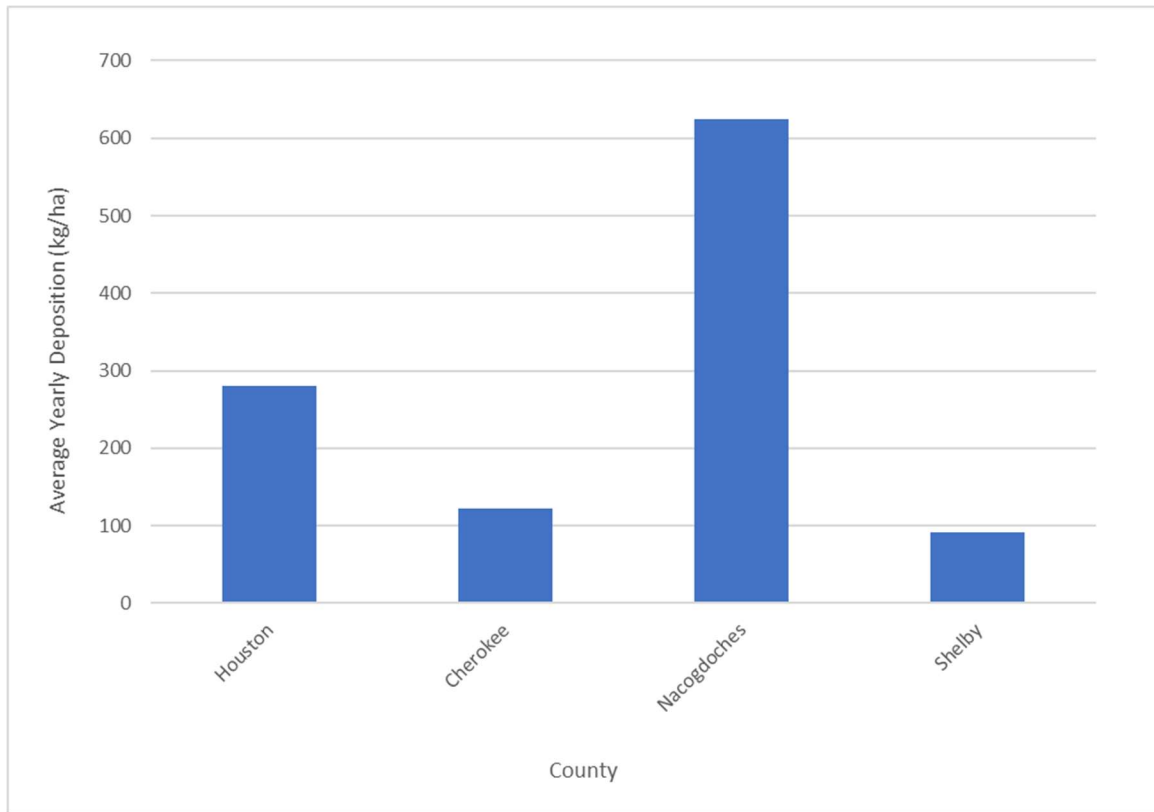


Figure 9. Average yearly particulate weight recorded at each of the counties between October 20th, 2018 and October 19th, 2019. Sites are displayed from westernmost to easternmost location as well as southernmost to northernmost location. Particulate weight is recorded in kg/ha per year. Six of the sites used were in Stephen F. Austin University Real Estate Foundation’s STMicroelectronics carbon sequestration project and one site was located at Stephen F. Austin State University’s Beef Farm at the Agriculture Center.

As longitude increased, the deposition decreased with the exception of Nacogdoches, which experienced more deposition than any of the other counties (Figure 9). One reason why Nacogdoches county may have experienced a higher total deposition than the other sites is due to its location further south and its close proximity to a bee hive box. Bees have been reported to increase pollen deposition in surrounding areas (Sáez et al., 2014). This could be due to pollen initially adhering to their bodies then becoming

airborne as they move from plant to plant. Using the average monthly particle size as a reference, pollen particles were more common at this site during the spring, when bees are typically more active.

Additionally, there were often bulls in this pen, and cattle hair has been observed to contain elements like B, Ba, Cu, Fe, Ca, K, Pb, Si, Na, Zn, Mg, Mn, P, and Ag (Washburn et al., 1958). Of these, Si, Ba, Na, K, and Fe were consistently observed at the Agriculture Center, and Ca was observed during every month aside from July 2019-August 2019. The presence of these elements indicates that a portion of the particulate weight observed may have been influenced by local dust generation from cattle activity.

Unpaved roads and geographic barriers may have influenced the total deposition measured at each site. This is because unpaved roads are vulnerable to wind erosion during dry periods as vehicles move on them, causing dust to rise off of the road, where wind can blow it to another area. The sites closest to roads with few geographic barriers likely had a higher input of deposition from these roads than the sites further away with many geographic barriers, provided the wind was blowing from the road towards the sampler. However, it should be noted that there was not a definitive way to differentiate between local particulate matter and that from more distant sources in this study.

At the SFA Agriculture Center, there was a line of trees between the sampler and an unpaved road 82m from the sampler, so some incoming dust from this area could have been blocked by the vegetation. Since the Agriculture Center recorded higher levels of

deposition than Bagley Road despite the road being further away, it stands to reason that due to the sampler at Bagley Road having more geographic barriers including trees and a dilapidated structure between the sampler and the unpaved road 79m from it, it experienced less deposition from this road. The sampler at Atoy was 18m from an unpaved road and had some forested barriers between it and the unpaved road, but for the most part, it was less influenced by geographic barriers than the other Bagley Road and Swink.

The sampler at Arbor Grove was 17m from an unpaved path leading into the property and had no geographic barriers with the exception of a cattle fence. It often experienced the most monthly deposition of the seven sites. Although an unpaved road was located 9m from Maxwell's sampler, it had more trees acting as barriers than Arbor Grove did. This correlates to Maxwell often experiencing less monthly deposition than Arbor Grove with the exception of high pollen count months. At the Hilliard property, there was an unpaved road less than 6m from the sampler that may have contributed to mineral deposition observed. However, the unpaved road was located north of the sampler so it mostly received mineral deposition from this road when the winds were blowing from the north.

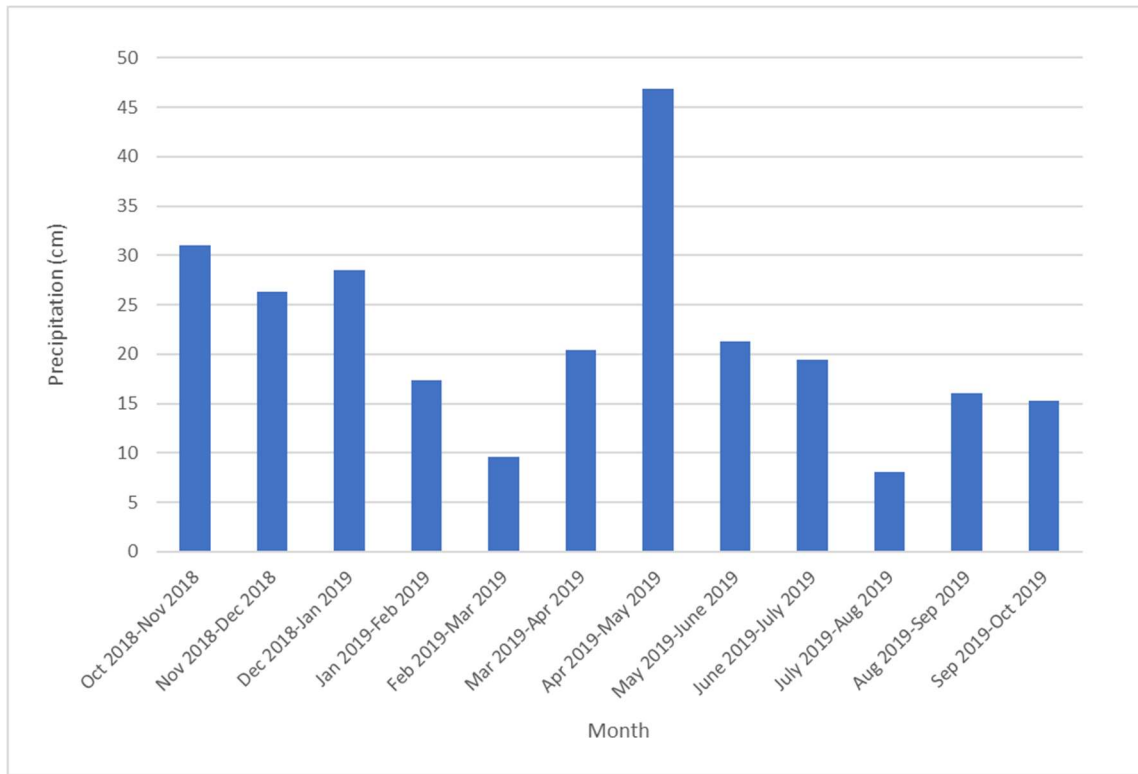


Figure 10. Arithmetic monthly mean precipitation in cm depth collected during the sampling period of October 20th, 2018-October 19th, 2019 at each sampling location. Six of the properties used were in Stephen F. Austin University Real Estate Foundation’s STMicroelectronics carbon sequestration project and one site was located at the SFA Beef Farm.

High periods of recorded deposition correlated with high periods of pollen deposition (Figure 7 and Houston Health Department, 2019). This indicates that during the months of January-March and September-October, the recorded sample deposition was influenced by pollen particles in the area. However, other months, such as March-April and October-January, did not appear to correlate to high periods of pollen deposition and may have had a higher input of mineral deposition during this time period (Figure 7 and Houston Health Department, 2019). The four months with the heaviest

rainfall had low recorded depositions (Figure 7 and Figure 10). This may be due to saturated soils being less cohesive and less susceptible to wind erosion. In Figure 10, rainfall was higher during the months of October-January and April-May, and these months received less deposition than the drier months of May-August.

Monthly Results and Observations

Table 4. Particulate weight in kg/ha per month for samples assessing monthly deposition between October 20th, 2018 and October 19th, 2019 at six of the sites in Stephen F. Austin University Real Estate Foundation’s STMicroelectronics carbon sequestration project and one site at the Stephen F. Austin Beef Farm.

| Date Range | Particulate Deposition (kg/ha) | | | | | | |
|-----------------------|--------------------------------|-------------|------|-------------|----------|---------|-------|
| | Agriculture Facility | Arbor Grove | Atoy | Bagley Road | Hilliard | Maxwell | Swink |
| 10/20/2018-11/21/2018 | 0.04 | 8.37 | 1.14 | 0.12 | 1.30 | 1.69 | 1.77 |
| 11/21/2018-12/19/2018 | 1.89 | 3.85 | 0.59 | - | - | 1.85 | 3.38 |
| 12/19/2018-1/19/2019 | 0.79 | 3.50 | 1.45 | 0.31 | 0 | 1.22 | 1.22 |
| 1/19/2019-2/22/2019 | - | 4.20 | 8.06 | 1.14 | 1.18 | 2.48 | 3.65 |
| 2/22/2019-3/20/2019 | 1.77 | 7.35 | 1.96 | 1.65 | 4.05 | 1.65 | 1.34 |
| 3/20/2019-4/18/2019 | 2.20 | 5.31 | 0.43 | 0.55 | 0.71 | 3.30 | 0.55 |
| 4/18/2019-5/22/2019 | 1.53 | 1.10 | 0.04 | 0.35 | 0.20 | 0.51 | 0.08 |
| 5/22/2019-6/21/2019 | 1.22 | 2.16 | 0.43 | 0.79 | 0.04 | 0.86 | 0.79 |
| 6/21/2019-7/20/2019 | 0.39 | 0.51 | 0.55 | 0.31 | 0.98 | 0.63 | 2.40 |
| 7/20/2019-8/22/2019 | 2.91 | 0.98 | 0.55 | 0.63 | 0.47 | 0.94 | 2.32 |
| 8/22/2019-9/21/2019 | 0.39 | 0.51 | 0.28 | 0.39 | 1.18 | 0.12 | 0.24 |
| 9/21/2019-10/19/2019 | 7.44 | 2.27 | 7.22 | 0.63 | 5.04 | 12.75 | 1.69 |

For the first collection month, samples were analyzed after six days (Table 4). During the initial drying process, the temperature was accidentally raised to 160°C instead of 60°C. This may have transformed some of the particulates and may have influenced the results for this part of the study. Sometime during the sampling period,

the collection funnel at the Swink sampling site was dislodged from the rest of the sampler. For consistency in calculations, deionized water was run through the connecting tube instead of the funnel. Afterwards, the funnel was reattached and secured with additional hose clamps and cable ties.

At the Hilliard property, stagnant water was observed in the collection funnel. The source of this drainage issue (a glass marble) was removed from the hose, and drainage capacity increased. At the Agriculture facility, the pail overflowed so its liquid contents were observed to be greater than 18927mL. Future studies should account for heavy rainfall potential.

The first collection month reported a large amount of deposition in kg/ha (Table 4). During this time period, the maximum particulate weight was recorded at Arbor Grove, which was the westernmost sampling site in Houston county. These properties reported a higher average deposition than the others observed this month. Hilliard Creek and Arbor Grove had the highest average micron size, indicating the potential for a higher percentage of pollen grains in comparison to the other sampling sites (Figure 11). The Agriculture facility had the lowest average micron size and reported the lowest amount of deposition during this time period (Figure 7 and Figure 11).

Of the three Cherokee county properties, Swink had the highest deposition rate at 1.77 kg/ha per month. Since it also had the largest clearing size of the three properties, it

may have been subject to mineral deposition from the unpaved road leading into the property.

Nacogdoches county had the lowest particulate weight recorded for this month at 0.0393 kg/ha (Table 4). With the smaller average particle size indicating low relative pollen counts as well as the low wind speeds and evenly dispersed wind directions indicating slow particulate movement, it is reasonable to conclude that this site likely experienced a reduced opportunity for depositional transport in comparison to the other sites (Figure 11, Figure 23, and Houston Health Department, 2019).

During the second month, samples were analyzed after two days (Table 4). The samples from Bagley Road and Hilliard Creek spilled during transport. Hilliard had a remaining sample of 2050mL and was analyzed for elemental analysis and particle size analysis. Bagley Road was left out of this month's observations due to lack of remaining sample.

During this sampling period, the maximum particulate weight was recorded at Arbor Grove, which is the site furthest west and south in Houston county (Table 4). It should be noted that the particulate weight at Arbor Grove decreased significantly from the previous month's sampling results, and this was a low period of deposition overall.

Of the two documented Cherokee county properties, Swink had the highest deposition rate at 3.3796 kg/ha per month and Atoy had the lowest (Table 4). This could have been due to different landscapes surrounding the samplers.

Nacogdoches county had the third highest particulate weight recorded for this month at 1.8863 kg/ha (Table 4). Small average particle size may have influenced the depositional transport at this site during this time period (Figure 11). Additionally, this site experienced a reduced amount of deposition in comparison to areas with higher elevations like Arbor Grove and Swink and experienced more deposition than areas with low elevation like Maxwell and Atoy (Figure 3 and Figure 7). This indicates that elevation/geographic barriers may have had an influence on depositional transport at these sites during this month.

For the third month, samples were analyzed after five days (Table 4). To reduce sample loss during transportation, each lid was securely attached to its corresponding pail using an adhesive with polyethylene coating and a cotton mesh base. This was a low period of deposition overall (Figure 7).

Sample sites further south appeared to have higher deposition rates this month (Figure 3 and Table 4). The maximum particulate weight during this time period was recorded at Arbor Grove as 3.4975 kg/ha (Table 4). Maxwell, another southern sampling site, tied with Swink for the third highest particulate weight recorded during this time period (Table 4).

The county with the fourth highest particulate weight recorded during this time period was Nacogdoches county at 0.7860 kg/ha per month (Table 4). Low average

particle size of deposition may have enabled greater depositional transport in this area (Figure 11).

Shelby county had the lowest deposition recorded for this month (Table 4). This could have been due to filter mass lost during transport from the glass petri dish to the disposable petri dish. In future studies, measuring the mass of the filter with the glass petri dish before and after collecting the deposition on the filter could help prevent this. Small average particle size may have impacted the site's depositional transport capacity for this time period (Figure 11).

For the fourth month, samples were analyzed after two days (Table 4). Overall, this was a period of high particulate deposition and intermediate mean particle size, which indicated a higher amount of pollen granules than previous months (Figure 7 and Figure 11). Cherokee and Houston county made up the highest depositional rates (Table 4). Houston county's location further south may have impacted its depositional transport capacity, and both Houston and Cherokee county may have been impacted by their location further west, where there were less trees between the samplers and more distant sources of mineral deposition from incoming western winds (Figure 21, Figure 22 and Table 32). This proximity to areas with less trees that may have reduced wind velocity could have provided the samplers within these counties with more deposition than the counties east of them, such as Shelby county, which had the second lowest particulate weight recorded for this month (Table 4, Figure 24 and Table 32).

For the fifth month, samples were analyzed after one day (Table 4). The maximum particulate weight collected during this time period was at Arbor Grove (Table 4). This was a period of high total deposition and high average particle size (Figure 7 and Figure 11). There was a correlation between high deposition rates and large clearing sizes (Table 1 and Table 4). During this time, the properties with the three largest clearing sizes were within the top four highest recorded depositions (Table 1 and Table 4).

For the sixth month, samples were collected analyzed after three days (Table 4). This was a period of intermediate particulate deposition as well as large mean particle size (Figure 7 and Figure 11). Houston county recorded the two highest particulate weights while Cherokee county recorded the lowest (Table 4). The Houston county sites contained ideal conditions for deposition during this time period. There was a nearby unpaved path with few geographic barriers south of the Arbor Grove sampler and an unpaved road near the Maxwell sampler. Also, they were the furthest south (Figure 3).

The Agriculture Center had the third highest particulate weight recorded during this time period at 2.2007 kg/ha per month (Table 4). Since this was a period of high pollen deposition and the densest area of trees was towards the east of the property, pollen deposition may have significantly contributed to the amount of deposition observed (Houston Health Department, 2019).

For the seventh month, samples were analyzed after three days (Table 4). Algae from Bagley Road and the Agriculture Center properties was visible on the samples after

filtration. This was a period of low particulate deposition and intermediate mean particle size (Figure 7 and Figure 11). The county with the highest particulate weight recorded during this time period was Nacogdoches county at 1.5326 kg/ha per month (Table 4). Since there was an unpaved road northwest of the sampler, the northwestern winds may have influenced this site's mineral input, especially considering the high winds present in this county at the time (Figure 23). Arbor Grove and Maxwell had the third highest particulate weight recorded during this time period. Since both properties contain unpaved roads/paths south of their samplers, these may have influenced their mineral input during this time period.

For the eighth month, samples were analyzed after one day (Table 4). The highest particulate weight during this time period was recorded at Arbor Grove, located at the westernmost sampling site, and the lowest particulate weight was recorded at Hilliard Creek, the easternmost sampling site (Table 4). This was a period of low particulate deposition and low mean particle size (Figure 7 and Figure 11).

Since the samplers at the Maxwell, Arbor Grove, Swink, and Bagley Road sites had unpaved roads and paths south of their samplers, they may have received mineral input from these sources. However, these samplers are also located closer to less forested regions west of Houston and Cherokee county and may have received more mineral input from these areas than sites further east like Hilliard Creek, which had the lowest particulate weight recorded for this month (Table 4).

For the ninth month, samples were analyzed after four days (Table 4). Algae was visible on the filter from the Maxwell property after filtration. The sample from Swink was dropped during transport and lost some of its contents. This was a period of low particle deposition and intermediate mean particle size (Figure 7 and Figure 11).

Since both Maxwell and Arbor Grove had unpaved roads and paths south of their samplers and are located the furthest south, they likely received mineral input from these paths. Out of the three Cherokee county properties, Swink had the highest deposition rate at 2.3971 kg/ha per month. This is likely due to the large clearing size around the sampler, the unpaved road south of it and the lack of obstacles between the road and the sampler (Table 1). The county with the second lowest particulate weight recorded during this time period was Nacogdoches county at 0.3930 kg/ha per month (Table 4).

For the tenth month, samples were analyzed after one day (Table 4). This was a period of high particulate deposition and intermediate average particle size (Figure 7 and Figure 11). Nacogdoches county and Houston county contain three of the four sites with the highest particulate deposition for this month. In Houston county, there were unpaved roads/paths south of both samplers so these unpaved roads may have contributed to the depositional input during this time period. The county with the highest deposition rate recorded during this time period was Nacogdoches county at 2.9080 kg/ha per month (Table 4). Shelby county had the lowest particulate weight recorded for this month (Table 4).

For the eleventh month, samples were analyzed after one day (Table 4). This was a period of intermediate particle deposition and intermediate mean particle size (Houston Health Department, 2019). Out of the three Cherokee county properties, Swink had the lowest deposition rate at 0.2358 kg/ha per month (Table 4). Mineral deposition from the unpaved path/road south of the Houston and Nacogdoches samplers may have contributed to their depositional inputs for this month.

For the final month, samples were analyzed after two days (Table 4). This was a period of high particulate deposition and intermediate mean particle size (Figure 7 and Figure 11). Out of the three Cherokee County properties, Atoy had the highest deposition rate at 7.2150 kg/ha per month (Table 4). Nacogdoches produced the second highest particulate weight recorded during this time period at 7.4378 kg/ha per month (Table 4).

Mixed Model ANOVA for Particle Size Distribution

The model for particle size distribution is $\text{Microns} = \mu + \text{Location} + \text{Sample}(\text{Location}) + X + Y + \text{Time}$ where Time was the coded date range of the sample, Location was the property the sample was taken at, Sample was the subsample taken from the sample filter after drying, X is the horizontal location of the filter on the stage, Y is the vertical location of the filter on the stage, and Microns is the measurement of one particle on the filter. The dependent variable in this model is Microns, and there were three independent variables or classes: location, sample, and time. Location had seven levels: one for each property in the study. Time had 12 values. Sample had four levels: one for each subsample of the filter. The significance level used for comparing P-values is 0.05. If $P \leq 0.05$, then the variable is statistically significant. If $P > 0.05$, then the variable is not statistically significant.

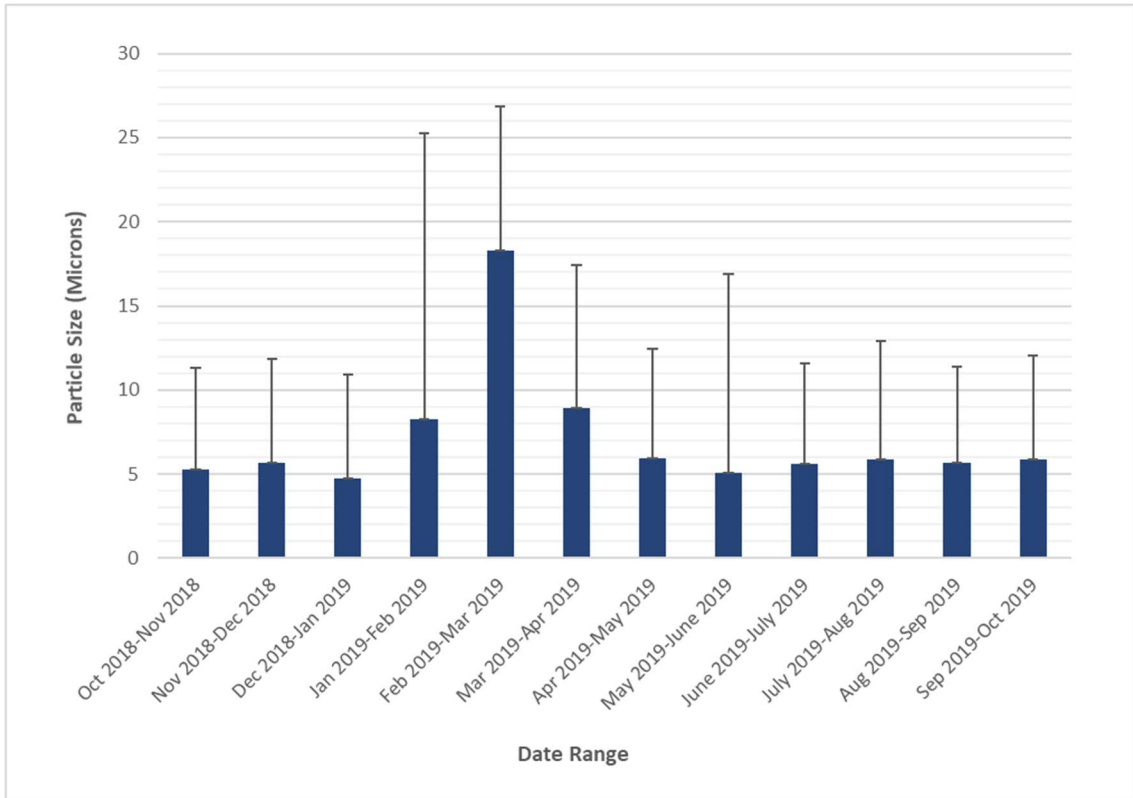


Figure 11. Arithmetic monthly mean size of sample particles across six sites in Stephen F. Austin University Real Estate Foundation’s STMicroelectronics carbon sequestration project and one site at the SFA Beef Farm. Units are in microns, and error bars are based on standard deviation of monthly mean particle sizes across sites.

In Figure 11, the average particle size appeared to follow a bell-curve pattern. From October 2018-February 2019, it gradually increased, then steeply peaked in February 2019-March 2019. Afterwards, it gradually decreased again before stabilizing around April 2019-May 2019 (Figure 11). Arbor Grove has a consistently higher mean particle size in comparison to the other sites, and this could be due to a higher pollen input than the other sites (Table 18).

Larger particles in this study tend to be associated with organic sources like pollen. January-April and September-October followed this pattern since these time periods had higher total pollen counts (Figure 11 and Houston Health Department, 2019). However, it should be noted that although pollen input may influence mean particle size, a higher total pollen count for an area does not always indicate that the majority of particles will be pollen in the sampler. If there was a lot of mineral deposition during a month with a high pollen count, then the average particle size may be lower than a month that had a lower pollen count but less mineral deposition. This is seen in the comparison between October 2018-November 2018 compared to November 2018-December 2018 (Figure 11 and Houston Health Department, 2019). November 2018-December 2018 has the higher pollen count, but it does not yield a higher average particulate size (Figure 11 and Houston Health Department, 2019).

Additionally, areas with small clearings bordered by dense trees and vegetation were more likely to be higher in pollen particles during certain months. All of the sites had either unpaved roads or unpaved paths within or leading up to the property. These sites likely contain smaller, mineral sourced particles from these roads and paths as dust became airborne with the presence of vehicles driving down the roads. The size of these mineral sourced particles (<0.002mm-2mm) would have been impacted by a variety of factors including distant particulate matter sources, imported materials used for unpaved roads, and bare soils. Low velocity winds would only have been able to transport smaller, less dense particles, while larger and denser particles would need high wind

velocities and less geographic obstacles to move across large distances. If the soils were very cohesive or had very dense particles, then they would likely not have moved very quickly across large distances.

During dry months recorded in Figure 10, the amount of mineral sourced particles may have increased due to the bare soil being less cohesive. Additionally, the presence of unpaved roads or cleared vegetation may have decreased the average particle size by providing more mineral particle input. Mechanical weathering in the pail over time could have shrunk some of the dry deposition during rain events providing large inputs of water during these time periods. Insoluble parts of the particles would likely not dissolve during these events, but separation of dry and wet deposition is a suggestion for future studies.

Elemental Composition of the Samples over Time

For each element, summary statistics were calculated using SAS, and a mixed model using repeated measures was used to process the data. The covariance structure was autoregressive. The estimation method was REML and the Residual Variance Method was profile. The Kenward-Roger method was used for both Fixed Effects SE and Degrees of Freedom. Date was coded as a numerical value for each analysis. Level 1 was October 2018-November 2018, 2 was November 2018-December 2018, 3 was December 2018-January 2019, 4 was January 2019-February 2019, 5 was February 2019-March 2019, 6 was March 2019-April 2019, 7 was April 2019-May 2019, 8 was May

2019-June 2019, 9 was June 2019-July 2019, 10 was July 2019-August 2019, 11 was August 2019-September 2019, and 12 was September 2019-October 2019.

It should be noted that Hydrogen and Helium were unable to be observed with the electron spectrometer due to the absence of core electrons and the presence of only valence electrons (Stojilovic, 2012). The units reported by the x-ray spectrometer for elemental composition were in mass percentage.

Summary Statistics for Si

Table 5. Arithmetic mean, standard deviation, minimum and maximum of Si sampled across seven sites over a twelve-month period. Four subsamples were collected per sample. One sample was collected per site per month. Six of the seven sampling sites are in Stephen F. Austin University Real Estate Foundation's STMicroelectronics carbon sequestration project and one sampling site is located at SFA's Beef Farm.

| Date Range | Mass Percentage of Si | | | |
|---------------------|-----------------------|--------------------|---------|---------|
| | Arithmetic Mean | Standard Deviation | Minimum | Maximum |
| Oct 2018-Nov 2018 | 48.37 | 2.87 | 41.11 | 51.75 |
| Nov 2018-Dec 2018 | 44.85 | 4.40 | 30.07 | 55.50 |
| Dec 2018-Jan 2019 | 47.35 | 4.04 | 27.36 | 57.86 |
| Jan 2019-Feb 2019 | 41.97 | 2.76 | 30.46 | 51.72 |
| Feb 2019-Mar 2019 | 21.94 | 3.59 | 5.52 | 44.55 |
| Mar 2019-Apr 2019 | 34.80 | 4.08 | 17.05 | 42.25 |
| Apr 2019-May 2019 | 41.57 | 4.61 | 28.73 | 56.39 |
| May 2019-June 2019 | 41.04 | 3.39 | 29.68 | 51.70 |
| June 2019-July 2019 | 43.60 | 3.43 | 28.34 | 52.85 |
| July 2019-Aug 2019 | 43.37 | 4.64 | 31.19 | 53.40 |
| Aug 2019-Sep 2019 | 43.65 | 2.97 | 35.10 | 50.50 |
| Sep 2019-Oct 2019 | 29.09 | 2.33 | 22.71 | 34.09 |

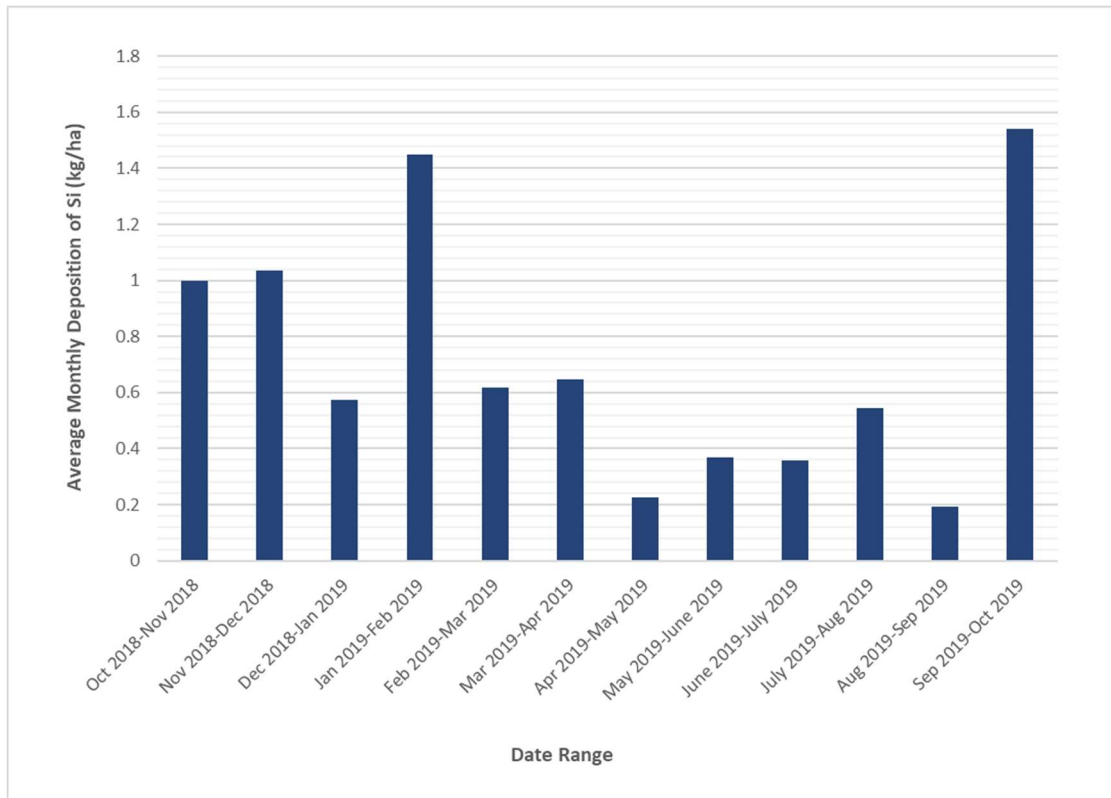


Figure 12. Arithmetic mean of Si in kg/ha sampled across seven sites over a twelve-month period. Four subsamples were collected per sample. One sample was collected per site per month. Six of the seven sampling sites are in Stephen F. Austin University Real Estate Foundation’s STMicroelectronics carbon sequestration project and one sampling site is located at SFA’s Beef Farm.

Mixed Model for Si

The model for Si is $Si = m + \text{Location} + \text{Plot}(\text{Location}) + \text{Time}$ where Time was the coded date range of the sample, Location was the property the sample was taken at, sample was the filter, Si was the Si concentration in mass percent for each subsample, and Subsample was the sample taken from the filter. The dependent variable in this model is Si, and there were three independent variables or classes: location, plot, and

time. Location had seven levels: one for each property in the study. Plot had four levels: one for each subsample of the filter. Time had 12 values. The AR(1) Covariance Parameter Estimate was 0.03288. Location was found to be significant at <0.0001 Pr>F. Plot(Location) was not found to be significant at 0.5236. Time was found to be significant at <0.0001 Pr>F. The interaction between Location and Time was found to be significant at <0.0001 Pr>F. Si deposition was recorded at a monthly range of 0.1939 kg/ha – 1.5393 kg/ha and had a yearly total of 8.5582 kg/ha deposition (Figure 12). There was a decrease in Si deposition in kg/ha from April to July, but the mass percentage of Si increased during these months, indicating a higher concentration of mineral matter (Figure 12, Table 5, and Table 19). This could be due to higher temperatures drying the soils and making them more susceptible to abrasion.

Cattle hair was observed to contain Si, but Si also has a correlation with soil particles (Washburn et al., 1958). Higher levels of Si are associated with different clay and primary minerals present in soils that release Si during chemical weathering (Makabe et al., 2009). This could indicate higher levels of mineral deposition during periods with high mass percentages of Si. However, since the filter was also made of Si composite, this data was likely influenced by the large percent of Si in the filter. Si appeared to remain stable with little fluctuation aside from two low peaks in February 2019-March 2019 and September 2019-October 2019.

Summary Statistics for O

Table 6. Arithmetic mean, standard deviation, minimum and maximum of O sampled across seven sites over a twelve-month period. Four subsamples were collected per sample. One sample was collected per site per month. Six of the seven sampling sites are in Stephen F. Austin University Real Estate Foundation’s STMicroelectronics carbon sequestration project and one sampling site is located at SFA’s Beef Farm.

| Date Range | Mass Percentage of O | | | |
|---------------------|----------------------|--------------------|---------|---------|
| | Arithmetic Mean | Standard Deviation | Minimum | Maximum |
| Oct 2018-Nov 2018 | 32.02 | 1.72 | 27.79 | 37.93 |
| Nov 2018-Dec 2018 | 32.77 | 3.19 | 27.41 | 41.67 |
| Dec 2018-Jan 2019 | 30.58 | 1.85 | 23.17 | 36.82 |
| Jan 2019-Feb 2019 | 28.27 | 1.56 | 21.11 | 32.54 |
| Feb 2019-Mar 2019 | 29.86 | 4.20 | 13.45 | 48.45 |
| Mar 2019-Apr 2019 | 29.70 | 1.74 | 20.61 | 38.59 |
| Apr 2019-May 2019 | 28.38 | 1.85 | 23.73 | 38.03 |
| May 2019-June 2019 | 28.12 | 1.42 | 22.40 | 33.18 |
| June 2019-July 2019 | 30.49 | 1.62 | 24.71 | 34.11 |
| July 2019-Aug 2019 | 30.11 | 1.79 | 25.92 | 34.70 |
| Aug 2019-Sep 2019 | 29.46 | 1.36 | 26.76 | 33.54 |
| Sep 2019-Oct 2019 | 33.17 | 1.66 | 29.54 | 37.96 |

Repeated Mixed Model for O

The model for O is $O = \mu + \text{Location} + \text{Plot}(\text{Location}) + \text{Time}$ where Time was the coded date range of the sample, Location was the property the sample was taken at, sample was the filter, O was the O concentration in mass percent for each subsample, and Subsample was the sample taken from the filter. The dependent variable in this model is Ca, and there were three independent variables or classes: location, plot, and time. Location had seven levels: one for each property in the study. Plot had four levels: one for each subsample of the filter. Time had 12 levels. The AR(1) Covariance Parameter Estimate was -0.03234, indicating next year’s data should reflect values less than this

year. Location was found to be significant at <0.0001 Pr>F. Plot(Location) was not found to be significant at 0.6348. Time was found to be significant at <0.0001 Pr>F. The interaction between Location and Time was found to be significant at <0.0001 Pr>F. Since the subsamples were briefly exposed to air, this data was likely influenced by O absorbed by the filter rather than O deposition. The average O of all seven sites appears to remain stable with some small fluctuation aside from two high peaks in October 2018-November 2018 and February 2019-March 2019 (Table 6 and Table 20). However there is a great variance between sites, which may indicate environmental factors such as a greater concentration of pollen or anthropogenic factors such as pollution if the O is combined with another element like N or S, neither of which were observed in this investigation.

Pollen spores could be a source of O in these samples due to the O present in the sporopollenin, cytoplasm, and pectin of the microspore (University of Bern, 2003). All three of these components are composed of C, H, and O (University of Bern, 2003). Since the outermost cell wall (exine) of the microspore is very high in sporopollenin, which encases the spore and is largely resistant to organic acid and alkaline inputs, its inert chemical makeup could have been preserved (University of Bern, 2003).

Summary Statistics for C

Table 7. Arithmetic mean, standard deviation, minimum and maximum of C sampled across seven sites over a twelve-month period. Four subsamples were collected per sample. One sample was collected per site per month. Six of the seven sampling sites are in Stephen F. Austin University Real Estate Foundation’s STMicroelectronics carbon sequestration project and one sampling site is located at SFA’s Beef Farm.

| Date Range | Mass Percentage of C | | | |
|---------------------|----------------------|--------------------|---------|---------|
| | Arithmetic Mean | Standard Deviation | Minimum | Maximum |
| Oct 2018-Nov 2018 | 6.85 | 0.16 | 0.00 | 10.06 |
| Nov 2018-Dec 2018 | 11.73 | 0.48 | 6.04 | 23.88 |
| Dec 2018-Jan 2019 | 4.66 | 0.96 | 0.00 | 18.84 |
| Jan 2019-Feb 2019 | 7.97 | 0.60 | 0.00 | 16.60 |
| Feb 2019-Mar 2019 | 24.33 | 6.26 | 9.44 | 59.37 |
| Mar 2019-Apr 2019 | 12.10 | 2.89 | 7.53 | 35.58 |
| Apr 2019-May 2019 | 6.95 | 0.19 | 0.00 | 14.15 |
| May 2019-June 2019 | 4.91 | 0.20 | 0.00 | 10.06 |
| June 2019-July 2019 | 5.84 | 1.52 | 0.00 | 17.27 |
| July 2019-Aug 2019 | 8.11 | 2.20 | 4.07 | 16.56 |
| Aug 2019-Sep 2019 | 5.90 | 1.01 | 3.52 | 12.43 |
| Sep 2019-Oct 2019 | 7.13 | 0.70 | 5.09 | 13.66 |

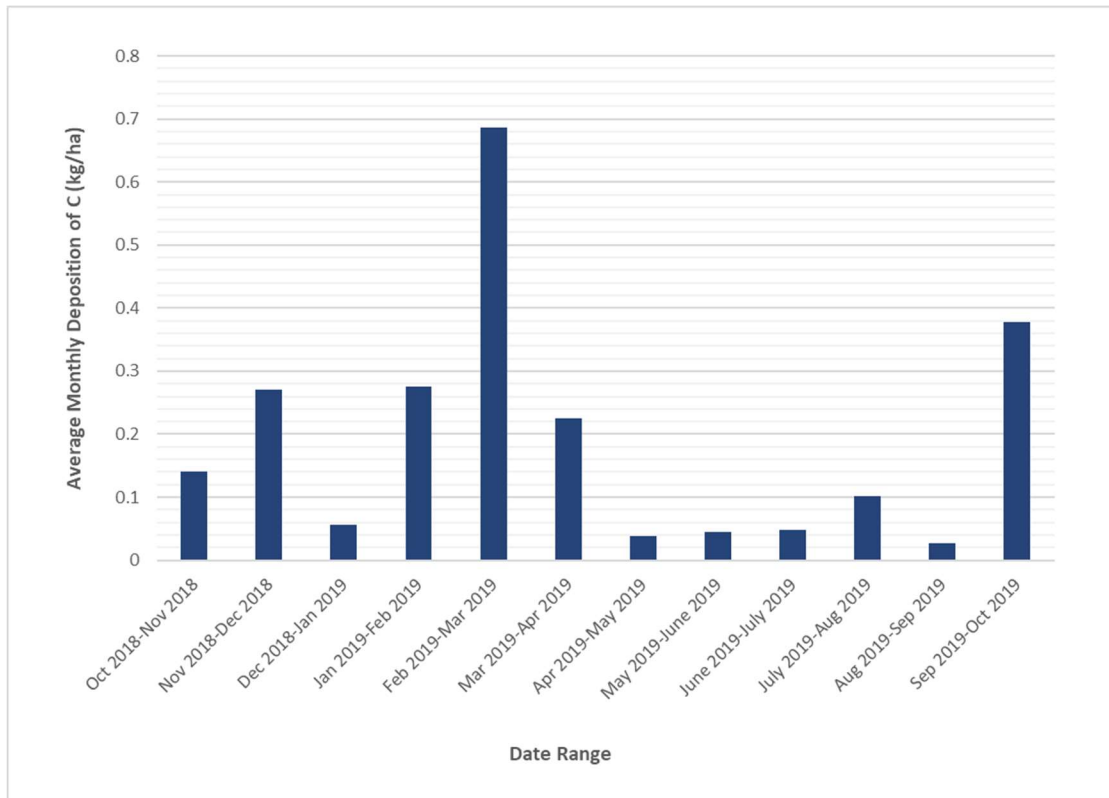


Figure 13. C in kg/ha sampled across seven sites over a twelve-month period. Four subsamples were collected per sample. One sample was collected per site per month. Six of the seven sampling sites are in Stephen F. Austin University Real Estate Foundation’s STMicroelectronics carbon sequestration project and one sampling site is located at SFA’s Beef Farm.

Repeated Mixed Model for C

The model for C is $C = m + \text{Location} + \text{Plot}(\text{Location}) + \text{Time}$ where Time was the coded date range of the sample, Location was the property the sample was taken at, sample was the filter, C was the C concentration in mass percent for each subsample, and Plot was the sample taken from the filter. The dependent variable in this model is C, and there were three independent variables or classes: location, plot, and time. Location had seven levels: one for each property in the study. Plot had four levels: one for each

subsample of the filter. Time had 12 levels. Level 1 was October 2018-November 2018, 2 was November 2018-December 2018, 3 was December 2018-January 2019, 4 was January 2019-February 2019, 5 was February 2019-March 2019, 6 was March 2019-April 2019, 7 was April 2019-May 2019, 8 was May 2019-June 2019, 9 was June 2019-July 2019, 10 was July 2019-August 2019, 11 was August 2019-September 2019, and 12 was September 2019-October 2019. The AR(1) Covariance Parameter Estimate was 0.08013. Location was found to be significant at <0.0001 Pr>F. Plot(Location) was not found to be significant at 0.2438. Time was found to be significant at <0.0001 Pr>F. The interaction between Location and Time was found to be significant at <0.0001 Pr>F. C deposition was recorded at a monthly range of 0.0262 kg/ha – 0.6871 kg/ha and had a yearly total of 2.2923 kg/ha deposition (Table 33). C deposition appears to increase drastically during months with traditionally high pollen counts (Table 7, Table 21, Figure 13 and Houston Health Department, 2019).

Pollen spores as well as CO₂ could have been sources of C in these samples due to CO₂ in the surrounding atmosphere and C present in sporopollenin, cytoplasm, and the pectin of microspores (University of Bern, 2003). All three of these components are made of C, H, and O (University of Bern, 2003). Since the outermost cell wall (exine) of the microspore is very high in sporopollenin, which encases the spore and is largely resistant to organic acid and alkaline inputs, its inert chemical makeup could have been preserved (University of Bern, 2003). Additional evidence that points to pollen being a

source of C deposition is the pollen jump observed between February-April, when pollen was observed to be very high at the seven sites.

Summary Statistics for Ba

Table 8. Arithmetic mean, standard deviation, minimum and maximum of Ba sampled across seven sites over a twelve-month period. Four subsamples were collected per sample. One sample was collected per site per month. Six of the seven sampling sites are in Stephen F. Austin University Real Estate Foundation's STMicroelectronics carbon sequestration project and one sampling site is located at SFA's Beef Farm.

| Date Range | Mass Percentage of Ba | | | |
|---------------------|-----------------------|--------------------|---------|---------|
| | Arithmetic Mean | Standard Deviation | Minimum | Maximum |
| Oct 2018-Nov 2018 | 8.12 | 1.77 | 0.00 | 13.60 |
| Nov 2018-Dec 2018 | 5.16 | 4.22 | 0.00 | 10.76 |
| Dec 2018-Jan 2019 | 8.40 | 2.37 | 0.00 | 11.86 |
| Jan 2019-Feb 2019 | 7.46 | 0.81 | 4.93 | 9.98 |
| Feb 2019-Mar 2019 | 3.91 | 0.85 | 0.00 | 7.80 |
| Mar 2019-Apr 2019 | 6.01 | 1.17 | 0.00 | 7.75 |
| Apr 2019-May 2019 | 6.98 | 2.10 | 0.00 | 11.03 |
| May 2019-June 2019 | 5.67 | 2.58 | 0.00 | 10.28 |
| June 2019-July 2019 | 6.65 | 3.06 | 0.00 | 12.78 |
| July 2019-Aug 2019 | 7.00 | 3.76 | 0.00 | 11.07 |
| Aug 2019-Sep 2019 | 9.16 | 0.66 | 6.38 | 10.76 |
| Sep 2019-Oct 2019 | 5.64 | 0.63 | 3.84 | 7.19 |

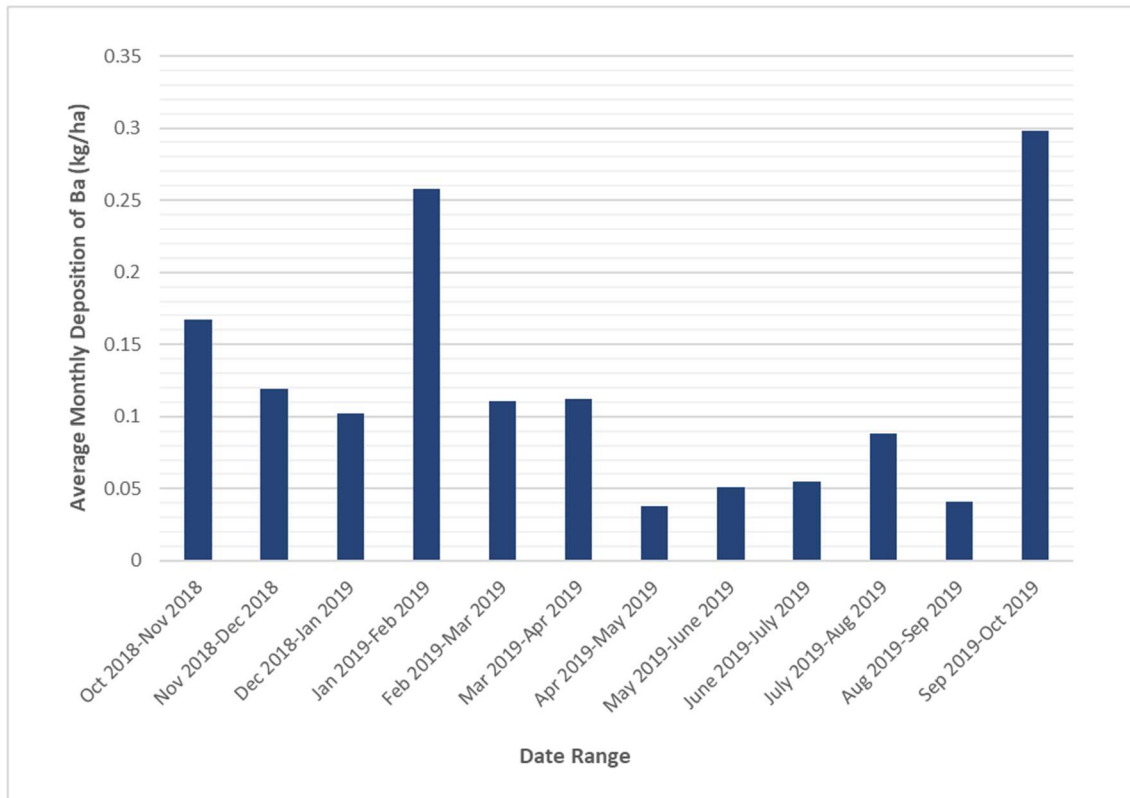


Figure 14. Ba in kg/ha sampled across seven sites over a twelve-month period. Four subsamples were collected per sample. One sample was collected per site per month. Six of the seven sampling sites are in Stephen F. Austin University Real Estate Foundation’s STMicroelectronics carbon sequestration project and one sampling site is located at SFA’s Beef Farm.

Repeated Mixed Model for Ba

The model for Ba is $Ba = m + \text{Location} + \text{Plot}(\text{Location}) + \text{Time}$ where Time was the coded date range of the sample, Location was the property the sample was taken at, sample was the filter, Ba was the Ba concentration in mass percent for each subsample, and Subsample was the sample taken from the filter. The dependent variable in this model is Ba, and there were three independent variables or classes: location, plot, and time. Location had seven levels: one for each property in the study. Plot had four levels:

one for each subsample of the filter. Time had 12 levels. The AR(1) Covariance Parameter Estimate was 0.03444. Location was found to be significant at 0.0097 Pr>F. Plot(Location) was not found to be significant at 0.6545. Time was found to be significant at <0.0001 Pr>F. The interaction between Location and Time was found to be significant at <0.0001 Pr>F. Ba deposition was recorded at a monthly range of 0.0380 kg/ha – 0.2984 kg/ha and had a yearly total of 1.43942 kg/ha deposition (Table 33). Ba is present in soils within and surrounding East Texas and appears higher throughout months with more total deposition (Table 4, Figure 14, and USGS, 1984). However, Ba makes up a larger mass percentage of the sample from June 2019-September 2019, which may indicate a higher mineral content during these months (Table 8 and Figure 14).

Hilliard, Arbor Grove, and Atoy displayed the highest values for Ba content so Ba content appeared to be influenced by a variety of factors other than longitude location. Average Ba content was high in October 2018-November 2018, then its content gradually decreased until it reached its lowest point in February 2019-March 2019 (Table 8 and Table 22). Then it peaked in March-April before gradually increasing from the level of February 2019-March 2019 (Table 8 and Table 22). This indicates that periods of temperature extremes or low moisture content could increase the amount of Ba observed in deposition. Periods of low moisture content would be ideal for mineral deposition since the soils would be dry and less cohesive. If a high wind occurs or calm winds consistently occur, this could move particulates easily across some landscapes.

It was noted that the Agriculture Center consistently reported high amounts of Ba in comparison to the other sites. This may have been influenced by the presence of cattle. Cattle are known to have Ba in the chemical composition of their hair, and it is possible that some of this shed hair blew into the sampler (Washburn et al., 1958).

Summary Statistics for Na

Table 9. Arithmetic mean, standard deviation, minimum and maximum of Na sampled across seven sites over a twelve-month period. Four subsamples were collected per sample. One sample was collected per site per month. Six of the seven sampling sites are in Stephen F. Austin University Real Estate Foundation's STMicroelectronics carbon sequestration project and one sampling site is located at SFA's Beef Farm.

| Date Range | Mass Percentage of Na | | | |
|---------------------|-----------------------|--------------------|---------|---------|
| | Arithmetic Mean | Standard Deviation | Minimum | Maximum |
| Oct 2018-Nov 2018 | 7.16 | 0.85 | 1.49 | 9.53 |
| Nov 2018-Dec 2018 | 6.74 | 1.59 | 0.00 | 9.14 |
| Dec 2018-Jan 2019 | 7.21 | 0.72 | 4.07 | 8.94 |
| Jan 2019-Feb 2019 | 6.32 | 0.66 | 3.04 | 8.66 |
| Feb 2019-Mar 2019 | 3.98 | 0.92 | 0.00 | 6.81 |
| Mar 2019-Apr 2019 | 5.91 | 0.97 | 2.63 | 7.81 |
| Apr 2019-May 2019 | 6.97 | 0.98 | 5.11 | 8.98 |
| May 2019-June 2019 | 6.78 | 1.24 | 4.47 | 10.63 |
| June 2019-July 2019 | 6.87 | 0.67 | 3.20 | 9.10 |
| July 2019-Aug 2019 | 6.83 | 0.92 | 5.11 | 9.20 |
| Aug 2019-Sep 2019 | 7.43 | 0.69 | 4.86 | 10.33 |
| Sep 2019-Oct 2019 | 6.84 | 0.71 | 5.37 | 8.80 |

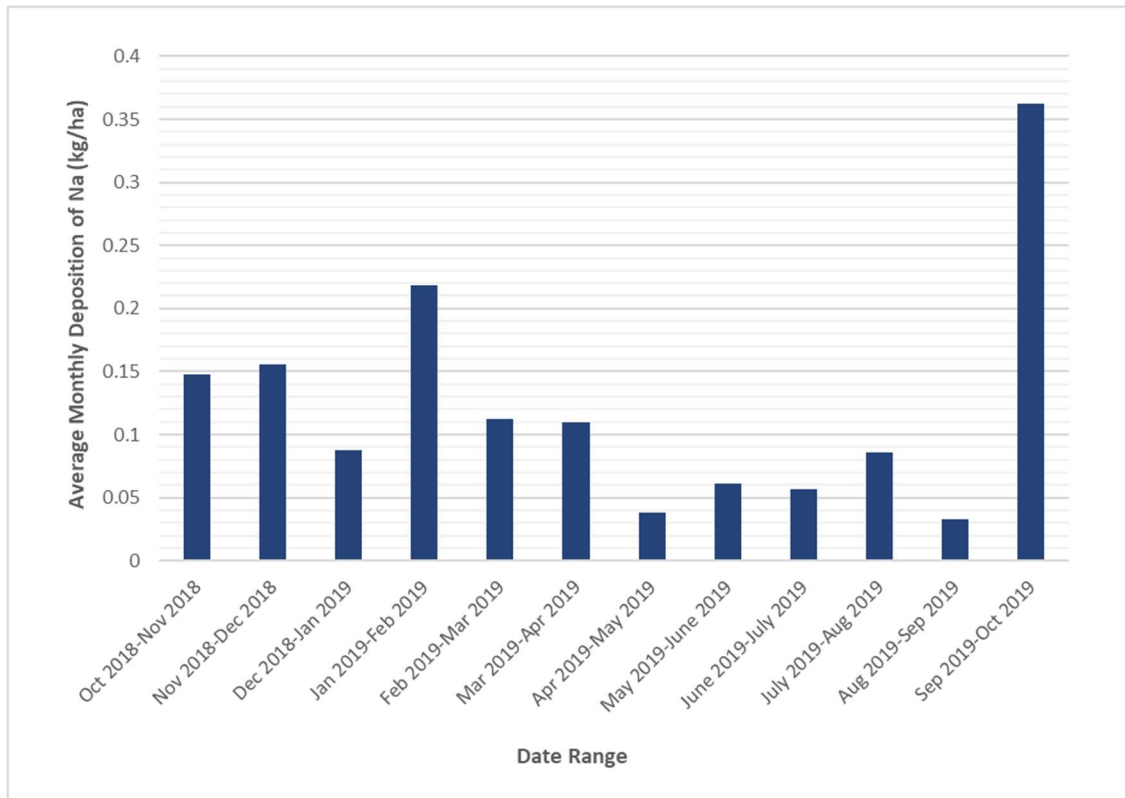


Figure 15. Arithmetic mean of Na in kg/ha sampled across seven sites over a twelve-month period. Four subsamples were collected per sample. One sample was collected per site per month. Six of the seven sampling sites are in Stephen F. Austin University Real Estate Foundation’s STMicroelectronics carbon sequestration project and one sampling site is located at SFA’s Beef Farm.

Repeated Mixed Model for Na

The model for Na is $Na = m + Location + Plot(Location) + Time$ where Time was the coded date range of the sample, Location was the property the sample was taken at, sample was the filter, Na was the Na concentration in mass percent for each subsample, and Subsample was the sample taken from the filter. The dependent variable in this model is Na, and there were three independent variables or classes: location, plot, and time. Location had seven levels: one for each property in the study. Plot had four levels:

one for each subsample of the filter. Time had 12 levels. The AR(1) Covariance Parameter Estimate was -0.02386. Location was found to be significant at <0.0001 Pr>F. Plot(Location) was not found to be significant at 0.2674. Time was found to be significant at <0.0001 Pr>F. The interaction between Location and Time was found to be significant at <0.0001 Pr>F. Na deposition was recorded at a monthly range of 0.0330 kg/ha – 0.3619 kg/ha and had a yearly total of 1.4679 kg/ha deposition (Table 33). Na is present in soils within and surrounding East Texas (USGS, 1984). Although the overall deposition is low in April 2019 - Sept 2019, Na mass percentage of the sample is fairly high, which may indicate higher percentages of mineral deposition during these months (Table 9 and Figure 15).

Average Na content was high in October 2018, then its content gradually decreased until it reached its lowest point in February 2019-March 2019 (Table 9 and Table 23). Then it peaked in March-April before gradually increasing from the levels of February 2019-March 2019 (Table 9 and Table 23). This indicates that periods of temperature extremes or low moisture content could increase the amount of Na content observed in deposition. Winter and Summer would be ideal times for mineral deposition to occur since the soils would dry and become less cohesive. If a high wind occurs or calm winds consistently occur, this could move particulates easily across some landscapes.

It was noted that the Agriculture Center consistently reported high amounts of Na in comparison to the other sites. This may have been influenced by the presence of cattle.

Cattle are known to have Na in the chemical composition of their hair, and it is possible that some of this shed hair blew into the sampler (Washburn et al., 1958).

Summary Statistics for Al

Table 10. Arithmetic mean, standard deviation, minimum and maximum of Al sampled across seven sites over a twelve-month period. Four subsamples were collected per sample. One sample was collected per site per month. Six of the seven sampling sites are in Stephen F. Austin University Real Estate Foundation’s STMicroelectronics carbon sequestration project and one sampling site is located at SFA’s Beef Farm.

| Date Range | Mass Percentage of Al | | | |
|---------------------|-----------------------|--------------------|---------|---------|
| | Arithmetic Mean | Standard Deviation | Minimum | Maximum |
| Oct 2018-Nov 2018 | 3.79 | 0.61 | 3.00 | 4.34 |
| Nov 2018-Dec 2018 | 3.21 | 0.95 | 1.92 | 4.06 |
| Dec 2018-Jan 2019 | 3.41 | 0.78 | 2.37 | 4.08 |
| Jan 2019-Feb 2019 | 3.70 | 0.49 | 3.11 | 4.27 |
| Feb 2019-Mar 2019 | 2.29 | 0.49 | 1.88 | 2.96 |
| Mar 2019-Apr 2019 | 3.10 | 0.49 | 2.54 | 3.65 |
| Apr 2019-May 2019 | 3.37 | 0.72 | 2.39 | 4.04 |
| May 2019-June 2019 | 2.59 | 0.91 | 1.81 | 3.74 |
| June 2019-July 2019 | 3.23 | 0.76 | 2.42 | 4.03 |
| July 2019-Aug 2019 | 3.45 | 0.42 | 3.01 | 3.91 |
| Aug 2019-Sep 2019 | 3.54 | 0.39 | 3.13 | 4.04 |
| Sep 2019-Oct 2019 | 3.17 | 0.43 | 2.75 | 3.69 |

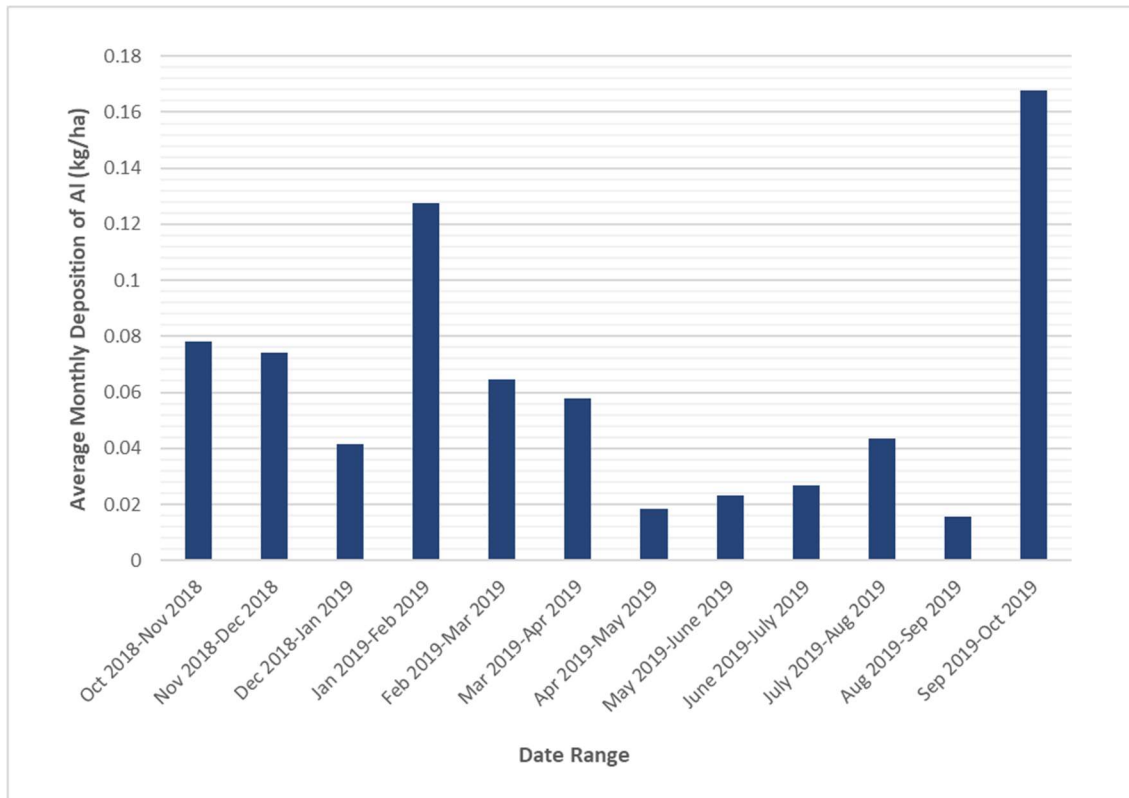


Figure 16. Arithmetic mean of Al in kg/ha sampled across seven sites over a twelve-month period. Four subsamples were collected per sample. One sample was collected per site per month. Six of the seven sampling sites are in Stephen F. Austin University Real Estate Foundation’s STMicroelectronics carbon sequestration project and one sampling site is located at SFA’s Beef Farm.

Repeated Mixed Model for Al

The model for Al is $Al = m + Location + Plot(Location) + Time$ where Time was the coded date range of the sample, Location was the property the sample was taken at, sample was the filter, Al was the Al concentration in mass percent for each subsample, and Subsample was the sample taken from the filter. The dependent variable in this model is Al, and there were three independent variables or classes: location, plot, and

time. Location had seven levels: one for each property in the study. Plot had four levels: one for each subsample of the filter. Time had 12 levels. The AR(1) Covariance Parameter Estimate was 0.07981. Location was found to be significant at 0.0123 Pr>F. Plot(Location) was not found to be significant at 0.3150. Time was found to be significant at <0.0001 Pr>F. The interaction between Location and Time was found to be significant at <0.0001 Pr>F. Al deposition was recorded at a monthly range of 0.0157 kg/ha – 0.1676 kg/ha and had a yearly total of 0.7389 kg/ha deposition (Table 33). Al is present in soils within and surrounding East Texas (USGS, 1984). Although the overall deposition is low in April 2019 - Sept 2019, Al mass percentage of the sample is fairly high, which may indicate higher percentages of mineral deposition during these months (Table 10 and Figure 16).

Swink exhibited a higher arithmetic mean of Al content than the other properties did throughout the year. This could be due to various unpaved areas across the property that allowed people to drive through. Unlike many of the other properties, this unpaved area was expansive, and a small body of water served as the primary depositional barrier between the road and the sampler. Peaks in Al appear to occur between October-January, March-June, and August-October (Table 10 and Table 24). This indicates that periods of temperature extremes or low moisture content could increase the amount of Al content observed in deposition. Winter and Summer would be ideal times for mineral deposition to occur since the soils would dry and become less cohesive. If a high wind occurs or

calm winds consistently occur, this could move particulates easily across some landscapes.

Summary Statistics for K

Table 11. Arithmetic mean, standard deviation, minimum and maximum of K sampled across seven sites over a twelve-month period. Four subsamples were collected per sample. One sample was collected per site per month. Six of the seven sampling sites are in Stephen F. Austin University Real Estate Foundation’s STMicroelectronics carbon sequestration project and one sampling site is located at SFA’s Beef Farm.

| Date Range | Mass Percentage of K | | | |
|---------------------|----------------------|--------------------|---------|---------|
| | Arithmetic Mean | Standard Deviation | Minimum | Maximum |
| Oct 2018-Nov 2018 | 4.09 | 0.42 | 2.32 | 5.99 |
| Nov 2018-Dec 2018 | 3.06 | 0.95 | 0.00 | 4.79 |
| Dec 2018-Jan 2019 | 3.47 | 0.56 | 0.00 | 4.19 |
| Jan 2019-Feb 2019 | 4.04 | 0.37 | 2.71 | 5.50 |
| Feb 2019-Mar 2019 | 2.37 | 0.43 | 0.00 | 4.40 |
| Mar 2019-Apr 2019 | 3.40 | 0.44 | 1.60 | 5.14 |
| Apr 2019-May 2019 | 4.13 | 0.47 | 2.79 | 6.23 |
| May 2019-June 2019 | 3.59 | 0.80 | 0.00 | 5.65 |
| June 2019-July 2019 | 3.76 | 0.38 | 2.23 | 5.21 |
| July 2019-Aug 2019 | 3.30 | 0.73 | 0.00 | 5.12 |
| Aug 2019-Sep 2019 | 4.28 | 0.26 | 3.51 | 4.92 |
| Sep 2019-Oct 2019 | 3.24 | 0.19 | 2.70 | 3.74 |

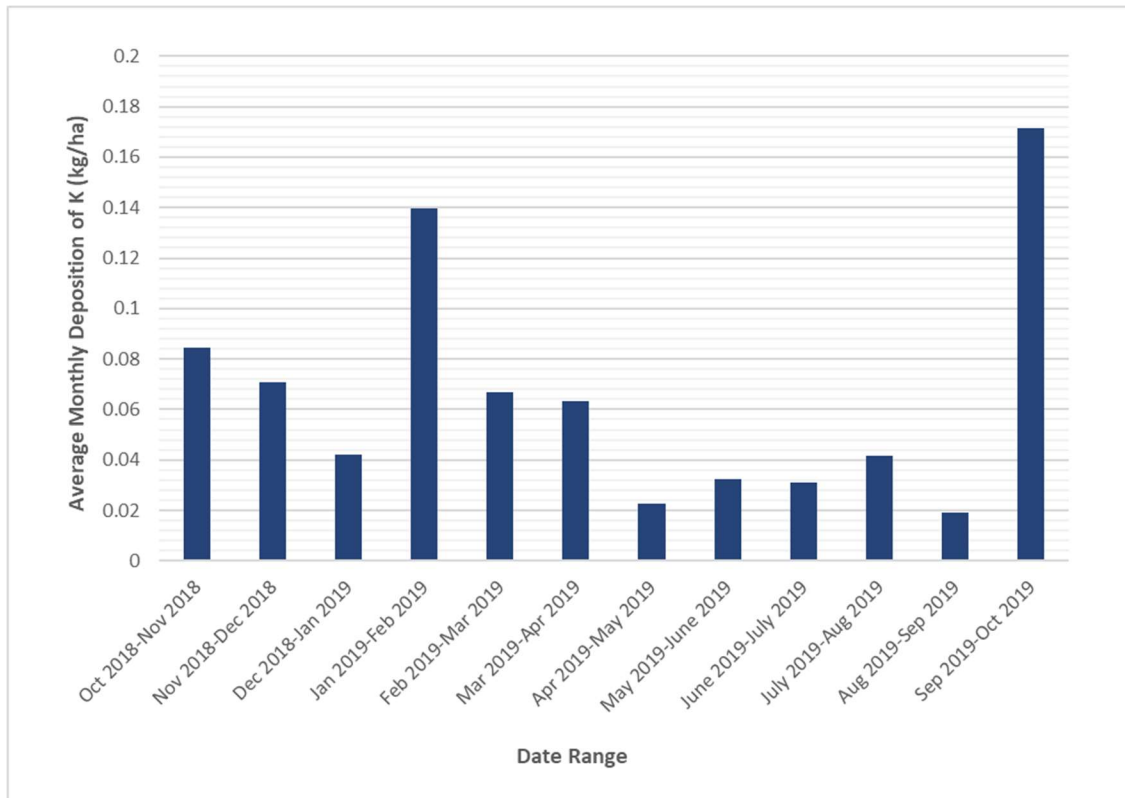


Figure 17. Arithmetic mean of K in kg/ha sampled across seven sites over a twelve-month period. Four subsamples were collected per sample. One sample was collected per site per month. Six of the seven sampling sites are in Stephen F. Austin University Real Estate Foundation’s STMicroelectronics carbon sequestration project and one sampling site is located at SFA’s Beef Farm.

Repeated Mixed Model for K

The model for K is $K = m + \text{Location} + \text{Plot}(\text{Location}) + \text{Time}$ where Time was the coded date range of the sample, Location was the property the sample was taken at, sample was the filter, K was the K concentration in mass percent for each subsample, and Subsample was the sample taken from the filter. The dependent variable in this model is K, and there were three independent variables or classes: location, plot, and time.

Location had seven levels: one for each property in the study. Plot had four levels: one

for each subsample of the filter. Time had 12 levels. The AR(1) Covariance Parameter Estimate was -0.1418. Location was found to be significant at <0.0001 Pr>F. Plot(Location) was not found to be significant at 0.4115. Time was found to be significant at <0.0001 Pr>F. The interaction between Location and Time was found to be significant at <0.0001 Pr>F. K deposition was recorded at a monthly range of 0.0190 kg/ha – 0.1714 kg/ha and had a yearly total of 0.7846 kg/ha deposition (Table 33).

K is present in soils within and surrounding East Texas so there may be a link between periods of low mineral deposition and periods of low K deposition (USGS, 1984). Low mass percentages of K deposition occurred between November 2018-December 2018 and February 2019-March 2019, while low periods of K deposition in kg/ha occurred during periods of low overall deposition (Table 11, Table 25 and Figure 17). This could be due to poor sediment transport during this time period. However, the arithmetic mean of K between sites remained very consistent over the twelve sampling months.

It was noted that the Agriculture Center consistently reported high amounts of K in comparison to the other sites. This may have been influenced by the presence of cattle. Cattle are known to have K in the chemical composition of their hair, and it is possible that some of this shed hair blew into the sampler (Washburn et al., 1958).

Summary Statistics for Ca

Table 12. Arithmetic mean, standard deviation, minimum and maximum of Ca sampled across seven sites over a twelve-month period. Four subsamples were collected per sample. One sample was collected per site per month. Six of the seven sampling sites are in Stephen F. Austin University Real Estate Foundation's STMicroelectronics carbon sequestration project and one sampling site is located at SFA's Beef Farm.

| Date Range | Mass Percentage of Ca | | | |
|---------------------|-----------------------|--------------------|---------|---------|
| | Arithmetic Mean | Standard Deviation | Minimum | Maximum |
| Oct 2018-Nov 2018 | 2.04 | 0.25 | 0.00 | 3.93 |
| Nov 2018-Dec 2018 | 0.41 | 0.64 | 0.00 | 2.72 |
| Dec 2018-Jan 2019 | 0.18 | 0.20 | 0.00 | 2.59 |
| Jan 2019-Feb 2019 | 2.00 | 0.46 | 0.00 | 3.00 |
| Feb 2019-Mar 2019 | 1.01 | 0.46 | 0.00 | 2.42 |
| Mar 2019-Apr 2019 | 1.42 | 0.69 | 0.00 | 2.63 |
| Apr 2019-May 2019 | 1.36 | 0.62 | 0.00 | 2.81 |
| May 2019-June 2019 | 0.65 | 0.44 | 0.00 | 2.89 |
| June 2019-July 2019 | 1.30 | 0.29 | 0.00 | 2.84 |
| July 2019-Aug 2019 | 0.46 | 0.77 | 0.00 | 2.72 |
| Aug 2019-Sep 2019 | 2.56 | 0.17 | 2.08 | 3.10 |
| Sep 2019-Oct 2019 | 1.81 | 0.11 | 1.49 | 2.19 |

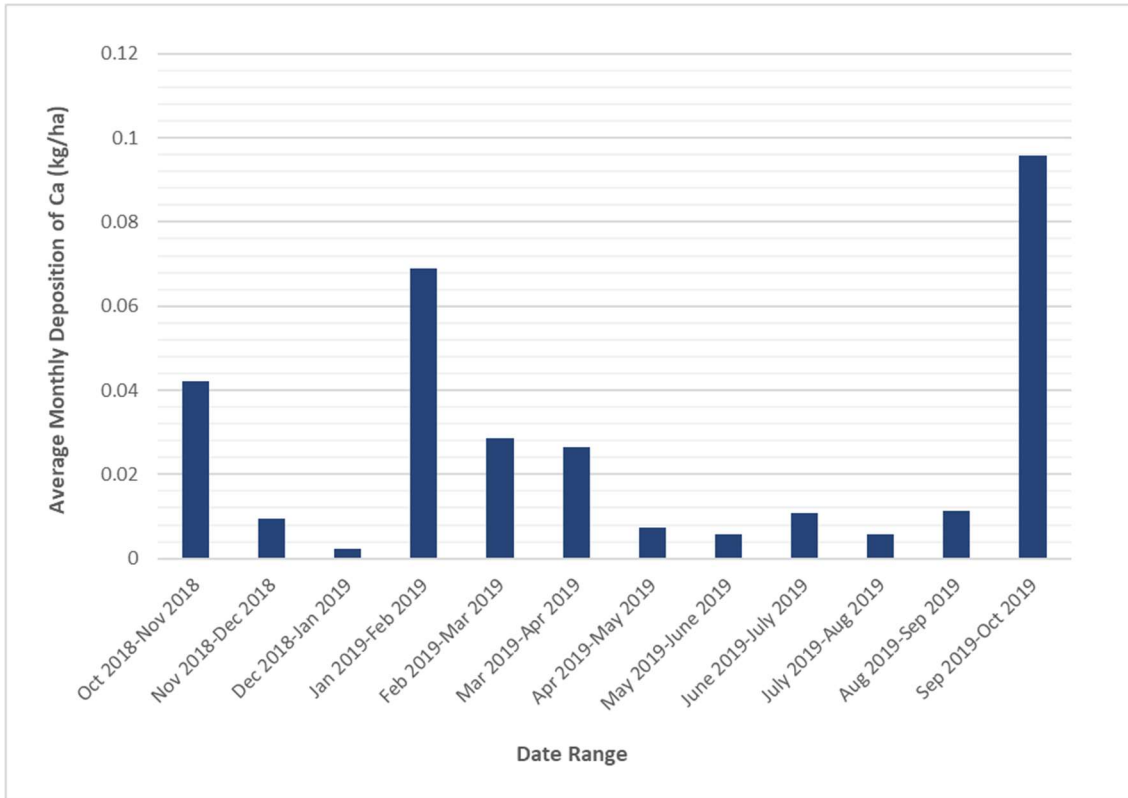


Figure 18. Arithmetic mean of Ca in kg/ha sampled across seven sites over a twelve-month period. Four subsamples were collected per sample. One sample was collected per site per month. Six of the seven sampling sites are in Stephen F. Austin University Real Estate Foundation’s STMicroelectronics carbon sequestration project and one sampling site is located at SFA’s Beef Farm.

Repeated Mixed Model for Ca

The model for Ca is $Ca = m + \text{Location} + \text{Plot}(\text{Location}) + \text{Time}$ where Time was the coded date range of the sample, Location was the property the sample was taken at, sample was the filter, Ca was the Ca concentration in mass percent for each subsample, and Subsample was the sample taken from the filter. The dependent variable in this model is Ca, and there were three independent variables or classes: location, plot, and time. Location had seven levels: one for each property in the study. Plot had four levels: one for each subsample of the filter. Time had 12 levels. The AR(1) Covariance Parameter Estimate was -0.02459. Location was found to be significant at $<0.0001 \text{ Pr}>F$. Plot(Location) was not found to be significant at 0.9948. Time was found to be significant at $<0.0001 \text{ Pr}>F$. The interaction between Location and Time was found to be significant at $<0.0001 \text{ Pr}>F$. Ca deposition was recorded at a monthly range of 0.0022 kg/ha – 0.0958 kg/ha and had a yearly total of 0.3146 kg/ha deposition (Table 33). There was an increase in both mass percentage of Ca and total deposition in kg/ha during the months of January 2019-April 2019 and September 2019-October 2019 (Table 12, Table 26 and Figure 18).

This Ca deposition may have been influenced by a CaCO_3 influx from the North or West (USGS, 1984 and Table 32). This may have influenced the productivity of surrounding soils by changing the pH over time and influencing the nutrient availability (Tsakelidou, 2008). Although the winds primarily blew from the south/southeast throughout the year, some months displayed winds blowing from the northwest (Figure

20 and Table 32). These months yielded a substantial amount of Ca and may have been influenced by the calcareous soils of central Texas (Johnston, 2010).

Ca deposition is present throughout most of the year, but it appears to peak with late summer and fall temperatures such as those between August and November. This would be an ideal time for mineral deposition to occur since the soils would dry and become less cohesive. If high winds or calm winds consistently occur, this could move particulates, such as Ca rich soil particles from Oklahoma, Central Texas, and West Texas, into East Texas forested regions and eventually cause a liming effect over time.

It was noted that the Agriculture Center consistently reported high amounts of Ca in comparison to the other sites. This may have been influenced by the presence of cattle. Cattle are known to have Ca in the chemical composition of their hair, and it is possible that some of this shed hair blew into the sampler (Washburn et al., 1958).

Summary Statistics for Zn

Table 13. Arithmetic mean, standard deviation, minimum and maximum of Zn sampled across seven sites over a twelve-month period. Four subsamples were collected per sample. One sample was collected per site per month. Six of the seven sampling sites are in Stephen F. Austin University Real Estate Foundation’s STMicroelectronics carbon sequestration project and one sampling site is located at SFA’s Beef Farm.

| Date Range | Mass Percentage of Zn | | | |
|---------------------|-----------------------|--------------------|---------|---------|
| | Arithmetic Mean | Standard Deviation | Minimum | Maximum |
| Oct 2018-Nov 2018 | 0 | 0 | 0 | 0 |
| Nov 2018-Dec 2018 | 0 | 0 | 0 | 0 |
| Dec 2018-Jan 2019 | 0 | 0 | 0 | 0 |
| Jan 2019-Feb 2019 | 0 | 0 | 0 | 0 |
| Feb 2019-Mar 2019 | 0.73 | 0.16 | 0 | 2.71 |
| Mar 2019-Apr 2019 | 0 | 0 | 0 | 0 |
| Apr 2019-May 2019 | 0 | 0 | 0 | 0 |
| May 2019-June 2019 | 0 | 0 | 0 | 0 |
| June 2019-July 2019 | 0 | 0 | 0 | 0 |
| July 2019-Aug 2019 | 0 | 0 | 0 | 0 |
| Aug 2019-Sep 2019 | 0 | 0 | 0 | 0 |
| Sep 2019-Oct 2019 | 5.11 | 0.62 | 3.61 | 6.86 |

Repeated Mixed Model for Zn

The model for Zn is $Zn = m + Location + Plot(Location) + Time$ where Time was the coded date range of the sample, Location was the property the sample was taken at, sample was the filter, Zn was the Zn concentration in mass percent for each subsample, and Subsample was the sample taken from the filter. The dependent variable in this model is Zn, and there were three independent variables or classes: location, plot, and time. Location had seven levels: one for each property in the study. Plot had four levels:

one for each subsample of the filter. Time had 12 levels. The AR(1) Covariance Parameter Estimate was 0.3805. Location was not found to be significant at 0.1421 $P > F$. Plot(Location) was not found to be significant at 0.4781. Time was found to be significant at $< 0.0001 P > F$. The interaction between Location and Time was found to be significant at $< 0.0001 P > F$. Zn is present in soils within and surrounding East Texas so there is no clear indicator where this element originated from (USGS, 1984). It appeared in February 2019-March 2019, which was when the other elements were at their lowest value, and September 2019-October 2019 (Table 13 and Table 27). This may be from the surrounding soil or it could be due to a sensitivity in the machine after the tungsten filament was changed. The filament was changed a day before the Sep 2019-Oct 2019 elemental analysis and two days before the Feb 2019-Mar 2019 elemental analysis, which indicates the filament change may have impacted the ability of the machine to identify elements.

Summary Statistics for Re

Table 14. Arithmetic mean, standard deviation, minimum and maximum of Re sampled across seven sites over a twelve-month period. Four subsamples were collected per sample. One sample was collected per site per month. Six of the seven sampling sites are in Stephen F. Austin University Real Estate Foundation’s STMicroelectronics carbon sequestration project and one sampling site is located at SFA’s Beef Farm.

| Date Range | Mass Percentage of Re | | | |
|---------------------|-----------------------|--------------------|---------|---------|
| | Arithmetic Mean | Standard Deviation | Minimum | Maximum |
| Oct 2018-Nov 2018 | 0 | 0 | 0 | 0 |
| Nov 2018-Dec 2018 | 0 | 0 | 0 | 0 |
| Dec 2018-Jan 2019 | 0 | 0 | 0 | 0 |
| Jan 2019-Feb 2019 | 0 | 0 | 0 | 0 |
| Feb 2019-Mar 2019 | 0.06 | 0.07 | 0 | 0.96 |
| Mar 2019-Apr 2019 | 0 | 0 | 0 | 0 |
| Apr 2019-May 2019 | 0 | 0 | 0 | 0 |
| May 2019-June 2019 | 0 | 0 | 0 | 0 |
| June 2019-July 2019 | 0 | 0 | 0 | 0 |
| July 2019-Aug 2019 | 0 | 0 | 0 | 0 |
| Aug 2019-Sep 2019 | 0 | 0 | 0 | 0 |
| Sep 2019-Oct 2019 | 1.39 | 1.46 | 0 | 4.33 |

Repeated Mixed Model for Re

The model for Re is $Re = m + Location + Plot(Location) + Time$ where Time was the coded date range of the sample, Location was the property the sample was taken at, sample was the filter, Re was the Re concentration in mass percent for each subsample, and Subsample was the sample taken from the filter. The dependent variable in this model is Re, and there were three independent variables or classes: location, plot, and time. Location had seven levels: one for each property in the study. Plot had four levels:

one for each subsample of the filter. Time had 12 levels. The AR(1) Covariance Parameter Estimate was 0.9905. Location was found to be significant at <0.0001 Pr>F. Plot(Location) was found to be significant at <0.0001 . Time was not found to be significant at 0.9388 Pr>F. The interaction between Location and Time was not found to be significant at 1.0000 Pr>F. Re is a rare metal additive used in tungsten alloys (RSC, 2019). Since tungsten filaments are used in the SEM, it is likely that this reading was not picked up from the deposition, but the SEM itself. It appeared in February 2019-March 2019 and September 2019-October 2019 (Table 14 and Table 28). Re may have been from the surrounding soil or it could have been detected due to varying sensitivity in the SEM after the tungsten filament was changed.

Summary Statistics for Ti

Table 15. Arithmetic mean, standard deviation, minimum and maximum of Ti sampled across seven sites over a twelve-month period. Four subsamples were collected per sample. One sample was collected per site per month. Six of the seven sampling sites are in Stephen F. Austin University Real Estate Foundation’s STMicroelectronics carbon sequestration project and one sampling site is located at SFA’s Beef Farm.

| Date Range | Mass Percentage of Ti | | | |
|---------------------|-----------------------|--------------------|---------|---------|
| | Arithmetic Mean | Standard Deviation | Minimum | Maximum |
| Oct 2018-Nov 2018 | 0.13 | 0.26 | 0 | 2.44 |
| Nov 2018-Dec 2018 | 0 | 0 | 0 | 0 |
| Dec 2018-Jan 2019 | 0.02 | 0.03 | 0 | 0.44 |
| Jan 2019-Feb 2019 | 0.02 | 0.04 | 0 | 0.59 |
| Feb 2019-Mar 2019 | 0 | 0 | 0 | 0 |
| Mar 2019-Apr 2019 | 0.05 | 0.09 | 0 | 0.67 |
| Apr 2019-May 2019 | 0 | 0 | 0 | 0 |
| May 2019-June 2019 | 0 | 0 | 0 | 0 |
| June 2019-July 2019 | 0.08 | 0.16 | 0 | 1.15 |
| July 2019-Aug 2019 | 0 | 0 | 0 | 0 |
| Aug 2019-Sep 2019 | 0.03 | 0.06 | 0 | 0.90 |
| Sep 2019-Oct 2019 | 0.09 | 0.14 | 0 | 0.70 |

Repeated Mixed Model for Ti

The model for Ti is $Ti = m + \text{Location} + \text{Plot}(\text{Location}) + \text{Time}$ where Time was the coded date range of the sample, Location was the property the sample was taken at, sample was the filter, Ti was the Ti concentration in mass percent for each subsample, and Subsample was the sample taken from the filter. The dependent variable in this model is Ti, and there were three independent variables or classes: location, plot, and time. Location had seven levels: one for each property in the study. Plot had four levels: one for each subsample of the filter. Time had 12 levels. The AR(1) Covariance

Parameter Estimate was 0.1045. Location was not found to be significant at 0.2150 Pr>F. Plot(Location) was not found to be significant at 0.8701. Time was not found to be significant at 0.2455 Pr>F. The interaction between Location and Time was not found to be significant at 0.8633 Pr>F. Ti is abundant in both nature and commercial processing so it is difficult to determine its source (RSC, 2019). Since the monthly mass percentage of Ti recorded was less than 0.2%, it was likely static from the SEM (Table 15 and Table 29).

Summary Statistics for Fe

Table 16. Arithmetic mean, standard deviation, minimum and maximum of Fe sampled across seven sites over a twelve-month period. Four subsamples were collected per sample. One sample was collected per site per month. Six of the seven sampling sites are in Stephen F. Austin University Real Estate Foundation's STMicroelectronics carbon sequestration project and one sampling site is located at SFA's Beef Farm.

| Date Range | Mass Percentage of Fe | | | |
|---------------------|-----------------------|--------------------|---------|---------|
| | Arithmetic Mean | Standard Deviation | Minimum | Maximum |
| Oct 2018-Nov 2018 | 7.16 | 0.85 | 1.49 | 9.53 |
| Nov 2018-Dec 2018 | 6.74 | 1.59 | 0 | 9.14 |
| Dec 2018-Jan 2019 | 7.21 | 0.72 | 4.07 | 8.94 |
| Jan 2019-Feb 2019 | 6.32 | 0.66 | 3.04 | 8.66 |
| Feb 2019-Mar 2019 | 3.98 | 0.92 | 0 | 6.81 |
| Mar 2019-Apr 2019 | 5.91 | 0.97 | 2.63 | 7.81 |
| Apr 2019-May 2019 | 6.97 | 0.98 | 5.11 | 8.98 |
| May 2019-June 2019 | 6.78 | 1.24 | 4.47 | 10.63 |
| June 2019-July 2019 | 6.87 | 0.67 | 3.20 | 9.10 |
| July 2019-Aug 2019 | 6.83 | 0.92 | 5.11 | 9.20 |
| Aug 2019-Sep 2019 | 7.43 | 0.69 | 4.86 | 10.33 |
| Sep 2019-Oct 2019 | 6.84 | 0.71 | 5.37 | 8.80 |

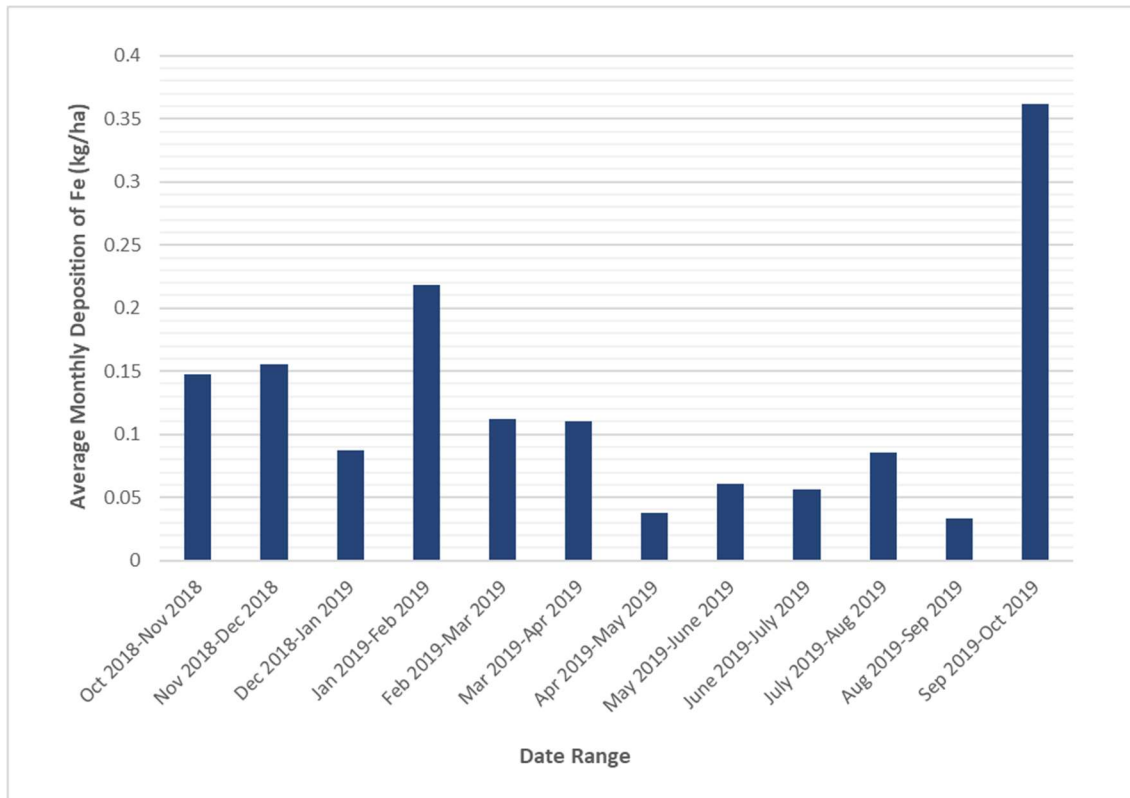


Figure 19. Arithmetic mean of Fe in kg/ha sampled across seven sites over a twelve-month period. Four subsamples were collected per sample. One sample was collected per site per month. Six of the seven sampling sites are in Stephen F. Austin University Real Estate Foundation’s STMicroelectronics carbon sequestration project and one sampling site is located at SFA’s Beef Farm.

Repeated Mixed Model for Fe

The model for Fe is $Fe = m + Location + Plot(Location) + Time$ where Time was the coded date range of the sample, Location was the property the sample was taken at, sample was the filter, Fe was the Fe concentration in mass percent for each subsample, and Subsample was the sample taken from the filter. The dependent variable in this model is Fe, and there were three independent variables or classes: location, plot, and

time. Location had seven levels: one for each property in the study. Plot had four levels: one for each subsample of the filter. Time had 12 levels. The AR(1) Covariance Parameter Estimate was 0.03199. Location was found to be significant at <0.0001 Pr>F. Plot(Location) was not found to be significant at 0.8523. Time was found to be significant at <0.0001 Pr>F. The interaction between Location and Time was found to be significant at <0.0001 Pr>F. Fe can be found in some soils within East Texas and Central Texas (Johnson, 2010). Fe deposition was recorded at a monthly range of 0.0330 kg/ha – 0.3619 kg/ha and had a yearly total of 1.4679 kg/ha deposition (Table 33). Although the total deposition in kg/ha does not decrease very much in February 2019-March 2019, the mass percentage of Fe in the samples decreases considerably during this time (Table 16, Table 30, and Figure 19). This may be due to less mobile soil particulates in the area during this time.

Fe was detected from only three properties: Arbor Grove in October 2018-November 2018, Atoy in January 2019-February 2019, and Swink in January 2019-February 2019 and May 2019-June 2019. This may be due to Fe present in nearby soils and the lack of reduced conditions since all three samplers are on elevated terrain.

Summary Statistics for Ce

Table 17. Arithmetic mean, standard deviation, minimum and maximum of Ce sampled across seven sites over a twelve-month period. Four subsamples were collected per sample. One sample was collected per site per month. Six of the seven sampling sites are in Stephen F. Austin University Real Estate Foundation’s STMicroelectronics carbon sequestration project and one sampling site is located at SFA’s Beef Farm.

| Date Range | Mass Percentage of Ce | | | |
|---------------------|-----------------------|--------------------|---------|---------|
| | Arithmetic Mean | Standard Deviation | Minimum | Maximum |
| Oct 2018-Nov 2018 | 0 | 0 | 0 | 0 |
| Nov 2018-Dec 2018 | 0 | 0 | 0 | 0 |
| Dec 2018-Jan 2019 | 0 | 0 | 0 | 0 |
| Jan 2019-Feb 2019 | 0.06 | 0.12 | 0 | 1.66 |
| Feb 2019-Mar 2019 | 0 | 0 | 0 | 0 |
| Mar 2019-Apr 2019 | 0 | 0 | 0 | 0 |
| Apr 2019-May 2019 | 0 | 0 | 0 | 0 |
| May 2019-June 2019 | 0 | 0 | 0 | 0 |
| June 2019-July 2019 | 0.10 | 0.19 | 0 | 2.66 |
| July 2019-Aug 2019 | 0 | 0 | 0 | 0 |
| Aug 2019-Sep 2019 | 0 | 0 | 0 | 0 |
| Sep 2019-Oct 2019 | 0 | 0 | 0 | 0 |

Repeated Mixed Model for Ce

The model for Ce is $Ce = m + \text{Location} + \text{Plot}(\text{Location}) + e$ where Time was the coded date range of the sample, Location was the property the sample was taken at, sample was the filter, Ce was the Ce concentration in mass percent for each subsample, and Subsample was the sample taken from the filter. The dependent variable in this model is Ce, and there were three independent variables or classes: location, plot, and time. Location had seven levels: one for each property in the study. Plot had four levels: one for each subsample of the filter. Time had 12 levels. The AR(1) Covariance

Parameter Estimate was 0.01543. Location was not found to be significant at 0.5154 Pr>F. Plot(Location) was not found to be significant at 0.4390. Time was not found to be significant at 0.5425 Pr>F. The interaction between Location and Time was not found to be significant at 0.4681 Pr>F. Ce is commonly found in natural minerals and is used commercially as a catalyst for various things like cigarette lighters and self-cleaning ovens (RSC, 2019). It is also used in flat screen TVs and lights (RSC, 2019). Since the monthly mass percentage of Ce recorded was less than 0.2%, it was likely static from the SEM (Table 17 and Table 31).

Summary Statistics for Trace Elements

The trace elements observed in this study include In, F, Mo, and Ru. All of these were found in only one sample, not statically significant, and allotted for less than <1.50% as their maximum mass percentage. The following paragraphs outline the summary statistics for each element.

In was found in one sample during this study (Hilliard February 2019-March 2019). Among this sample's four subsamples, the average element mass percentage was 0.38%, the standard deviation was 0.75, the minimum value was 0%, and the maximum value was 1.50%. All other readings for In recorded 0%.

F was found in one sample during this study (Atoy May 2019-June 2019). Among this sample's four subsamples, the average element mass percentage was 0.02%,

the standard deviation was 0.04, the minimum value was 0%, and the maximum value was 0.08%. All other readings for F recorded 0%.

Mo was found in one sample during this study (Hilliard February 2019-March 2019). Among this sample's four subsamples, the average element mass percentage was 0.04%, the standard deviation was 0.07, the minimum value was 0%, and the maximum value was 0.14%. All other readings for Mo recorded 0%.

Ru was found in one sample during this study (Agriculture Farm December 2018-January 2019). Among this sample's four subsamples, the average element mass percentage was 0.01%, the standard deviation was 0.02, the minimum value was 0%, and the maximum value was 0.04%. All other readings for Ru recorded 0%.

Repeated Mixed Model for Trace Elements

The model for In is $In = m + Location + Plot(Location) + Time$ where Time was the coded date range of the sample, Location was the property the sample was taken at, sample was the filter, In was the In concentration in mass percent for each subsample, and Subsample was the sample taken from the filter. The dependent variable in this model is In, and there were three independent variables or classes: location, plot, and time. Location had seven levels: one for each property in the study. Plot had four levels: one for each subsample of the filter. Time had 12 levels. The AR(1) Covariance Parameter Estimate was -0.01543. Location was not found to be significant at 0.4129 $Pr > F$. Plot(Location) was not found to be significant at 0.4390. Time was not found to be

significant at 0.4643 Pr>F. The interaction between Location and Time was not found to be significant at 0.4955 Pr>F. With the outlier sample removed, no variables were significant.

In is not typically found uncombined in nature, but when it is, it is often associated with other elements such as Zn (RSC, 2019). It is common in However, it is used in indium-tin oxide coated glass slides that are used in SEM analysis (Pluk, 2009). Indium-tin oxide is also common in touch screen technology, flat screens, and solar panels (RSC, 2019). Due to this element being more common in the industrial setting rather than nature, it is likely the In in this reading was unsubstantial.

The model for F is $F = m + \text{Location} + \text{Plot}(\text{Location}) + \text{Time}$ where Time was the coded date range of the sample, Location was the property the sample was taken at, sample was the filter, F was the F concentration in mass percent for each subsample, and Subsample was the sample taken from the filter. The dependent variable in this model is F, and there were three independent variables or classes: location, plot, and time. Location had seven levels: one for each property in the study. Plot had four levels: one for each subsample of the filter. Time had 12 levels. The AR(1) Covariance Parameter Estimate was -0.01543. Location was not found to be significant at 0.4129 Pr>F. Plot(Location) was not found to be significant at 0.4390. Time was not found to be significant at 0.4643 Pr>F. The interaction between Location and Time was not found to be significant at 0.4955 Pr>F. With the outlier sample removed, no variables were significant. Combined F is very common in Nature and can be found in trace amounts

within bodies of water and various minerals like fluorite, cryolite, and fluorspar (RSC, 2019).

The model for Mo is $Mo = m + Location + Plot(Location) + Time$ where Time was the coded date range of the sample, Location was the property the sample was taken at, sample was the filter, Mo was the Mo concentration in mass percent for each subsample, and Subsample was the sample taken from the filter. The dependent variable in this model is Mo, and there were three independent variables or classes: location, plot, and time. Location had seven levels: one for each property in the study. Plot had four levels: one for each subsample of the filter. Time had 12 levels. The AR(1) Covariance Parameter Estimate was -0.01543. Location was not found to be significant at 0.4129 Pr>F. Plot(Location) was not found to be significant at 0.4390. Time was not found to be significant at 0.4643 Pr>F. The interaction between Location and Time was not found to be significant at 0.4955 Pr>F. With the outlier sample removed, no variables were significant. Mo is present in soils within and surrounding East Texas so there is no clear indicator where this element originated from (USGS, 1984).

The model for Ru is $Ru = m + Location + Plot(Location) + Time$ where Time was the coded date range of the sample, Location was the property the sample was taken at, sample was the filter, Ru was the Ru concentration in mass percent for each subsample, and Subsample was the sample taken from the filter. The dependent variable in this model is Ru, and there were three independent variables or classes: location, plot, and time. Location had seven levels: one for each property in the study. Plot had four levels:

one for each subsample of the filter. Time had 12 levels. The AR(1) Covariance Parameter Estimate was -0.01543. Location was not found to be significant at 0.4129 $Pr>F$. Plot(Location) was not found to be significant at 0.4390. Time was not found to be significant at 0.4644 $Pr>F$. The interaction between Location and Time was not found to be significant at 0.4953 $Pr>F$. With the outlier sample removed, no variables were significant. Ru is an extremely rare metal, and is used most often in the electronic industry (RSC, 2019).

CONCLUSIONS

The deposition collected for this study was significantly influenced by location of the sampler and time. Other factors that could have influenced the amount of deposition collected were surrounding groundcover, precipitation, wind direction, wind velocity, clearing size, pollen deposition, geologic barriers, unpaved roads, etc. Calm winds are unlikely to carry larger particles over great distances and would be susceptible to geologic and natural barriers such as trees reducing their velocity. However, areas with higher wind speeds and sparse trees would be more susceptible to nonnative particulates.

In Figure 10, months with the highest average precipitation had the lowest average particulate deposition. This could be due to precipitation events reducing the mobility of particulates. Large precipitation events may also temporarily increase the cohesiveness of incoming particulate matter, making particle transport more difficult.

Surrounding groundcover appeared to influence the amount of deposition in the sampler since different types of pollen were released during different parts of the year (Houston Health Department, 2019). Particle size data helped identify this trend. Since pollen is associated with larger particles, particle size data was used to identify the

relative pollen concentrations across different sites over the sampling year. Higher average particle sizes correlated to higher amounts of particle deposition and lower amounts of precipitation. This trend may correlate with a higher amount of dry deposition or pollen during these time periods.

Particle size data also provided information about the potential origins of particulate deposition during different sampling periods. Months with low mean particle size may be indicative of distant sources of mineral deposition due to wind and mechanical weathering altering the size and morphology of mineral matter as it moved across the landscape. Since these months were often months with higher rates of precipitation, this data may also be indicative of higher rates of wet deposition.

The total yearly deposition recorded in this study was 22.9865 kg/ha. Of this yearly deposition, 8.5582 kg/ha was Si deposition, 2.2923 kg/ha was C deposition, 1.4394 kg/ha was Ba deposition, 1.4679 kg/ha was Na deposition, 0.7389 kg/ha was Al deposition, 0.3146 kg/ha was Ca deposition, 0.7846 kg/ha was K deposition, and 1.4679 kg/ha was Fe deposition (Table 33). Si deposition had a monthly range of 0.1939 kg/ha – 1.5393 kg/ha, C deposition had a monthly range of 0.0262 kg/ha – 0.6871 kg/ha, Ba had a monthly range of 0.0380 kg/ha – 0.2984 kg/ha, Na had a monthly range of 0.0330 kg/ha – 0.3619 kg/ha, Al had a monthly range of 0.0157 kg/ha – 0.1676 kg/ha, Ca had a monthly range of 0.0022 kg/ha – 0.0958 kg/ha, K had a monthly range of 0.0190 kg/ha – 0.1714 kg/ha, and Fe had a monthly range of 0.0330 kg/ha – 0.3619 kg/ha (Table 33). Mean particle size increased from January 2019-April 2019 (Figure 11).

Total deposition displayed seasonal patterns, with higher deposition during the Spring and Fall and lower deposition during the Summer and Winter (Figure 7). Particle size increased during high pollen months and wetter seasons such as Spring and decreased during traditionally drier months like Summer (Figure 11 and Houston Health Department, 2019). This may indicate higher amounts of organic deposition during high pollen seasons and higher amounts of mineral deposition in drier months. Elements found in soils tended to make up a larger percentage of the deposition during drier Summer and Winter months (Figure 10, Table 18, Table 22, Table 23, Table 24, Table 25, Table 26 and Table 30).

The highest deposition was recorded at Maxwell, and Arbor Grove maintained the highest average deposition for six out of twelve recorded months. These two properties are the furthest properties to the west and south. They have the least number of trees between the plains of central Texas and their location. Peak deposition was observed between September 2018-November 2018, and January 2019-April 2019. Peak deposition appears to correspond to traditionally dry seasons and pollen season.

Water levels in the samplers were accounted for in the deposition calculations. However, during some months, the pails overflowed or spilled, and this likely influenced the calculations. Future studies should account for these possibilities by using larger pails to hold the deposition. To reduce spilling during transport, the lids should be sealed and spill-proof.

It may benefit future studies to collect an unfiltered water sample for elemental analysis using an ICP-MS and nitric acid digestion. Due to the early disposal of sample solution after recordings were made, this was not a viable option. The high silica content of the filters used in this study made this option unusable because the silica would form a gel that could interfere with the results collected.

While H and He were not recorded by the SEM-EDS technology, there is a high probability that H was present due to its abundance in pollen granules and water. Si, O, C, Ba, Na, Al, K, Ca and Fe were observed at >1.00% mass. Of these, Si, O, C, Ba, Na, Al, K, Ca, and Fe were found to be statistically significant by time, location, and the interaction between time and location using the ANOVA Mixed Model statistics method.

Si makes up a large portion of soil particles and the glass filter used in this study so its readings may correlate with both the filter and surrounding soils. While O and C are present in pollen grains, they are also present in CO₂, and O is present in H₂O and O₂. Therefore, these may have many sources other than deposition. Fe is present in some East Texas soils. Ba, Na, Al, Ca, and K are all common in East Texas soils. Ca is also common in Central Texas soils, which could indicate that more research into the transport of particulates should be analyzed.

East Texas soils may have been impacted in a variety of ways by the incoming particulate matter from different regions. O deposition from air and water may have increased the efficiency of cellular respiration in plants while incoming C may have

influenced photosynthesis rates (University of Missouri, 2017). Also, since soils tend to act as C sinks, this may have allowed elements that were combined with C to remain in the soil longer than they would have uncombined (Oertel et al., 2016). Deposition of Micronutrients Zn and Fe as well as macronutrients Ca and K may have increased soil fertility over time. However, CaO_3 deposition may impact pH and nutrient availability (Tsakelidou, 2008). Na deposition may have increased soil salinity when combined to form various salts. Depending on the amount and chemical combination of Al found in East Texas soils as well as the soil's pH, Al could have been harmful to surrounding plant growth, inconsequential, or beneficial (Bojórquez-Quintal et al., 2017).

LITERATURE CITED

- Adriaenssens S., Staelens J., Baeten L., Verstraeten A., Boeckx P., Samson R., and Verheyen K. 2013. Influence of canopy budget model approaches on atmospheric deposition estimates to forests [Online]. Available at <https://link.springer.com/article/10.1007/s10533-013-9846-0>. Springer Nature, Switzerland, AG.
- Al-Taani A.A., Rashdan M., and Khashashneh S. 2014. Atmospheric dry deposition of mineral dust to the Gulf of Aqaba, Red Sea: Rate and trace elements [Online]. Available at <https://www.sciencedirect.com/science/article/pii/S0025326X14008005>. Elsevier B.V., Amsterdam, Netherlands.
- ArcGIS. 2018. Weather Stations [Online]. Available at <https://www.arcgis.com/home/webmap/viewer.html?layers=7a02bf800a7f4ead84b94ac860f6844c>. Esri.
- Arisci S., Rogora M., Marchetto A., and Dichiaro F. 2011. The role of forest type in the variability of DOC in atmospheric deposition at forest plots in Italy [Online]. Available at <https://link.springer.com/article/10.1007/s10661-011-2196-2>. Springer Nature, Switzerland, AG.
- ASTM. 2017. ASTM D1739 – 98(2017) Standard Test Method for Collection and Measurement of Dustfall (Settleable Particulate Matter). ASTM International, West Conshohocken, PA.
- Aulirantio-Lehtimäki, Helander M.L., Pessi A-M. 1991. Circadian periodicity of airborne pollen and spores; significance of sampling height [Online]. Available at <https://link.springer.com/article/10.1007/BF02270681>. Springer Nature, Switzerland, AG.
- Biret F. 2014. X-Ray Diffraction Table [Online]. Available at <http://www.webmineral.com/MySQL/xray.php#.W3Rd6yBOnCs>. Mineralogy Database.

- Bojórquez-Quintal E., Escalante-Magaña C., Echevarría-Machado I. and Martínez-Estévez M. 2017. Aluminum, a Friend or Foe of Higher Plants in Acid Soils [Online]. Available at <https://www.frontiersin.org/articles/10.3389/fpls.2017.01767/full>.
- Campbell, K., and J. Wendelberger. 1994. Non-detect data in environmental investigations. Non-detect data in environmental investigations (Conference) | OSTI.GOV. Available at <https://www.osti.gov/servlets/purl/10156972/>.
- Desboeufs K., Leblond N., Wagener T., Nguyen E.B., and Guieu C. 2013. Chemical fate and settling of mineral dust in surface seawater after atmospheric deposition observed from dust seeding experiments in large mesocosms [Online]. Available at https://www.researchgate.net/profile/Cecile_Guieu/publication/267154183_Chemical_fate_and_settling_of_mineral_dust_in_surface_seawater_after_atmospheric_deposition_observed_from_dust_seeding_experiments_in_large_mesocosms/links/544692660cf2f14fb80f7a86.pdf. Biogeosciences Discussions. Biogeosciences Discussions.
- Diebold, F. X. 2019. Introduction to Time Series Regression and Forecasting (SW Chapter 14) [Online]. Available at https://www.sas.upenn.edu/~fdiebold/Teaching104/Ch14_slides.pdf. University of Pennsylvania, Philadelphia, PA.
- Dörr N., Kaiser K., Sauheitl L., Lamersdorf N., S tange, C.F., and Guggenberger G. 2010. Fate of ammonium ¹⁵N in a Norway spruce forest under long-term reduction in atmospheric N deposition [Online]. Available at <https://link.springer.com/content/pdf/10.1007/s10533-010-9561-z.pdf>. ebscohost. Springer Nature, Switzerland, AG.
- Draaijers, G.P.J., and J.W. Erisman. 1995. A canopy budget model to assess atmospheric deposition from throughfall measurements [Online]. Available at <https://link.springer.com/article/10.1007/BF01186169>. Springer Nature, Switzerland, AG.
- EPA. 2008. Standard Operating Procedure for Sample Preparation and Analysis of PM₁₀ and PM_{2.5} Samples by Scanning Electron Microscopy [Online]. Available at <https://www3.epa.gov/ttnamti1/files/ambient/pm25/spec/RTISEMSOPFINAL.pdf>. Environmental and Industrial Sciences Division Research Triangle Institute Research Triangle Park, North Carolina.

- EPA. 2016. Ecoregions of North America [Online]. Available at <https://www.epa.gov/eco-research/ecoregions-north-america>. EPA.
- EPA. 2018. Guidance for Determining the Acceptability of Environmental Fate Studies Conducted with Foreign Soils [Online]. Available at <https://www.epa.gov/pesticide-science-and-assessing-pesticide-risks/guidance-determining-acceptability-environmental>. EPA.
- Gregory P.H. 2009. The dispersion of air-borne spores [Online]. Available at <https://www.sciencedirect.com/science/article/pii/S0007153645800414>. Egyptian Journal of Medical Human Genetics. Elsevier B.V., Amsterdam, Netherlands.
- Hartmann J., Kunimatsu T., and Levy J. 2007. The impact of Eurasian dust storms and anthropogenic emissions on atmospheric nutrient deposition rates in forested Japanese catchments and adjacent regional seas [Online]. Available at <https://www.sciencedirect.com/science/article/pii/S092181810700121X>. Egyptian Journal of Medical Human Genetics. Elsevier B.V., Amsterdam, Netherlands.
- Helwig, N. (2019). Linear Mixed-Effects Regression [Online]. Available at <http://users.stat.umn.edu/~helwig/notes/lmer-Notes.pdf>.
- Hirst J.M. 2009. Changes in atmospheric spore content: Diurnal periodicity and the effects of weather [Online]. Available at <https://www.sciencedirect.com/science/article/pii/S0007153653800343>. Egyptian Journal of Medical Human Genetics. Elsevier B.V., Amsterdam, Netherlands.
- Houston Health Department. Pollen and Mold Spore Reports. Houston Health Department - Pollen and Mold. Available at <http://www.houstontx.gov/health/Pollen-Mold/> (verified 18 May 2020).
- Illinois State Water Survey. 1989. Using copper sulfate to control algae in water supply impoundments [Online]. Available at <https://www.isws.illinois.edu/pubdoc/MP/ISWSMP-111.pdf>. Miscellaneous Publication 111, Illinois State Water Survey, Champaign, Illinois.
- Johnson H.E. 2010. SOILS [Online]. Available at <https://tshaonline.org/handbook/online/articles/gps01>

- Lancaster N. 2009. Monitoring Aeolian Features and Processes (U.S. National Park Service) [Online]. Available at <http://www.nps.gov/articles/aeolian.htm>. National Parks Service. Geological Society of America, Boulder, Colorado.
- Lakes Environmental. 2018. Wind Rose Plots for Meteorological Data [Online]. Available at <http://www.weblakes.com/>. Lakes Environmental Software, Ontario, Waterloo.
- Lee E.J. and Booth T. 2003. Macronutrient input from pollen in two regenerating pine stands in southeast Korea [Online]. Available at <https://link.springer.com/article/10.1046/j.1440-1703.2003.00566.x>. Springer Nature, Switzerland, AG.
- Lequy É., Conil S., Nicolas M., and Turpaul M-P. 2013. Relationship Between Atmospheric Dissolved Deposition and Mineral Dust Deposition in French Forests [Online]. Available at <https://link.springer.com/article/10.1007/s11270-013-1680-4>. Springer Nature, Switzerland, AG.
- Li W., Gao F., Liao X. 2013. Estimating Chemical Exchange between Atmospheric Deposition and Forest Canopy in Guizhou, China [Online]. Available at <https://dl-sciencesocieties-org.steenproxy.sfasu.edu/publications/jeq/pdfs/42/2/332>. Journal of Environmental Quality. American Society of Agronomy, Crop Science Society of America, and Soil Science Society of America, Madison, WI.
- Ličbínský R., Frýbort A., Huzlík J., Adamec V., Effenberger K., Mikuška P., Vojtěšek M., and Křůmal K. 2010. Usage of Scanning Electron Microscopy for Particulate Matter Sources Identification [Online]. Available at https://www.researchgate.net/publication/271050658_Usage_of_Scanning_Electron_Microscopy_for_Part particulate_Matter_Sources_Identification. ResearchGate, Berlin, Germany.
- Lower S. 2018. 7.10: Colloids and their Uses. Chemistry LibreTexts [Online]. Available at [https://chem.libretexts.org/Textbook_Maps/General_Chemistry/Book:_Chem1_\(Lower\)/07:_Solids_and_Liquids/7.10:_Colloids_and_their_Uses](https://chem.libretexts.org/Textbook_Maps/General_Chemistry/Book:_Chem1_(Lower)/07:_Solids_and_Liquids/7.10:_Colloids_and_their_Uses). LibreTexts, Vancouver, Canada.

- Makabe, S., Kakuda K., Sasaki Y., Ando T., Fujii H. & Ando H. 2009. Relationship between mineral composition or soil texture and available silicon in alluvial paddy soils on the Shounai Plain, Japan [Online]. Available at <https://www.tandfonline.com/doi/full/10.1111/j.1747-0765.2008.00352.x?scroll=top&needAccess=true>. Informa UK Limited, London, England.
- McDonnell T.C., Belyazid S., Sullivan T.J., Bell M., Clark C., Blett T., Evans T., Cass W., Hyduke A., and Sverdrup H. 2018. Vegetation dynamics associated with changes in atmospheric nitrogen deposition and climate in hardwood forests of Shenandoah and Great Smokey Mountains National Parks, USA [Online]. Available at <http://www.sciencedirect.com/science/article/pii/S0269749117334413>. Environmental Pollution. Elsevier B.V., Amsterdam, Netherlands.
- NASA, Voiland A., and Stevens J. 2018. Just Another Day on Aerosol Earth [Online]. Available at <https://earthobservatory.nasa.gov/images/92654/just-another-day-on-aerosol-earth>. NASA, Houston, Texas.
- Nathan, M.V. 2017. Soils, Plant Nutrition and Nutrient Management [Online]. Available at <https://extension.missouri.edu/mg4/>. University of Missouri, Columbia, Missouri.
- Natural Resources Conservation Service. Welcome to Southern Great Plains Soil Survey Region 9 [Online]. Available at <https://www.nrcs.usda.gov/wps/portal/nrcs/main/soils/survey/office/ssr9/>. NRCS, Temple, TX.
- NOAA. 2018. National Centers for Environmental Information Data Access [Online]. Available at <http://www.ncdc.noaa.gov/>. National Centers for Environmental Information, Asheville, NC.
- NOAA. 2019. National Centers for Environmental Information Data Access [Online]. Available at <http://www.ncdc.noaa.gov/>. National Centers for Environmental Information, Asheville, NC.
- NRCS. 2019. Web Soil Survey [Online]. Available at <https://websoilsurvey.nrcs.usda.gov/app>. NRCS, Washington, D.C., Virginia.

- Ophthalmol I.J. 2011. How to choose the right statistical test [Online]? Available at <https://www.ncbi.nlm.nih.gov/pmc/articles/PMC3116565/>. Medknow Publications, Mumbai, India.
- Oertel C., Matschullat J., Zurba K., Zimmermann F., and Erasmi S. 2016. Greenhouse gas emissions from soils—A review [Online]. Available at <https://www.sciencedirect.com/science/article/pii/S0009281916300551>. Elsevier B.V., Amsterdam, Netherlands.
- Phillips T. and Watmough S.A. 2012. A nutrient budget for a selection harvest: implications for long-term sustainability [Online]. Available at <http://www.nrcresearchpress.com/doi/10.1139/cjfr-2012-0224>. ebscohost. Canadian Journal of Forest Research. NRC Research Press, Ottawa, Ontario.
- Pluk, H., D.J. Stokes, B. Lich, B. Wieringa, and J. Fransen. 2009. Advantages of indium-tin oxide-coated glass slides in correlative scanning electron microscopy applications of uncoated cultured cells. *Journal of microscopy*. Available at <https://www.ncbi.nlm.nih.gov/pubmed/19250456> (verified 17 March 2020).
- Radnor. 1986. Atmospheric deposition and eastern forests: cooperative research. The Station, Broomall, PA.
- RSC. 2019. Element information, properties and uses | Periodic Table [Online]. Available at <http://www.rsc.org/periodic-table/element/>.
- Ruddy B., Lorenz D., and Mueller D. 2018. County-Level Estimates of Nutrient Inputs to the Land Surface of the Conterminous United States, 1982–2001 [Online]. Available at https://pubs.usgs.gov/sir/2006/5012/pdf/sir2006_5012.pdf. USGS. U.S. Geological Survey, Reston, Virginia.
- Sáez A., Morales C.L., Ramos L.Y., and Aizen M.A. 2014. Extremely frequent bee visits increase pollen deposition but reduce drupelet set in raspberry [Online]. Available at <https://besjournals.onlinelibrary.wiley.com/doi/abs/10.1111/1365-2664.12325> (verified 28 June 2020). British Ecological Society, London, UK.

- Scanza R.A., Mahowald N., Ghan S., Zender C.S., Kok, J., Liu X., Zhang Y., and Albani S. 2014. Modeling dust as component minerals in the Community Atmosphere Model: Development of framework and impact on radiative forcing [Online]. Available at <http://web.a.ebscohost.com.steenproxy.sfasu.edu:2048/ehost/pdfviewer/pdfviewer?vid=0&sid=98ce4bab-f4a2-4568-8500-19dfc380ce65@sessionmgr4009> (verified 19 May 2020). *ebscohost. Atmospheric Chemistry & Physics*. p. 537–561. *Atmospheric Chemistry & Physics*.
- Simpson S.H. 2015. Creating a Data Analysis Plan: What to Consider When Choosing Statistics for a Study [Online]. Available at <https://www.ncbi.nlm.nih.gov/pmc/articles/PMC4552232/> (verified 19 May 2020). *Canadian Journal of Hospital Pharmacy*, Ottawa, Ontario.
- Soil Science Society of America. 2018. Soil Science Society of America [Online]. Available at <https://www.soils.org/> (verified 19 May 2020). Soil Science Society of America.
- Stojilovic, N. 2012. Why Can't We See Hydrogen in X-ray Photoelectron Spectroscopy? *acs.org*. Available at <https://pubs.acs.org/doi/abs/10.1021/ed300057j> (verified 19 May 2020).
- Swapp S. 2017. Scanning Electron Microscopy (SEM) [Online]. Available at https://serc.carleton.edu/research_education/geochemsheets/techniques/SEM.html. Using Media to Enhance Teaching and Learning. University of Wyoming, Laramie, Wyoming.
- Taylor, J. 2019. Statistics 203: Introduction to Regression and Analysis of Variance Time Series Regression [Online]. Available at <http://statweb.stanford.edu/~jtaylo/courses/stats203/notes/time.series.regression.pdf>. Stanford University, Stanford, CA.
- TCEQ. 2018. Yearly Summary Report By Site [Online]. Available at https://www.tceq.texas.gov/cgi_bin/compliance/monops/particulates.pl?region_cri t=12. Texas Commission on Environmental Quality, Austin, Texas.
- Thomas R.Q., Canham C.D., Weathers K.C., and Goodale C.L. 2009. Increased tree carbon storage in response to nitrogen deposition in the US [Online]. Available at <https://www.nature.com/articles/ngeo721>. Nature Publishing Group, London, United Kingdom.
- TPWD. 2018. Red Tide in Texas Current Status [Online]. Available at <https://tpwd.texas.gov/landwater/water/environconcerns/hab/redtide/status.phtml>. TPWD, Austin, Texas.

- Türtscher S., Berger P., Lindebner L., and Berger T.W. 2017. Declining atmospheric deposition of heavy metals over the last three decades is reflected in soil and foliage of 97 beech (*Fagus sylvatica*) stands in the Vienna Woods [Online]. Available at <https://www.sciencedirect.com/science/article/pii/S0269749117309703>. Elsevier B.V., Amsterdam, Netherlands.
- Tsakelidou, K. 2008. Effect of calcium carbonate as determined by lime requirement buffer pH methods on soil characteristics and yield of sorghum plants [Online]. Available at <https://www.tandfonline.com/doi/abs/10.1080/00103620009370510>. Informa UK Limited, London, England.
- UCLA. 2006. Introduction to Linear Mixed Models [Online]. Available at <https://stats.idre.ucla.edu/other/mult-pkg/introduction-to-linear-mixed-models/>. UC REGENTS, Oakland, California.
- University of Bern. 2003. Morphology of Microspores. Available at http://www.botany.unibe.ch/pailo/pollen_e/morphology.htm (verified 19 May 2020).
- UNL. 2018. Soil Genesis and Development, Lesson 5 - Soil Classification and Geography [Online]. Available at <http://passel.unl.edu/pages/informationmodule.php?idinformationmodule=1130447032&topicorder=8&maxto=16>. Plant and Soil Sciences eLibrary.
- USGS. 1984. Element Concentrations in Soils and Other Surficial Materials of the Conterminous United States [Online]. Available at https://pubs.usgs.gov/pp/1270/pdf/PP1270_508.pdf (verified 19 May 2020).
- Washburn, R. G.; Gilmore, L. O.; Fechheimer, N. S. 1958. The Chemical Composition of Cattle Hair. I, The Fat, Ash and Nitrogen Content [Online]. Available at <http://citeseerx.ist.psu.edu/viewdoc/download?doi=10.1.1.925.3324&rep=rep1&type=pdf> (verified 28 June 2020). The Ohio Journal of Science.
- Wieder R.K., Vile M.A., Albright C.M., Scott K.D., Vitt D.H., Quinn J.C., and Burke-Scollet M. 2016. Effects of altered atmospheric nutrient deposition from Alberta oil sands development on *Sphagnum fuscum* growth and C, N and S accumulation in peat [Online]. Available at <https://link.springer.com/article/10.1007/s10533-016-0216-6>. Springer Nature, Switzerland, AG.

- Zak D.R., Holmes W.E., Tomlinson M.J., Pregitzer K.S., and Burton A.J. 2006. Microbial Cycling of C and N in Northern Hardwood Forests Receiving Chronic Atmospheric NO₃⁻ Deposition [Online]. <https://link.springer.com/article/10.1007/s10021-005-0085-7>. Springer Nature, Switzerland, AG.
- Zhang G., Zhang J., and Liu S. 2007. Characterization of nutrients in the atmospheric wet and dry deposition observed at the two monitoring sites over Yellow Sea and East China Sea [Online]. Available at <https://link.springer.com/article/10.1007/s10874-007-9060-3>. Springer Nature, Switzerland, AG.
- Živković T., Disney K., and Moore T.R. 2017. Variations in nitrogen, phosphorous, and $\delta^{15}\text{N}$ in Sphagnum mosses along a climatic and atmospheric deposition gradient in eastern Canada [Online]. Available at <http://www.nrcresearchpress.com/doi/full/10.1139/cjb-2016-0314>. Canadian Science Publishing, Ottawa, Ontario.

APPENDIX

Table 18. Arithmetic monthly mean, maximum and minimum size with standard deviation of sample particles from six sites outlined in Stephen F. Austin University Real Estate Foundation’s STMICROELECTRONICS carbon sequestration project and one site at the SFA Beef Farm. Units are in Microns.

| Date Range | Property | | | | | | | | | | | | | | | | | | | | | | | | | | | |
|---------------------|--------------------|------|--------|-------|-------------|------|--------|-------|---------|------|--------|-------|-------------|------|--------|-------|----------|------|--------|-------|---------|------|--------|-------|-------|------|--------|-------|
| | Agriculture Center | | | | Arbor Grove | | | | Atoy | | | | Bagley Road | | | | Hilliard | | | | Maxwell | | | | Swink | | | |
| | Microns | | | | Microns | | | | Microns | | | | Microns | | | | Microns | | | | Microns | | | | | | | |
| | Mean | Min | Max | SD | Mean | Min | Max | SD | Mean | Min | Max | SD | Mean | Min | Max | SD | Mean | Min | Max | SD | Mean | Min | Max | SD | Mean | Min | Max | SD |
| Oct 2018-Nov 2018 | 4.47 | 0.38 | 34.43 | 3.74 | 9.00 | 1.20 | 79.08 | 7.55 | 3.89 | 0.38 | 45.75 | 3.70 | 4.32 | 0.38 | 47.56 | 3.89 | 5.42 | 0.54 | 213.84 | 10.47 | 4.22 | 0.54 | 78.19 | 4.97 | 5.58 | 0.38 | 86.02 | 5.58 |
| Nov 2018-Dec 2018 | 4.10 | 0.38 | 56.73 | 3.96 | 7.75 | 0.38 | 97.03 | 8.40 | 4.55 | 0.38 | 40.10 | 3.93 | - | - | - | - | 4.47 | 0.38 | 44.99 | 4.40 | 7.19 | 0.38 | 162.04 | 11.41 | 6.15 | 0.38 | 159.37 | 10.43 |
| Dec 2018-Jan 2019 | 3.57 | 0.38 | 65.92 | 3.86 | 7.58 | 0.85 | 169.12 | 8.79 | 4.37 | 0.38 | 80.28 | 5.99 | 3.67 | 0.38 | 55.26 | 3.51 | 4.19 | 0.38 | 100.72 | 4.87 | 4.85 | 0.38 | 115.93 | 8.94 | 5.10 | 0.38 | 131.43 | 7.20 |
| Jan 2019-Feb 2019 | 5.10 | 0.38 | 91.77 | 6.36 | 11.39 | 0.76 | 86.21 | 9.88 | 11.00 | 1.14 | 134.87 | 11.98 | 6.83 | 0.76 | 260.14 | 8.53 | 6.30 | 0.38 | 77.80 | 7.13 | 7.11 | 0.38 | 63.25 | 5.94 | 10.00 | 0.54 | 108.84 | 10.18 |
| Feb 2019-Mar 2019 | 15.26 | 0.85 | 144.88 | 16.99 | 30.99 | 1.20 | 86.58 | 22.52 | 18.84 | 1.14 | 79.41 | 19.64 | 14.70 | 0.76 | 91.85 | 16.39 | 18.61 | 1.57 | 184.10 | 16.93 | 17.77 | 0.85 | 131.64 | 17.60 | 12.01 | 1.52 | 71.97 | 9.16 |
| Mar 2019-Apr 2019 | 8.88 | 0.85 | 80.57 | 9.78 | 10.00 | 0.76 | 160.28 | 13.10 | 8.68 | 0.54 | 89.10 | 12.14 | 8.18 | 0.38 | 77.84 | 11.63 | 8.55 | 0.38 | 77.76 | 10.73 | 9.90 | 0.54 | 153.78 | 13.20 | 8.46 | 0.38 | 85.98 | 12.05 |
| Apr 2019-May 2019 | 6.90 | 0.54 | 138.81 | 8.04 | 6.51 | 0.38 | 68.43 | 6.14 | 3.65 | 0.38 | 90.66 | 3.59 | 5.54 | 0.38 | 130.32 | 7.26 | 5.95 | 0.54 | 55.13 | 4.64 | 6.18 | 0.38 | 170.41 | 7.29 | 6.75 | 0.38 | 70.76 | 5.33 |
| May 2019-June 2019 | 4.68 | 0.38 | 83.52 | 6.18 | 4.44 | 0.38 | 99.21 | 5.33 | 5.65 | 0.38 | 103.17 | 6.61 | 6.33 | 0.54 | 111.05 | 6.47 | 3.71 | 0.38 | 80.23 | 3.91 | 4.84 | 0.38 | 138.81 | 6.71 | 5.85 | 0.76 | 127.45 | 6.78 |
| June 2019-July 2019 | 4.22 | 0.38 | 91.48 | 5.33 | 5.88 | 0.38 | 82.58 | 5.77 | 6.22 | 0.38 | 58.65 | 5.94 | 6.25 | 0.76 | 150.33 | 7.94 | 4.41 | 0.38 | 47.21 | 4.11 | 4.62 | 0.38 | 204.53 | 7.45 | 7.60 | 0.38 | 136.25 | 8.94 |
| July 2019-Aug 2019 | 7.59 | 1.08 | 127.69 | 7.96 | 5.21 | 0.38 | 124.92 | 7.65 | 5.70 | 0.54 | 119.16 | 7.31 | 5.27 | 0.38 | 108.74 | 7.52 | 4.34 | 0.38 | 169.48 | 7.17 | 5.82 | 0.38 | 115.88 | 7.14 | 7.04 | 0.38 | 492.44 | 14.39 |
| Aug 2019-Sep 2019 | 5.90 | 0.76 | 62.35 | 6.35 | 5.87 | 0.54 | 87.72 | 6.74 | 4.74 | 0.38 | 119.14 | 5.70 | 4.88 | 0.38 | 81.03 | 4.53 | 7.08 | 0.54 | 138.98 | 6.75 | 6.43 | 0.54 | 89.01 | 6.91 | 4.92 | 0.38 | 163.93 | 6.17 |
| Sep 2019-Oct 2019 | 6.48 | 0.85 | 104.13 | 6.15 | 5.44 | 0.54 | 80.91 | 5.62 | 5.68 | 0.38 | 64.35 | 5.72 | 4.58 | 0.38 | 54.78 | 4.23 | 6.97 | 1.20 | 146.07 | 6.94 | 7.09 | 1.14 | 179.03 | 9.38 | 5.01 | 0.76 | 69.28 | 4.91 |

Table 19. Arithmetic monthly mean, maximum and minimum mass percentage of Si with standard deviation of sample particles from six sites outlined in Stephen F. Austin University Real Estate Foundation's STMicronics carbon sequestration project and one site at the SFA Beef Farm.

| Date Range | Property | | | | | | | | | | | | | | | | | | | | | | | | | | | |
|---------------------|--------------------|-------|-------|------|--------------------|-------|-------|------|--------------------|-------|-------|------|--------------------|-------|-------|------|--------------------|-------|-------|------|--------------------|-------|-------|------|-------|-------|-------|------|
| | Agriculture Center | | | | Arbor Grove | | | | Atoy | | | | Bagley Road | | | | Hilliard | | | | Maxwell | | | | Swink | | | |
| | Mass Percentage Si | | | | Mass Percentage Si | | | | Mass Percentage Si | | | | Mass Percentage Si | | | | Mass Percentage Si | | | | Mass Percentage Si | | | | | | | |
| | Mean | Min | Max | SD | Mean | Min | Max | SD | Mean | Min | Max | SD | Mean | Min | Max | SD | Mean | Min | Max | SD | Mean | Min | Max | SD | Mean | Min | Max | SD |
| Oct 2018-Nov 2018 | 49.71 | 47.91 | 51.19 | 1.49 | 45.81 | 41.11 | 50.43 | 4.43 | 49.60 | 46.93 | 51.75 | 2.18 | 48.82 | 46.19 | 51.31 | 2.77 | 49.03 | 45.90 | 51.05 | 2.29 | 48.25 | 45.05 | 51.68 | 2.83 | 47.35 | 42.34 | 50.93 | 4.07 |
| Nov 2018-Dec 2018 | 49.28 | 48.15 | 49.94 | 0.85 | 38.51 | 35.09 | 43.36 | 3.48 | 45.75 | 41.88 | 49.23 | 3.81 | - | - | - | - | 44.16 | 41.79 | 46.93 | 2.14 | 48.52 | 39.48 | 55.50 | 6.85 | 42.88 | 30.07 | 50.80 | 9.29 |
| Dec 2018-Jan 2019 | 47.65 | 42.79 | 53.94 | 4.63 | 32.55 | 27.36 | 35.07 | 3.57 | 53.86 | 48.99 | 57.86 | 3.66 | 49.65 | 45.81 | 51.31 | 2.58 | 50.41 | 46.54 | 55.03 | 3.80 | 47.70 | 38.12 | 53.84 | 7.33 | 49.62 | 46.46 | 52.58 | 2.70 |
| Jan 2019-Feb 2019 | 47.19 | 46.38 | 48.32 | 0.82 | 34.86 | 31.15 | 38.24 | 2.96 | 45.93 | 41.56 | 51.72 | 4.49 | 45.79 | 44.47 | 47.37 | 1.36 | 44.17 | 40.41 | 48.14 | 3.28 | 36.40 | 30.46 | 40.94 | 4.36 | 39.42 | 37.63 | 41.42 | 2.07 |
| Feb 2019-Mar 2019 | 33.54 | 28.16 | 43.40 | 6.76 | 9.66 | 5.52 | 17.26 | 5.19 | 30.67 | 26.25 | 32.61 | 2.98 | 38.30 | 34.25 | 44.55 | 4.52 | 14.55 | 12.48 | 16.72 | 1.84 | 14.66 | 11.84 | 17.62 | 2.40 | 12.21 | 10.34 | 13.75 | 1.43 |
| Mar 2019-Apr 2019 | 28.73 | 22.36 | 35.47 | 5.36 | 29.58 | 17.05 | 38.15 | 9.52 | 39.29 | 35.08 | 42.25 | 3.32 | 35.53 | 33.03 | 37.56 | 1.87 | 36.40 | 33.27 | 40.35 | 2.93 | 35.84 | 32.60 | 40.16 | 3.21 | 38.24 | 35.90 | 41.18 | 2.37 |
| Apr 2019-May 2019 | 37.44 | 28.73 | 44.58 | 7.21 | 36.23 | 34.58 | 40.49 | 2.85 | 41.57 | 36.81 | 48.95 | 5.78 | 40.62 | 37.54 | 43.56 | 3.00 | 45.17 | 37.03 | 48.89 | 5.47 | 39.74 | 36.15 | 41.67 | 2.48 | 50.20 | 44.12 | 56.39 | 5.50 |
| May 2019-June 2019 | 39.18 | 38.55 | 39.82 | 0.58 | 42.91 | 38.61 | 45.55 | 3.00 | 46.41 | 39.63 | 51.70 | 5.07 | 35.54 | 29.68 | 39.32 | 4.13 | 48.59 | 48.13 | 49.42 | 0.58 | 39.35 | 32.95 | 47.72 | 6.18 | 35.28 | 30.95 | 40.39 | 4.18 |
| June 2019-July 2019 | 49.09 | 46.35 | 52.85 | 2.72 | 41.70 | 36.98 | 49.56 | 5.74 | 35.81 | 28.34 | 41.19 | 5.79 | 45.54 | 37.92 | 50.83 | 5.83 | 49.60 | 46.87 | 52.29 | 2.22 | 48.06 | 46.41 | 49.46 | 1.30 | 35.40 | 35.17 | 36.04 | 0.43 |
| July 2019-Aug 2019 | 37.47 | 31.19 | 46.18 | 6.97 | 41.79 | 37.27 | 45.46 | 3.95 | 46.56 | 40.25 | 51.96 | 5.08 | 44.80 | 37.77 | 49.69 | 5.62 | 49.89 | 46.11 | 53.40 | 2.98 | 41.66 | 34.16 | 45.23 | 5.22 | 41.42 | 38.00 | 44.48 | 2.68 |
| Aug 2019-Sep 2019 | 46.65 | 42.89 | 49.92 | 2.91 | 44.17 | 42.72 | 47.40 | 2.19 | 45.74 | 41.85 | 49.65 | 3.20 | 42.83 | 40.19 | 46.76 | 3.00 | 38.86 | 35.10 | 44.65 | 4.07 | 42.88 | 42.27 | 44.09 | 0.83 | 44.44 | 39.32 | 50.50 | 4.60 |
| Sep 2019-Oct 2019 | 25.78 | 22.71 | 30.63 | 3.58 | 28.83 | 26.01 | 32.80 | 3.14 | 31.99 | 27.49 | 34.09 | 3.05 | 30.50 | 27.74 | 31.96 | 1.89 | 27.59 | 25.92 | 29.38 | 1.42 | 28.95 | 26.71 | 32.52 | 2.50 | 30.01 | 29.13 | 30.59 | 0.70 |

Table 20. Arithmetic monthly mean, maximum and minimum mass percentage of O with standard deviation of sample particles from six sites outlined in Stephen F. Austin University Real Estate Foundation's STMicroelectronics carbon sequestration project and one site at the SFA Beef Farm.

| Date Range | Property | | | | | | | | | | | | | | | | | | | | | | | | | | | |
|---------------------|--------------------|-------|-------|------|-------------------|-------|-------|------|-------------------|-------|-------|------|-------------------|-------|-------|------|-------------------|-------|-------|------|-------------------|-------|-------|------|-------|-------|-------|------|
| | Agriculture Center | | | | Arbor Grove | | | | Atoy | | | | Bagley Road | | | | Hilliard | | | | Maxwell | | | | Swink | | | |
| | Mass Percentage O | | | | Mass Percentage O | | | | Mass Percentage O | | | | Mass Percentage O | | | | Mass Percentage O | | | | Mass Percentage O | | | | | | | |
| | Mean | Min | Max | SD | Mean | Min | Max | SD | Mean | Min | Max | SD | Mean | Min | Max | SD | Mean | Min | Max | SD | Mean | Min | Max | SD | Mean | Min | Max | SD |
| Oct 2018-Nov 2018 | 32.47 | 30.78 | 34.31 | 1.54 | 30.35 | 27.79 | 33.39 | 2.58 | 32.9 | 32.19 | 33.71 | 0.63 | 32.2 | 30.9 | 32.87 | 0.89 | 32.65 | 30.26 | 37.93 | 3.56 | 31.91 | 29.71 | 32.91 | 1.48 | 31.69 | 30.27 | 33.17 | 1.39 |
| Nov 2018-Dec 2018 | 30.99 | 29.8 | 32.54 | 1.17 | 30.68 | 27.41 | 33.49 | 2.57 | 35.46 | 28.89 | 41.67 | 5.23 | - | - | - | - | 32.45 | 28.54 | 36.64 | 4.43 | 31.94 | 30.78 | 33.79 | 1.38 | 35.08 | 30.56 | 39.47 | 4.33 |
| Dec 2018-Jan 2019 | 32.58 | 29.46 | 36.82 | 3.08 | 25.48 | 23.17 | 27.78 | 1.98 | 32.87 | 30.65 | 34.87 | 1.83 | 30.25 | 28.98 | 31.9 | 1.27 | 30.20 | 28.21 | 32.39 | 1.80 | 32.49 | 29.81 | 35.38 | 2.36 | 30.20 | 29.61 | 31.11 | 0.64 |
| Jan 2019-Feb 2019 | 31.16 | 29.53 | 32.54 | 1.24 | 22.84 | 21.11 | 25.2 | 1.91 | 28.12 | 26.34 | 30.97 | 2.03 | 30.92 | 30.14 | 31.96 | 0.78 | 29.80 | 29.25 | 31.18 | 0.92 | 25.75 | 22.69 | 28.75 | 2.56 | 29.28 | 27.96 | 31.32 | 1.45 |
| Feb 2019-Mar 2019 | 24.44 | 22.32 | 28.58 | 2.84 | 19.77 | 13.45 | 31.36 | 7.99 | 22.19 | 18.91 | 25.05 | 2.99 | 27.36 | 24.55 | 30.05 | 2.26 | 42.93 | 33.06 | 48.45 | 6.80 | 40.10 | 35.52 | 46.33 | 4.55 | 32.25 | 30.14 | 34.47 | 1.94 |
| Mar 2019-Apr 2019 | 21.53 | 20.61 | 23.82 | 1.53 | 26.1 | 23.83 | 28.68 | 2.16 | 37.04 | 35.96 | 38.59 | 1.25 | 25.07 | 23.91 | 26.46 | 1.29 | 35.66 | 33.34 | 36.94 | 1.59 | 35.97 | 32.33 | 38.54 | 2.61 | 26.50 | 24.11 | 28.17 | 1.72 |
| Apr 2019-May 2019 | 25.99 | 23.73 | 29.6 | 2.52 | 24.54 | 23.84 | 25.87 | 0.92 | 29.29 | 26.87 | 31.44 | 1.92 | 26.52 | 24.64 | 29.23 | 1.98 | 30.95 | 30.72 | 31.19 | 0.20 | 26.68 | 23.94 | 28.06 | 1.90 | 34.69 | 30.01 | 38.03 | 3.48 |
| May 2019-June 2019 | 27.25 | 24.81 | 29.74 | 2.34 | 28.72 | 27.2 | 30.2 | 1.56 | 30.85 | 29.99 | 32.15 | 0.94 | 26.98 | 26.74 | 27.22 | 0.2 | 30.26 | 28.89 | 31.15 | 0.96 | 29.40 | 25.42 | 33.18 | 3.17 | 23.37 | 22.40 | 24.33 | 0.79 |
| June 2019-July 2019 | 31.68 | 29.57 | 33.24 | 1.59 | 30.21 | 26 | 32.08 | 2.83 | 26.19 | 24.71 | 27.46 | 1.15 | 31.43 | 30.48 | 33.07 | 1.16 | 32.73 | 31.42 | 34.11 | 1.41 | 31.13 | 30.29 | 32.30 | 0.85 | 30.04 | 26.53 | 31.52 | 2.38 |
| July 2019-Aug 2019 | 29.26 | 28.09 | 32.38 | 2.09 | 27.7 | 25.92 | 29.26 | 1.38 | 32.12 | 29.43 | 34.7 | 2.23 | 30.81 | 29.49 | 32.52 | 1.52 | 30.75 | 29.64 | 31.38 | 0.76 | 29.03 | 27.86 | 30.18 | 1.27 | 31.11 | 27.71 | 34.14 | 3.31 |
| Aug 2019-Sep 2019 | 31.32 | 30.05 | 32.68 | 1.44 | 29.62 | 28.61 | 30.53 | 0.89 | 30.03 | 27.83 | 31.61 | 1.58 | 29.38 | 28.63 | 31.26 | 1.26 | 27.67 | 26.76 | 29.05 | 1.01 | 28.23 | 27.22 | 29.15 | 0.80 | 29.94 | 27.68 | 33.54 | 2.52 |
| Sep 2019-Oct 2019 | 32.69 | 32.08 | 33.6 | 0.64 | 32.01 | 29.54 | 34.15 | 2.46 | 35.44 | 32.27 | 37.96 | 2.35 | 34.19 | 32.44 | 36.1 | 1.5 | 31.32 | 30.71 | 31.83 | 0.48 | 32.84 | 29.84 | 36.70 | 2.94 | 33.70 | 32.34 | 35.19 | 1.27 |

Table 21. Arithmetic monthly mean, maximum and minimum mass percentage of C with standard deviation of sample particles from six sites outlined in Stephen F. Austin University Real Estate Foundation's STMicroelectronics carbon sequestration project and one site at the SFA Beef Farm.

| Date Range | Property | | | | | | | | | | | | | | | | | | | | | | | | | | | | | | | |
|---------------------|--------------------|-------|-------|------|-------------------|-------|-------|-------|-------------------|-------|-------|------|-------------------|-------|-------|------|-------------------|-------|-------|------|-------------------|-------|-------|------|-------|-------|-------|------|------|------|------|------|
| | Agriculture Center | | | | Arbor Grove | | | | Atoy | | | | Bagley Road | | | | Hilliard | | | | Maxwell | | | | Swink | | | | | | | |
| | Mass Percentage C | | | | Mass Percentage C | | | | Mass Percentage C | | | | Mass Percentage C | | | | Mass Percentage C | | | | Mass Percentage C | | | | | | | | | | | |
| | Mean | Min | Max | SD | Mean | Min | Max | SD | Mean | Min | Max | SD | Mean | Min | Max | SD | Mean | Min | Max | SD | Mean | Min | Max | SD | Mean | Min | Max | SD | | | | |
| Oct 2018-Nov 2018 | 10.06 | 10.06 | 10.06 | 0 | 8.41 | 7.49 | 9.19 | 0.74 | 10.06 | 10.06 | 10.06 | 0 | 3.91 | 3.91 | 3.91 | 0 | 0 | 0 | 0 | 0 | 10.06 | 10.06 | 10.06 | 0 | 10.06 | 10.06 | 10.06 | 0 | 5.45 | 4.98 | 5.91 | 0.38 |
| Nov 2018-Dec 2018 | 10.06 | 10.06 | 10.06 | 0 | 9.87 | 6.50 | 12.01 | 2.50 | 10.06 | 10.06 | 10.06 | 0 | - | - | - | - | 10.06 | 10.06 | 10.06 | 0 | 6.47 | 6.04 | 6.91 | 0.36 | 23.88 | 23.88 | 23.88 | 0 | 0 | 0 | 0 | 0 |
| Dec 2018-Jan 2019 | 2.14 | 0 | 4.27 | 1.74 | 17.60 | 16.70 | 18.84 | 0.98 | 0 | 0 | 0 | 0 | 0 | 0 | 0 | 0 | 10.06 | 10.06 | 10.06 | 0 | 2.83 | 0 | 8.49 | 4 | 0 | 0 | 0 | 0 | 0 | 0 | 0 | 0 |
| Jan 2019-Feb 2019 | 10.06 | 10.06 | 10.06 | 0 | 15.07 | 13.54 | 16.60 | 1.25 | 4.52 | 3.19 | 5.75 | 1.05 | 0 | 0 | 0 | 0 | 4.72 | 4.42 | 4.98 | 0.23 | 10.06 | 10.06 | 10.06 | 0 | 11.37 | 9.77 | 13.28 | 1.68 | 0 | 0 | 0 | 0 |
| Feb 2019-Mar 2019 | 18.38 | 15.78 | 19.74 | 1.84 | 36.68 | 28.22 | 59.37 | 15.14 | 17.14 | 11.7 | 26.53 | 6.67 | 11.55 | 9.44 | 14.75 | 2.36 | 35.53 | 22.11 | 45.72 | 12 | 31.81 | 25.43 | 34.14 | 4.26 | 19.24 | 17.31 | 20.77 | 1.59 | 0 | 0 | 0 | 0 |
| Mar 2019-Apr 2019 | 10.06 | 10.06 | 10.06 | 0 | 21.44 | 10.19 | 35.58 | 12.24 | 9.02 | 7.67 | 10.78 | 1.56 | 10.06 | 10.06 | 10.06 | 0 | 10.67 | 7.53 | 14.95 | 3.16 | 13.38 | 10.38 | 17.54 | 3.24 | 10.06 | 10.06 | 10.06 | 0 | 0 | 0 | 0 | 0 |
| Apr 2019-May 2019 | 10.06 | 10.06 | 10.06 | 0 | 12.49 | 10.83 | 14.15 | 1.36 | 2.99 | 2.99 | 2.99 | 0 | 13.04 | 13.04 | 13.04 | 0 | 0 | 0 | 0 | 0 | 10.06 | 10.06 | 10.06 | 0 | 0 | 0 | 0 | 0 | 0 | 0 | 0 | 0 |
| May 2019-June 2019 | 10.06 | 10.06 | 10.06 | 0 | 7.63 | 6.46 | 9.61 | 1.41 | 0 | 0 | 0 | 0 | 0 | 0 | 0 | 0 | 6.62 | 6.62 | 6.62 | 0 | 0 | 0 | 0 | 0 | 10.06 | 10.06 | 10.06 | 0 | 0 | 0 | 0 | 0 |
| June 2019-July 2019 | 0 | 0 | 0 | 0 | 6.70 | 5.58 | 7.22 | 0.76 | 12.08 | 9.83 | 14.89 | 2.30 | 4.89 | 0 | 9.02 | 3.72 | 0 | 0 | 0 | 0 | 4.36 | 3.78 | 5.55 | 0.81 | 12.86 | 10.24 | 17.27 | 3.08 | 0 | 0 | 0 | 0 |
| July 2019-Aug 2019 | 12.27 | 7.88 | 16.56 | 3.61 | 9.40 | 8.22 | 11.36 | 1.41 | 7.02 | 4.48 | 10.56 | 2.58 | 7.66 | 5.83 | 11.40 | 2.57 | 4.30 | 4.07 | 4.53 | 0.19 | 8.10 | 4.90 | 12.76 | 3.32 | 8.00 | 6.43 | 10.43 | 1.74 | 0 | 0 | 0 | 0 |
| Aug 2019-Sep 2019 | 3.61 | 3.52 | 3.70 | 0.07 | 7.22 | 6.34 | 7.72 | 0.62 | 4.13 | 3.85 | 4.43 | 0.24 | 7.24 | 4.87 | 12.43 | 3.49 | 6.00 | 5.39 | 7.20 | 0.83 | 6.04 | 5.22 | 6.61 | 0.61 | 7.08 | 5.8 | 8.43 | 1.22 | 0 | 0 | 0 | 0 |
| Sep 2019-Oct 2019 | 10.79 | 6.78 | 13.66 | 3.18 | 5.82 | 5.39 | 6.25 | 0.35 | 10.06 | 10.06 | 10.06 | 0 | 5.74 | 5.74 | 5.74 | 0 | 6.37 | 5.28 | 7.27 | 0.88 | 5.62 | 5.09 | 6.24 | 0.48 | 5.54 | 5.54 | 5.54 | 0 | 0 | 0 | 0 | 0 |

Table 22. Arithmetic monthly mean, maximum and minimum mass percentage of Ba with standard deviation of sample particles from six sites outlined in Stephen F. Austin University Real Estate Foundation's STMicronics carbon sequestration project and one site at the SFA Beef Farm.

| Date Range | Property | | | | | | | | | | | | | | | | | | | | | | | | | | | |
|---------------------|--------------------|------|-------|------|--------------------|------|-------|------|--------------------|------|-------|------|--------------------|-------|-------|------|--------------------|------|-------|------|--------------------|------|-------|------|-------|------|-------|------|
| | Agriculture Center | | | | Arbor Grove | | | | Atoy | | | | Bagley Road | | | | Hilliard | | | | Maxwell | | | | Swink | | | |
| | Mass Percentage Ba | | | | Mass Percentage Ba | | | | Mass Percentage Ba | | | | Mass Percentage Ba | | | | Mass Percentage Ba | | | | Mass Percentage Ba | | | | | | | |
| | Mean | Min | Max | SD | Mean | Min | Max | SD | Mean | Min | Max | SD | Mean | Min | Max | SD | Mean | Min | Max | SD | Mean | Min | Max | SD | Mean | Min | Max | SD |
| Oct 2018-Nov 2018 | 10.48 | 8.90 | 13.6 | 2.12 | 1.39 | 0 | 5.54 | 2.77 | 9.31 | 8.54 | 10.1 | 0.64 | 9.32 | 8.80 | 9.89 | 0.45 | 7.43 | 0 | 10.42 | 4.97 | 9.43 | 8.03 | 10.55 | 1.04 | 9.48 | 8.98 | 9.86 | 0.37 |
| Nov 2018-Dec 2018 | 9.75 | 8.83 | 10.28 | 0.63 | 1.92 | 0 | 7.69 | 3.85 | 2.23 | 0 | 8.92 | 4.46 | - | - | - | - | 5.27 | 0 | 10.76 | 6.08 | 6.99 | 0 | 10.19 | 4.70 | 4.82 | 0 | 9.86 | 5.57 |
| Dec 2018-Jan 2019 | 7.79 | 0 | 11.09 | 5.21 | 3.66 | 0 | 7.69 | 4.24 | 9.45 | 8.62 | 10.18 | 0.81 | 11.15 | 10.32 | 11.86 | 0.76 | 9.84 | 9.45 | 10.36 | 0.39 | 7.10 | 0 | 10.88 | 4.86 | 9.80 | 9.48 | 10.13 | 0.29 |
| Jan 2019-Feb 2019 | 9.14 | 8.54 | 9.98 | 0.71 | 5.92 | 4.93 | 7.54 | 1.13 | 6.87 | 5.33 | 7.74 | 1.06 | 8.35 | 7.23 | 8.90 | 0.79 | 8.88 | 8.38 | 9.13 | 0.34 | 6.59 | 5.12 | 7.84 | 1.14 | 6.47 | 6.15 | 7.16 | 0.47 |
| Feb 2019-Mar 2019 | 6.06 | 3.94 | 7.80 | 1.61 | 2.07 | 0 | 4.58 | 1.91 | 5.75 | 5.02 | 6.36 | 0.69 | 5.57 | 4.85 | 6.03 | 0.51 | 2.28 | 1.83 | 2.70 | 0.37 | 3.00 | 2.51 | 3.34 | 0.35 | 2.65 | 2.23 | 3.35 | 0.51 |
| Mar 2019-Apr 2019 | 4.07 | 0 | 7.75 | 3.19 | 6.31 | 4.21 | 7.43 | 1.48 | 6.43 | 6.03 | 6.97 | 0.39 | 6.67 | 6.27 | 7.22 | 0.44 | 6.28 | 5.10 | 7.37 | 1.01 | 5.53 | 4.01 | 6.44 | 1.07 | 6.78 | 6.14 | 7.45 | 0.60 |
| Apr 2019-May 2019 | 6.55 | 4.91 | 7.65 | 1.22 | 7.92 | 7.04 | 8.71 | 0.70 | 6.20 | 5.07 | 7.36 | 0.94 | 5.92 | 5.27 | 6.62 | 0.58 | 7.53 | 0 | 10.78 | 5.06 | 7.11 | 5.84 | 8.14 | 1.09 | 7.63 | 0 | 11.03 | 5.13 |
| May 2019-June 2019 | 7.28 | 6.13 | 8.84 | 1.14 | 9.05 | 8.04 | 9.58 | 0.72 | 6.57 | 0 | 10.07 | 4.48 | 1.48 | 0 | 5.90 | 2.95 | 9.65 | 9.33 | 10.28 | 0.43 | 1.94 | 0 | 7.76 | 3.88 | 3.70 | 0 | 9.07 | 4.48 |
| June 2019-July 2019 | 9.90 | 8.09 | 11.66 | 1.48 | 4.15 | 0 | 8.69 | 4.80 | 4.72 | 0 | 10.26 | 5.49 | 7.89 | 0 | 12.78 | 5.50 | 8.93 | 7.52 | 9.55 | 0.95 | 9.72 | 9.24 | 10.86 | 0.77 | 1.23 | 0 | 4.92 | 2.46 |
| July 2019-Aug 2019 | 4.25 | 0 | 9.15 | 4.93 | 8.81 | 8.32 | 9.36 | 0.43 | 7.47 | 0 | 10.58 | 5.03 | 7.24 | 0 | 10.26 | 4.85 | 9.69 | 8.79 | 11.07 | 1.05 | 6.86 | 0 | 9.66 | 4.60 | 4.65 | 0 | 10.14 | 5.41 |
| Aug 2019-Sep 2019 | 9.83 | 9.36 | 10.76 | 0.64 | 9.40 | 8.78 | 10.12 | 0.69 | 10.05 | 9.23 | 10.65 | 0.60 | 9.03 | 7.70 | 9.70 | 0.92 | 7.30 | 6.38 | 7.80 | 0.63 | 9.62 | 8.51 | 10.19 | 0.76 | 8.91 | 8.56 | 9.31 | 0.41 |
| Sep 2019-Oct 2019 | 5.01 | 3.91 | 5.67 | 0.77 | 5.49 | 4.90 | 5.92 | 0.45 | 6.28 | 5.68 | 6.57 | 0.41 | 5.91 | 5.40 | 6.32 | 0.38 | 5.08 | 3.84 | 5.74 | 0.84 | 5.33 | 4.38 | 6.46 | 0.89 | 6.38 | 5.67 | 7.19 | 0.66 |

Table 23. Arithmetic monthly mean, maximum and minimum mass percentage of Na with standard deviation of sample particles from six sites outlined in Stephen F. Austin University Real Estate Foundation's STMicroelectronics carbon sequestration project and one site at the SFA Beef Farm.

| Date Range | Property | | | | | | | | | | | | | | | | | | | | | | | | | | | |
|---------------------|--------------------|------|------|------|--------------------|------|------|------|--------------------|------|------|------|--------------------|------|------|------|--------------------|------|------|------|--------------------|------|-------|------|-------|------|-------|------|
| | Agriculture Center | | | | Arbor Grove | | | | Atoy | | | | Bagley Road | | | | Hilliard | | | | Maxwell | | | | Swink | | | |
| | Mass Percentage Na | | | | Mass Percentage Na | | | | Mass Percentage Na | | | | Mass Percentage Na | | | | Mass Percentage Na | | | | Mass Percentage Na | | | | | | | |
| | Mean | Min | Max | SD | Mean | Min | Max | SD | Mean | Min | Max | SD | Mean | Min | Max | SD | Mean | Min | Max | SD | Mean | Min | Max | SD | Mean | Min | Max | SD |
| Oct 2018-Nov 2018 | 7.96 | 7.05 | 9.10 | 0.85 | 2.52 | 1.49 | 4.13 | 1.16 | 8.08 | 7.31 | 9.33 | 0.92 | 8.12 | 7.48 | 8.54 | 0.45 | 7.95 | 6.29 | 9.53 | 1.49 | 7.83 | 7.18 | 8.77 | 0.70 | 7.63 | 7.28 | 8.06 | 0.39 |
| Nov 2018-Dec 2018 | 7.82 | 7.22 | 8.22 | 0.45 | 6.04 | 4.98 | 6.90 | 0.81 | 5.71 | 0 | 8.35 | 3.93 | - | - | - | - | 7.98 | 6.53 | 9.14 | 1.14 | 6.31 | 5.09 | 7.72 | 1.18 | 6.60 | 4.01 | 8.92 | 2.02 |
| Dec 2018-Jan 2019 | 7.66 | 6.29 | 8.82 | 1.06 | 4.65 | 4.07 | 5.17 | 0.45 | 7.67 | 6.94 | 8.94 | 0.88 | 7.85 | 7.23 | 8.69 | 0.61 | 7.76 | 7.28 | 8.48 | 0.53 | 7.15 | 5.94 | 7.82 | 0.83 | 7.76 | 6.93 | 8.50 | 0.65 |
| Jan 2019-Feb 2019 | 8.48 | 8.18 | 8.66 | 0.21 | 4.10 | 3.04 | 5.05 | 0.94 | 4.49 | 3.43 | 5.16 | 0.74 | 7.17 | 6.73 | 7.89 | 0.53 | 7.37 | 7.15 | 7.54 | 0.18 | 6.98 | 5.15 | 8.35 | 1.59 | 5.63 | 5.10 | 6.09 | 0.45 |
| Feb 2019-Mar 2019 | 5.42 | 4.43 | 6.10 | 0.80 | 0.94 | 0 | 2.57 | 1.22 | 5.29 | 3.32 | 6.52 | 1.41 | 6.39 | 5.39 | 6.81 | 0.67 | 2.64 | 1.90 | 3.71 | 0.78 | 4.11 | 2.89 | 5.70 | 1.19 | 3.10 | 2.76 | 3.49 | 0.39 |
| Mar 2019-Apr 2019 | 4.82 | 3.41 | 6.80 | 1.61 | 4.84 | 2.63 | 6.67 | 1.84 | 6.49 | 5.95 | 7.71 | 0.82 | 6.03 | 5.31 | 6.87 | 0.72 | 7.19 | 6.78 | 7.81 | 0.44 | 5.71 | 4.91 | 6.66 | 0.79 | 6.31 | 5.61 | 6.79 | 0.57 |
| Apr 2019-May 2019 | 7.17 | 5.56 | 8.66 | 1.44 | 6.21 | 5.47 | 7.30 | 0.81 | 7.28 | 6.56 | 8.98 | 1.15 | 6.75 | 5.42 | 7.72 | 0.96 | 7.66 | 6.88 | 8.70 | 0.77 | 6.79 | 5.11 | 7.92 | 1.22 | 6.92 | 6.36 | 7.38 | 0.53 |
| May 2019-June 2019 | 7.30 | 5.13 | 8.98 | 1.64 | 6.96 | 5.39 | 8.68 | 1.58 | 6.85 | 6.56 | 7.04 | 0.21 | 5.63 | 4.47 | 7.10 | 1.28 | 6.73 | 6.40 | 7.42 | 0.47 | 7.72 | 6.09 | 10.63 | 2.08 | 6.24 | 4.99 | 8.21 | 1.39 |
| June 2019-July 2019 | 7.82 | 7.26 | 8.35 | 0.52 | 6.95 | 5.43 | 7.68 | 1.06 | 5.73 | 5.51 | 6.09 | 0.28 | 6.33 | 6.01 | 6.89 | 0.39 | 8.08 | 7.31 | 9.10 | 0.81 | 8.18 | 7.55 | 8.39 | 0.42 | 5.03 | 3.20 | 5.80 | 1.23 |
| July 2019-Aug 2019 | 6.34 | 5.62 | 7.64 | 0.89 | 6.57 | 5.31 | 7.84 | 1.04 | 7.49 | 6.69 | 8.09 | 0.58 | 7.10 | 5.25 | 9.20 | 1.62 | 7.29 | 6.77 | 7.70 | 0.40 | 6.68 | 5.11 | 7.61 | 1.10 | 6.32 | 5.29 | 7.05 | 0.79 |
| Aug 2019-Sep 2019 | 8.17 | 7.60 | 9.34 | 0.81 | 7.44 | 6.86 | 7.94 | 0.51 | 8.07 | 7.33 | 8.98 | 0.77 | 7.02 | 6.74 | 7.37 | 0.26 | 5.39 | 4.86 | 5.82 | 0.40 | 7.76 | 6.83 | 8.27 | 0.64 | 8.18 | 7.36 | 10.33 | 1.44 |
| Sep 2019-Oct 2019 | 6.32 | 5.37 | 7.65 | 1.07 | 7.17 | 6.39 | 8.33 | 0.89 | 7.20 | 5.73 | 8.80 | 1.36 | 7.06 | 6.59 | 7.26 | 0.32 | 6.21 | 5.92 | 6.33 | 0.19 | 7.02 | 6.81 | 7.53 | 0.35 | 6.92 | 6.22 | 7.86 | 0.76 |

Table 24. Arithmetic monthly mean, maximum and minimum mass percentage of Al with standard deviation of sample particles from six sites outlined in Stephen F. Austin University Real Estate Foundation's STMicroelectronics carbon sequestration project and one site at the SFA Beef Farm.

| Date Range | Property | | | | | | | | | | | | | | | | | | | | | | | | | | | |
|---------------------|--------------------|------|------|------|--------------------|------|------|------|--------------------|------|------|------|--------------------|------|------|------|--------------------|------|------|------|--------------------|------|------|------|-------|------|------|------|
| | Agriculture Center | | | | Arbor Grove | | | | Atoy | | | | Bagley Road | | | | Hilliard | | | | Maxwell | | | | Swink | | | |
| | Mass Percentage Al | | | | Mass Percentage Al | | | | Mass Percentage Al | | | | Mass Percentage Al | | | | Mass Percentage Al | | | | Mass Percentage Al | | | | | | | |
| | Mean | Min | Max | SD | Mean | Min | Max | SD | Mean | Min | Max | SD | Mean | Min | Max | SD | Mean | Min | Max | SD | Mean | Min | Max | SD | Mean | Min | Max | SD |
| Oct 2018-Nov 2018 | 3.70 | 3.46 | 4.12 | 0.30 | 5.46 | 4.49 | 6.17 | 0.78 | 3.67 | 3.20 | 4.04 | 0.40 | 3.62 | 3.28 | 4.03 | 0.32 | 2.75 | 0 | 4.04 | 1.85 | 3.57 | 3.21 | 3.92 | 0.30 | 3.77 | 3.33 | 4.08 | 0.34 |
| Nov 2018-Dec 2018 | 3.65 | 3.39 | 3.99 | 0.27 | 2.34 | 0 | 3.57 | 1.59 | 3.34 | 2.77 | 4.18 | 0.61 | - | - | - | - | 3.18 | 2.96 | 3.45 | 0.21 | 2.93 | 0 | 4.61 | 2.04 | 3.82 | 2.37 | 4.54 | 1.00 |
| Dec 2018-Jan 2019 | 3.62 | 3.05 | 4.35 | 0.55 | 2.25 | 0 | 3.35 | 1.52 | 4.11 | 3.83 | 4.41 | 0.27 | 3.71 | 3.54 | 4.04 | 0.23 | 3.70 | 3.21 | 4.27 | 0.44 | 3.73 | 2.97 | 4.25 | 0.58 | 2.78 | 0 | 3.86 | 1.86 |
| Jan 2019-Feb 2019 | 3.67 | 3.43 | 3.86 | 0.19 | 3.17 | 2.59 | 4.00 | 0.60 | 5.62 | 4.31 | 6.70 | 1.00 | 3.62 | 3.42 | 3.74 | 0.14 | 3.27 | 2.85 | 3.96 | 0.49 | 3.12 | 2.13 | 3.84 | 0.72 | 3.43 | 3.07 | 3.80 | 0.31 |
| Feb 2019-Mar 2019 | 3.29 | 2.63 | 4.47 | 0.87 | 0.63 | 0.00 | 1.67 | 0.80 | 2.64 | 2.26 | 3.48 | 0.58 | 3.22 | 2.90 | 3.55 | 0.27 | 2.59 | 2.27 | 3.07 | 0.34 | 1.89 | 1.58 | 2.46 | 0.39 | 1.79 | 1.53 | 2.01 | 0.21 |
| Mar 2019-Apr 2019 | 2.69 | 2.26 | 3.26 | 0.49 | 2.45 | 1.40 | 3.28 | 0.78 | 3.28 | 2.68 | 3.60 | 0.42 | 3.30 | 2.76 | 4.12 | 0.58 | 3.05 | 2.54 | 3.40 | 0.39 | 3.22 | 2.88 | 3.79 | 0.40 | 3.70 | 3.24 | 4.09 | 0.39 |
| Apr 2019-May 2019 | 2.73 | 2.15 | 3.19 | 0.43 | 3.19 | 2.78 | 3.61 | 0.34 | 3.94 | 3.03 | 4.98 | 0.80 | 3.46 | 3.09 | 3.89 | 0.34 | 3.47 | 2.50 | 3.89 | 0.65 | 3.73 | 3.21 | 4.05 | 0.39 | 3.08 | 0 | 4.66 | 2.09 |
| May 2019-June 2019 | 3.30 | 3.09 | 3.74 | 0.30 | 3.20 | 3.02 | 3.51 | 0.23 | 3.66 | 3.04 | 3.99 | 0.42 | 2.58 | 0 | 4.47 | 1.93 | 3.70 | 3.54 | 3.84 | 0.13 | 0.85 | 0 | 3.39 | 1.70 | 0.82 | 0 | 3.27 | 1.63 |
| June 2019-July 2019 | 3.92 | 3.66 | 4.52 | 0.41 | 3.31 | 2.92 | 4.19 | 0.59 | 1.50 | 0 | 3.27 | 1.74 | 2.77 | 0 | 4.23 | 1.90 | 3.99 | 3.61 | 4.42 | 0.33 | 3.95 | 3.87 | 4.10 | 0.10 | 3.14 | 2.89 | 3.48 | 0.27 |
| July 2019-Aug 2019 | 3.29 | 2.62 | 3.90 | 0.71 | 3.17 | 2.68 | 3.53 | 0.43 | 3.81 | 3.51 | 4.23 | 0.32 | 3.75 | 3.24 | 4.52 | 0.54 | 3.75 | 3.40 | 4.13 | 0.32 | 3.35 | 2.82 | 3.77 | 0.40 | 3.05 | 2.81 | 3.32 | 0.22 |
| Aug 2019-Sep 2019 | 3.63 | 3.12 | 4.14 | 0.42 | 3.86 | 3.59 | 4.22 | 0.26 | 3.50 | 2.78 | 4.17 | 0.57 | 3.49 | 3.29 | 3.68 | 0.20 | 3.35 | 3.07 | 4.01 | 0.44 | 3.29 | 3.13 | 3.47 | 0.14 | 3.63 | 2.94 | 4.59 | 0.69 |
| Sep 2019-Oct 2019 | 2.86 | 2.32 | 3.74 | 0.62 | 3.08 | 2.71 | 3.69 | 0.46 | 3.59 | 3.17 | 3.89 | 0.33 | 3.23 | 2.89 | 3.55 | 0.35 | 3.14 | 2.91 | 3.33 | 0.20 | 3.07 | 2.52 | 3.91 | 0.63 | 3.20 | 2.72 | 3.70 | 0.40 |

Table 25. Arithmetic monthly mean, maximum and minimum mass percentage of K with standard deviation of sample particles from six sites outlined in Stephen F. Austin University Real Estate Foundation's STMicroelectronics carbon sequestration project and one site at the SFA Beef Farm.

| Date Range | Property | | | | | | | | | | | | | | | | | | | | | | | | | | | |
|---------------------|--------------------|------|------|------|-------------------|------|------|------|-------------------|------|------|------|-------------------|------|------|------|-------------------|------|------|------|-------------------|------|------|------|-------|------|------|------|
| | Agriculture Center | | | | Arbor Grove | | | | Atoy | | | | Bagley Road | | | | Hilliard | | | | Maxwell | | | | Swink | | | |
| | Mass Percentage K | | | | Mass Percentage K | | | | Mass Percentage K | | | | Mass Percentage K | | | | Mass Percentage K | | | | Mass Percentage K | | | | | | | |
| | Mean | Min | Max | SD | Mean | Min | Max | SD | Mean | Min | Max | SD | Mean | Min | Max | SD | Mean | Min | Max | SD | Mean | Min | Max | SD | Mean | Min | Max | SD |
| Oct 2018-Nov 2018 | 4.77 | 4.04 | 5.99 | 0.85 | 2.68 | 2.32 | 3.49 | 0.56 | 4.39 | 4.18 | 4.62 | 0.19 | 4.31 | 4.14 | 4.48 | 0.15 | 3.66 | 2.76 | 4.04 | 0.61 | 4.38 | 3.72 | 4.83 | 0.47 | 4.41 | 4.32 | 4.50 | 0.08 |
| Nov 2018-Dec 2018 | 4.15 | 3.35 | 4.79 | 0.68 | 2.15 | 0 | 3.35 | 1.48 | 2.15 | 0 | 2.93 | 1.44 | - | - | - | - | 3.51 | 2.85 | 4.12 | 0.69 | 3.34 | 2.54 | 3.82 | 0.56 | 3.04 | 1.95 | 3.74 | 0.83 |
| Dec 2018-Jan 2019 | 3.97 | 3.77 | 4.12 | 0.16 | 2.73 | 2.11 | 3.34 | 0.52 | 3.75 | 3.60 | 3.98 | 0.17 | 3.03 | 0 | 4.19 | 2.02 | 3.71 | 3.37 | 3.92 | 0.24 | 3.48 | 2.87 | 3.91 | 0.50 | 3.59 | 3.34 | 4.08 | 0.33 |
| Jan 2019-Feb 2019 | 4.48 | 4.30 | 4.82 | 0.23 | 3.42 | 2.71 | 4.40 | 0.71 | 3.72 | 3.10 | 4.06 | 0.42 | 4.33 | 4.17 | 4.48 | 0.13 | 4.00 | 3.76 | 4.16 | 0.17 | 4.71 | 3.81 | 5.50 | 0.70 | 3.60 | 3.41 | 3.91 | 0.22 |
| Feb 2019-Mar 2019 | 3.55 | 2.80 | 4.40 | 0.67 | 1.01 | 0 | 2.05 | 0.85 | 3.38 | 2.56 | 4.39 | 0.77 | 3.69 | 3.63 | 3.77 | 0.06 | 1.18 | 0.90 | 1.73 | 0.38 | 1.97 | 1.76 | 2.06 | 0.14 | 1.79 | 1.61 | 1.92 | 0.14 |
| Mar 2019-Apr 2019 | 3.10 | 1.60 | 3.78 | 1.01 | 3.00 | 2.10 | 3.59 | 0.69 | 3.10 | 2.84 | 3.25 | 0.18 | 3.99 | 3.80 | 4.31 | 0.22 | 3.13 | 2.68 | 3.42 | 0.35 | 2.83 | 2.68 | 2.96 | 0.11 | 4.63 | 4.18 | 5.14 | 0.50 |
| Apr 2019-May 2019 | 4.71 | 3.98 | 6.23 | 1.05 | 3.76 | 3.46 | 4.25 | 0.36 | 4.81 | 4.55 | 5.10 | 0.24 | 3.69 | 3.26 | 3.98 | 0.32 | 3.44 | 2.79 | 3.83 | 0.45 | 4.40 | 3.90 | 4.80 | 0.43 | 4.13 | 3.59 | 4.54 | 0.45 |
| May 2019-June 2019 | 4.84 | 3.64 | 5.65 | 0.85 | 3.71 | 3.40 | 3.96 | 0.23 | 3.41 | 2.75 | 3.88 | 0.48 | 3.52 | 2.60 | 4.83 | 0.94 | 3.66 | 3.44 | 4.01 | 0.25 | 3.33 | 2.37 | 4.05 | 0.75 | 2.68 | 0 | 5.04 | 2.08 |
| June 2019-July 2019 | 4.55 | 4.34 | 4.92 | 0.26 | 3.10 | 2.64 | 3.72 | 0.48 | 3.27 | 2.85 | 3.64 | 0.36 | 3.99 | 3.09 | 5.21 | 0.95 | 4.47 | 4.20 | 4.61 | 0.19 | 4.42 | 4.21 | 4.58 | 0.17 | 2.49 | 2.23 | 2.78 | 0.23 |
| July 2019-Aug 2019 | 1.27 | 0 | 2.68 | 1.47 | 3.43 | 3.31 | 3.54 | 0.09 | 3.75 | 2.71 | 4.51 | 0.82 | 3.82 | 3.00 | 4.51 | 0.66 | 4.00 | 3.38 | 5.12 | 0.77 | 3.46 | 2.46 | 4.14 | 0.72 | 3.36 | 2.79 | 3.92 | 0.56 |
| Aug 2019-Sep 2019 | 4.59 | 4.47 | 4.79 | 0.14 | 4.33 | 4.19 | 4.53 | 0.16 | 4.53 | 4.35 | 4.92 | 0.26 | 4.37 | 3.73 | 4.78 | 0.45 | 3.74 | 3.51 | 4.19 | 0.31 | 4.43 | 4.11 | 4.69 | 0.27 | 3.99 | 3.68 | 4.20 | 0.22 |
| Sep 2019-Oct 2019 | 3.15 | 2.92 | 3.32 | 0.20 | 3.07 | 2.85 | 3.23 | 0.17 | 3.42 | 3.30 | 3.67 | 0.17 | 3.52 | 3.24 | 3.74 | 0.23 | 2.92 | 2.70 | 3.02 | 0.15 | 3.18 | 2.82 | 3.41 | 0.25 | 3.45 | 3.36 | 3.65 | 0.14 |

Table 26. Arithmetic monthly mean, maximum and minimum mass percentage of Ca with standard deviation of sample particles from six sites outlined in Stephen F. Austin University Real Estate Foundation's STMicroelectronics carbon sequestration project and one site at the SFA Beef Farm.

| Date Range | Property | | | | | | | | | | | | | | | | | | | | | | | | | | | |
|---------------------|--------------------|------|------|------|--------------------|------|------|------|--------------------|------|------|------|--------------------|------|------|------|--------------------|------|------|------|--------------------|------|------|------|-------|------|------|------|
| | Agriculture Center | | | | Arbor Grove | | | | Atoy | | | | Bagley Road | | | | Hilliard | | | | Maxwell | | | | Swink | | | |
| | Mass Percentage Ca | | | | Mass Percentage Ca | | | | Mass Percentage Ca | | | | Mass Percentage Ca | | | | Mass Percentage Ca | | | | Mass Percentage Ca | | | | | | | |
| | Mean | Min | Max | SD | Mean | Min | Max | SD | Mean | Min | Max | SD | Mean | Min | Max | SD | Mean | Min | Max | SD | Mean | Min | Max | SD | Mean | Min | Max | SD |
| Oct 2018-Nov 2018 | 2.87 | 2.49 | 3.93 | 0.71 | 1.09 | 0.88 | 1.43 | 0.24 | 2.62 | 2.47 | 2.76 | 0.16 | 2.60 | 2.37 | 2.85 | 0.20 | 0 | 0 | 0 | 0 | 2.58 | 2.15 | 2.84 | 0.31 | 2.52 | 2.41 | 2.62 | 0.11 |
| Nov 2018-Dec 2018 | 1.32 | 0 | 2.72 | 1.53 | 0.56 | 0 | 2.24 | 1.12 | 0 | 0 | 0 | 0 | - | - | - | - | 0 | 0 | 0 | 0 | 0.59 | 0 | 2.34 | 1.17 | 0 | 0 | 0 | 0 |
| Dec 2018-Jan 2019 | 1.24 | 0 | 2.59 | 1.43 | 0 | 0 | 0 | 0 | 0 | 0 | 0 | 0 | 0 | 0 | 0 | 0 | 0 | 0 | 0 | 0 | 0 | 0 | 0 | 0 | 0 | 0 | 0 | 0 |
| Jan 2019-Feb 2019 | 2.70 | 2.48 | 3.00 | 0.26 | 0.51 | 0 | 2.05 | 1.03 | 2.07 | 1.56 | 2.41 | 0.36 | 2.43 | 2.27 | 2.63 | 0.15 | 2.46 | 2.38 | 2.53 | 0.06 | 1.89 | 0 | 2.74 | 1.27 | 1.91 | 1.78 | 2.00 | 0.10 |
| Feb 2019-Mar 2019 | 1.20 | 0 | 2.42 | 1.38 | 0 | 0 | 0 | 0 | 1.35 | 0 | 2.20 | 0.96 | 2.05 | 1.71 | 2.34 | 0.28 | 0.55 | 0 | 0.93 | 0.40 | 0.98 | 0.87 | 1.07 | 0.08 | 0.91 | 0.80 | 1.01 | 0.09 |
| Mar 2019-Apr 2019 | 1.06 | 0 | 2.33 | 1.24 | 1.79 | 1.27 | 2.19 | 0.40 | 1.76 | 1.62 | 1.87 | 0.11 | 0.66 | 0 | 2.63 | 1.32 | 1.88 | 1.67 | 2.26 | 0.27 | 1.60 | 1.45 | 1.69 | 0.11 | 1.20 | 0 | 2.51 | 1.38 |
| Apr 2019-May 2019 | 2.31 | 2.02 | 2.63 | 0.30 | 0 | 0 | 0 | 0 | 2.42 | 2.15 | 2.66 | 0.21 | 1.61 | 0 | 2.33 | 1.08 | 0 | 0 | 0 | 1.29 | 0 | 2.64 | 1.49 | 1.86 | 0 | 2.81 | 1.27 | 0 |
| May 2019-June 2019 | 2.63 | 2.19 | 2.89 | 0.32 | 1.17 | 0 | 2.49 | 1.35 | 0 | 0 | 0 | 0 | 0.72 | 0 | 2.87 | 1.44 | 0 | 0 | 0 | 0 | 0 | 0 | 0 | 0 | 0 | 0 | 0 | 0 |
| June 2019-July 2019 | 2.62 | 2.54 | 2.73 | 0.09 | 0 | 0 | 0 | 0 | 0 | 0 | 0 | 0 | 1.39 | 0 | 2.84 | 1.61 | 2.53 | 2.16 | 2.76 | 0.28 | 2.55 | 2.51 | 2.62 | 0.05 | 0 | 0 | 0 | 0 |
| July 2019-Aug 2019 | 0 | 0 | 0 | 0 | 0 | 0 | 0 | 0 | 0.68 | 0 | 2.72 | 1.36 | 1.30 | 0 | 2.65 | 1.50 | 0.63 | 0 | 2.53 | 1.27 | 0.62 | 0 | 2.46 | 1.23 | 0 | 0 | 0 | 0 |
| Aug 2019-Sep 2019 | 2.59 | 2.27 | 2.88 | 0.29 | 2.61 | 2.52 | 2.72 | 0.09 | 2.77 | 2.65 | 3.10 | 0.22 | 2.41 | 2.08 | 2.56 | 0.22 | 2.69 | 2.60 | 2.76 | 0.07 | 2.55 | 2.39 | 2.76 | 0.18 | 2.30 | 2.16 | 2.49 | 0.14 |
| Sep 2019-Oct 2019 | 1.68 | 1.49 | 1.85 | 0.17 | 1.77 | 1.69 | 1.86 | 0.10 | 1.97 | 1.82 | 2.19 | 0.18 | 1.87 | 1.67 | 1.95 | 0.13 | 1.72 | 1.63 | 1.81 | 0.07 | 1.73 | 1.58 | 1.83 | 0.11 | 1.92 | 1.88 | 1.98 | 0.04 |

Table 27. Arithmetic monthly mean, maximum and minimum mass percentage of Zn with standard deviation of sample particles from six sites outlined in Stephen F. Austin University Real Estate Foundation's STMicroelectronics carbon sequestration project and one site at the SFA Beef Farm.

| Date Range | Property | | | | | | | | | | | | | | | | | | | | | | | | | | | | | | | |
|---------------------|--------------------|------|------|------|--------------------|------|------|------|--------------------|------|------|------|--------------------|------|------|------|--------------------|------|------|------|--------------------|------|------|------|-------|------|------|------|---|---|---|---|
| | Agriculture Center | | | | Arbor Grove | | | | Atoy | | | | Bagley Road | | | | Hilliard | | | | Maxwell | | | | Swink | | | | | | | |
| | Mass Percentage Zn | | | | Mass Percentage Zn | | | | Mass Percentage Zn | | | | Mass Percentage Zn | | | | Mass Percentage Zn | | | | Mass Percentage Zn | | | | | | | | | | | |
| | Mean | Min | Max | SD | Mean | Min | Max | SD | Mean | Min | Max | SD | Mean | Min | Max | SD | Mean | Min | Max | SD | Mean | Min | Max | SD | Mean | Min | Max | SD | | | | |
| Oct 2018-Nov 2018 | 0 | 0 | 0 | 0 | 0 | 0 | 0 | 0 | 0 | 0 | 0 | 0 | 0 | 0 | 0 | 0 | 0 | 0 | 0 | 0 | 0 | 0 | 0 | 0 | 0 | 0 | 0 | 0 | 0 | 0 | 0 | 0 |
| Nov 2018-Dec 2018 | 0 | 0 | 0 | 0 | 0 | 0 | 0 | 0 | 0 | 0 | 0 | 0 | - | - | - | - | 0 | 0 | 0 | 0 | 0 | 0 | 0 | 0 | 0 | 0 | 0 | 0 | 0 | 0 | 0 | 0 |
| Dec 2018-Jan 2019 | 0 | 0 | 0 | 0 | 0 | 0 | 0 | 0 | 0 | 0 | 0 | 0 | 0 | 0 | 0 | 0 | 0 | 0 | 0 | 0 | 0 | 0 | 0 | 0 | 0 | 0 | 0 | 0 | 0 | 0 | 0 | 0 |
| Jan 2019-Feb 2019 | 0 | 0 | 0 | 0 | 0 | 0 | 0 | 0 | 0 | 0 | 0 | 0 | 0 | 0 | 0 | 0 | 0 | 0 | 0 | 0 | 0 | 0 | 0 | 0 | 0 | 0 | 0 | 0 | 0 | 0 | 0 | 0 |
| Feb 2019-Mar 2019 | 0 | 0 | 0 | 0 | 0 | 0 | 0 | 0 | 0 | 0 | 0 | 0 | 0 | 0 | 0 | 0 | 1.44 | 0.28 | 1.11 | 1.72 | 2.20 | 0.44 | 1.66 | 2.71 | 1.49 | 0.42 | 1.04 | 2.02 | | | | |
| Mar 2019-Apr 2019 | 0 | 0 | 0 | 0 | 0 | 0 | 0 | 0 | 0 | 0 | 0 | 0 | 0 | 0 | 0 | 0 | 0 | 0 | 0 | 0 | 0 | 0 | 0 | 0 | 0 | 0 | 0 | 0 | 0 | 0 | 0 | 0 |
| Apr 2019-May 2019 | 0 | 0 | 0 | 0 | 0 | 0 | 0 | 0 | 0 | 0 | 0 | 0 | 0 | 0 | 0 | 0 | 0 | 0 | 0 | 0 | 0 | 0 | 0 | 0 | 0 | 0 | 0 | 0 | 0 | 0 | 0 | 0 |
| May 2019-June 2019 | 0 | 0 | 0 | 0 | 0 | 0 | 0 | 0 | 0 | 0 | 0 | 0 | 0 | 0 | 0 | 0 | 0 | 0 | 0 | 0 | 0 | 0 | 0 | 0 | 0 | 0 | 0 | 0 | 0 | 0 | 0 | 0 |
| June 2019-July 2019 | 0 | 0 | 0 | 0 | 0 | 0 | 0 | 0 | 0 | 0 | 0 | 0 | 0 | 0 | 0 | 0 | 0 | 0 | 0 | 0 | 0 | 0 | 0 | 0 | 0 | 0 | 0 | 0 | 0 | 0 | 0 | 0 |
| July 2019-Aug 2019 | 0 | 0 | 0 | 0 | 0 | 0 | 0 | 0 | 0 | 0 | 0 | 0 | 0 | 0 | 0 | 0 | 0 | 0 | 0 | 0 | 0 | 0 | 0 | 0 | 0 | 0 | 0 | 0 | 0 | 0 | 0 | 0 |
| Aug 2019-Sep 2019 | 0 | 0 | 0 | 0 | 0 | 0 | 0 | 0 | 0 | 0 | 0 | 0 | 0 | 0 | 0 | 0 | 0 | 0 | 0 | 0 | 0 | 0 | 0 | 0 | 0 | 0 | 0 | 0 | 0 | 0 | 0 | 0 |
| Sep 2019-Oct 2019 | 4.48 | 0.70 | 3.78 | 5.25 | 5.44 | 0.18 | 5.27 | 5.68 | 5.27 | 0.96 | 4.41 | 6.59 | 6.12 | 0.52 | 5.65 | 6.86 | 4.55 | 0.94 | 3.61 | 5.74 | 4.77 | 0.39 | 4.32 | 5.26 | 5.15 | 0.62 | 4.44 | 5.90 | | | | |

Table 28. Arithmetic monthly mean, maximum and minimum mass percentage of Re with standard deviation of sample particles from six sites outlined in Stephen F. Austin University Real Estate Foundation's STMicroelectronics carbon sequestration project and one site at the SFA Beef Farm.

| Date Range | Property | | | | | | | | | | | | | | | | | | | | | | | | | | | |
|---------------------|--------------------|------|-----|------|--------------------|------|-----|------|--------------------|------|-----|------|--------------------|------|-----|------|--------------------|------|-----|------|--------------------|------|-----|------|-------|------|-----|------|
| | Agriculture Center | | | | Arbor Grove | | | | Atoy | | | | Bagley Road | | | | Hillard | | | | Maxwell | | | | Swink | | | |
| | Mass Percentage Re | | | | Mass Percentage Re | | | | Mass Percentage Re | | | | Mass Percentage Re | | | | Mass Percentage Re | | | | Mass Percentage Re | | | | | | | |
| | Mean | Min | Max | SD | Mean | Min | Max | SD | Mean | Min | Max | SD | Mean | Min | Max | SD | Mean | Min | Max | SD | Mean | Min | Max | SD | Mean | Min | Max | SD |
| Oct 2018-Nov 2018 | 0 | 0 | 0 | 0 | 0 | 0 | 0 | 0 | 0 | 0 | 0 | 0 | 0 | 0 | 0 | 0 | 0 | 0 | 0 | 0 | 0 | 0 | 0 | 0 | 0 | 0 | 0 | |
| Nov 2018-Dec 2018 | 0 | 0 | 0 | 0 | 0 | 0 | 0 | 0 | 0 | 0 | 0 | 0 | - | - | - | - | 0 | 0 | 0 | 0 | 0 | 0 | 0 | 0 | 0 | 0 | | |
| Dec 2018-Jan 2019 | 0 | 0 | 0 | 0 | 0 | 0 | 0 | 0 | 0 | 0 | 0 | 0 | 0 | 0 | 0 | 0 | 0 | 0 | 0 | 0 | 0 | 0 | 0 | 0 | 0 | 0 | 0 | |
| Jan 2019-Feb 2019 | 0 | 0 | 0 | 0 | 0 | 0 | 0 | 0 | 0 | 0 | 0 | 0 | 0 | 0 | 0 | 0 | 0 | 0 | 0 | 0 | 0 | 0 | 0 | 0 | 0 | 0 | 0 | |
| Feb 2019-Mar 2019 | 0 | 0 | 0 | 0 | 0 | 0 | 0 | 0 | 0 | 0 | 0 | 0 | 0 | 0 | 0 | 0 | 0 | 0 | 0 | 0 | 0 | 0 | 0 | 0 | 0.41 | 0.49 | 0 | 0.96 |
| Mar 2019-Apr 2019 | 0 | 0 | 0 | 0 | 0 | 0 | 0 | 0 | 0 | 0 | 0 | 0 | 0 | 0 | 0 | 0 | 0 | 0 | 0 | 0 | 0 | 0 | 0 | 0 | 0 | 0 | 0 | |
| Apr 2019-May 2019 | 0 | 0 | 0 | 0 | 0 | 0 | 0 | 0 | 0 | 0 | 0 | 0 | 0 | 0 | 0 | 0 | 0 | 0 | 0 | 0 | 0 | 0 | 0 | 0 | 0 | 0 | 0 | |
| May 2019-June 2019 | 0 | 0 | 0 | 0 | 0 | 0 | 0 | 0 | 0 | 0 | 0 | 0 | 0 | 0 | 0 | 0 | 0 | 0 | 0 | 0 | 0 | 0 | 0 | 0 | 0 | 0 | 0 | |
| June 2019-July 2019 | 0 | 0 | 0 | 0 | 0 | 0 | 0 | 0 | 0 | 0 | 0 | 0 | 0 | 0 | 0 | 0 | 0 | 0 | 0 | 0 | 0 | 0 | 0 | 0 | 0 | 0 | 0 | |
| July 2019-Aug 2019 | 0 | 0 | 0 | 0 | 0 | 0 | 0 | 0 | 0 | 0 | 0 | 0 | 0 | 0 | 0 | 0 | 0 | 0 | 0 | 0 | 0 | 0 | 0 | 0 | 0 | 0 | 0 | |
| Aug 2019-Sep 2019 | 0 | 0 | 0 | 0 | 0 | 0 | 0 | 0 | 0 | 0 | 0 | 0 | 0 | 0 | 0 | 0 | 0 | 0 | 0 | 0 | 0 | 0 | 0 | 0 | 0 | 0 | 0 | |
| Sep 2019-Oct 2019 | 1.14 | 1.58 | 0 | 3.34 | 0.33 | 0.67 | 0 | 1.33 | 2.44 | 1.86 | 0 | 4.33 | 0.40 | 0.81 | 0 | 1.61 | 2.12 | 1.47 | 0 | 3.12 | 1.66 | 1.92 | 0 | 3.33 | 1.63 | 1.94 | 0 | 3.84 |

Table 29. Arithmetic monthly mean, maximum and minimum mass percentage of Ti with standard deviation of sample particles from six sites outlined in Stephen F. Austin University Real Estate Foundation's STMicronics carbon sequestration project and one site at the SFA Beef Farm.

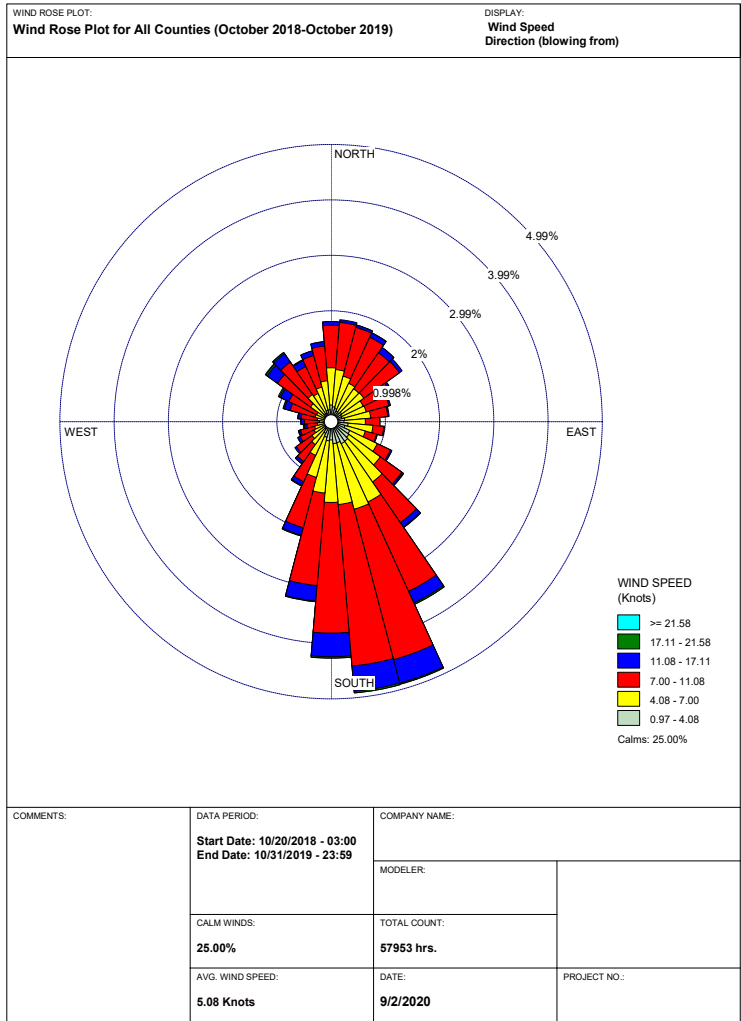
| Date Range | Property | | | | | | | | | | | | | | | | | | | | | | | | | | | |
|---------------------|--------------------|------|-----|------|--------------------|-----|-----|----|--------------------|------|-----|------|--------------------|------|-----|------|--------------------|------|-----|------|--------------------|------|-----|------|-------|-----|-----|----|
| | Agriculture Center | | | | Arbor Grove | | | | Atoy | | | | Bagley Road | | | | Hilliard | | | | Maxwell | | | | Swink | | | |
| | Mass Percentage Ti | | | | Mass Percentage Ti | | | | Mass Percentage Ti | | | | Mass Percentage Ti | | | | Mass Percentage Ti | | | | Mass Percentage Ti | | | | | | | |
| | Mean | Min | Max | SD | Mean | Min | Max | SD | Mean | Min | Max | SD | Mean | Min | Max | SD | Mean | Min | Max | SD | Mean | Min | Max | SD | Mean | Min | Max | SD |
| Oct 2018-Nov 2018 | 0 | 0 | 0 | 0 | 0 | 0 | 0 | 0 | 0 | 0 | 0 | 0 | 0 | 0 | 0 | 0 | 0.61 | 1.22 | 0 | 2.44 | 0.29 | 0.58 | 0 | 1.15 | 0 | 0 | 0 | 0 |
| Nov 2018-Dec 2018 | 0 | 0 | 0 | 0 | 0 | 0 | 0 | 0 | 0 | 0 | 0 | 0 | - | - | - | - | 0 | 0 | 0 | 0 | 0 | 0 | 0 | 0 | 0 | 0 | 0 | 0 |
| Dec 2018-Jan 2019 | 0 | 0 | 0 | 0 | 0 | 0 | 0 | 0 | 0 | 0 | 0 | 0 | 0 | 0 | 0 | 0 | 0 | 0 | 0 | 0 | 0.11 | 0.22 | 0 | 0.44 | 0 | 0 | 0 | 0 |
| Jan 2019-Feb 2019 | 0 | 0 | 0 | 0 | 0 | 0 | 0 | 0 | 0 | 0 | 0 | 0 | 0.15 | 0.30 | 0 | 0.59 | 0 | 0 | 0 | 0 | 0 | 0 | 0 | 0 | 0 | 0 | 0 | 0 |
| Feb 2019-Mar 2019 | 0 | 0 | 0 | 0 | 0 | 0 | 0 | 0 | 0 | 0 | 0 | 0 | 0 | 0 | 0 | 0 | 0 | 0 | 0 | 0 | 0 | 0 | 0 | 0 | 0 | 0 | 0 | 0 |
| Mar 2019-Apr 2019 | 0 | 0 | 0 | 0 | 0 | 0 | 0 | 0 | 0.17 | 0.34 | 0 | 0.67 | 0 | 0 | 0 | 0 | 0 | 0 | 0 | 0 | 0.15 | 0.31 | 0 | 0.61 | 0 | 0 | 0 | 0 |
| Apr 2019-May 2019 | 0 | 0 | 0 | 0 | 0 | 0 | 0 | 0 | 0 | 0 | 0 | 0 | 0 | 0 | 0 | 0 | 0 | 0 | 0 | 0 | 0 | 0 | 0 | 0 | 0 | 0 | 0 | 0 |
| May 2019-June 2019 | 0 | 0 | 0 | 0 | 0 | 0 | 0 | 0 | 0 | 0 | 0 | 0 | 0 | 0 | 0 | 0 | 0 | 0 | 0 | 0 | 0 | 0 | 0 | 0 | 0 | 0 | 0 | 0 |
| June 2019-July 2019 | 0.26 | 0.52 | 0 | 1.03 | 0 | 0 | 0 | 0 | 0 | 0 | 0 | 0 | 0 | 0 | 0 | 0 | 0.29 | 0.58 | 0 | 1.15 | 0 | 0 | 0 | 0 | 0 | 0 | 0 | 0 |
| July 2019-Aug 2019 | 0 | 0 | 0 | 0 | 0 | 0 | 0 | 0 | 0 | 0 | 0 | 0 | 0 | 0 | 0 | 0 | 0 | 0 | 0 | 0 | 0 | 0 | 0 | 0 | 0 | 0 | 0 | 0 |
| Aug 2019-Sep 2019 | 0 | 0 | 0 | 0 | 0 | 0 | 0 | 0 | 0 | 0 | 0 | 0 | 0 | 0 | 0 | 0 | 0.23 | 0.45 | 0 | 0.90 | 0 | 0 | 0 | 0 | 0 | 0 | 0 | 0 |
| Sep 2019-Oct 2019 | 0.29 | 0.33 | 0 | 0.58 | 0 | 0 | 0 | 0 | 0 | 0 | 0 | 0 | 0 | 0 | 0 | 0 | 0.14 | 0.28 | 0 | 0.55 | 0.18 | 0.35 | 0 | 0.70 | 0 | 0 | 0 | 0 |

Table 30. Arithmetic monthly mean, maximum and minimum mass percentage of Fe with standard deviation of sample particles from six sites outlined in Stephen F. Austin University Real Estate Foundation's STMicroelectronics carbon sequestration project and one site at the SFA Beef Farm.

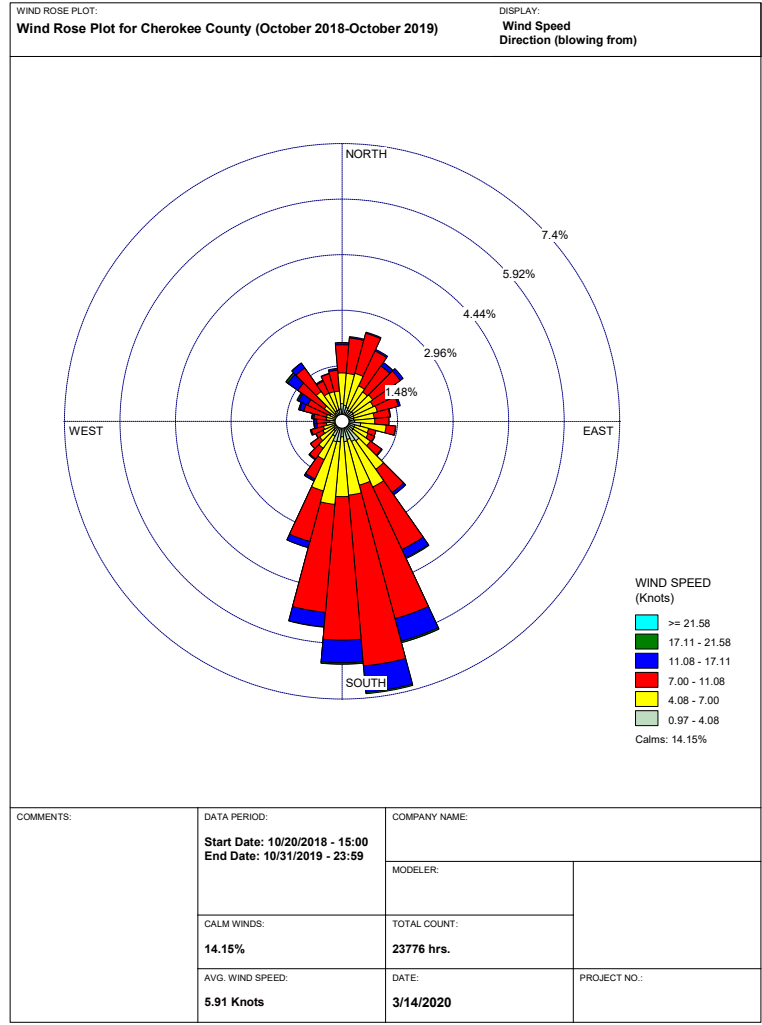
| Date Range | Property | | | | | | | | | | | | | | | | | | | | | | | | | | | | | | |
|---------------------|--------------------|------|------|------|--------------------|------|------|------|--------------------|------|------|------|--------------------|------|------|------|--------------------|------|------|------|--------------------|------|-------|------|-------|------|-------|------|-----|-----|----|
| | Agriculture Center | | | | Arbor Grove | | | | Atoy | | | | Bagly Road | | | | Hilliard | | | | Maxwell | | | | Swink | | | | | | |
| | Mass Percentage Fe | | | | Mass Percentage Fe | | | | Mass Percentage Fe | | | | Mass Percentage Fe | | | | Mass Percentage Fe | | | | Mass Percentage Fe | | | | | | | | | | |
| Mean | Min | Max | SD | Mean | Min | Max | SD | Mean | Min | Max | SD | Mean | Min | Max | SD | Mean | Min | Max | SD | Mean | Min | Max | SD | Mean | Min | Max | SD | Mean | Min | Max | SD |
| Oct 2018-Nov 2018 | 7.96 | 7.05 | 9.10 | 0.85 | 2.52 | 1.49 | 4.13 | 1.16 | 8.08 | 7.31 | 9.33 | 0.92 | 8.12 | 7.48 | 8.54 | 0.45 | 7.95 | 6.29 | 9.53 | 1.49 | 7.83 | 7.18 | 8.77 | 0.70 | 7.63 | 7.28 | 8.06 | 0.39 | | | |
| Nov 2018-Dec 2018 | 7.82 | 7.22 | 8.22 | 0.45 | 6.04 | 4.98 | 6.90 | 0.81 | 5.71 | 0 | 8.35 | 3.93 | - | - | - | - | 7.98 | 6.53 | 9.14 | 1.14 | 6.31 | 5.09 | 7.72 | 1.18 | 6.60 | 4.01 | 8.92 | 2.02 | | | |
| Dec 2018-Jan 2019 | 7.66 | 6.29 | 8.82 | 1.06 | 4.65 | 4.07 | 5.17 | 0.45 | 7.67 | 6.94 | 8.94 | 0.88 | 7.85 | 7.23 | 8.69 | 0.61 | 7.76 | 7.28 | 8.48 | 0.53 | 7.15 | 5.94 | 7.82 | 0.83 | 7.76 | 6.93 | 8.50 | 0.65 | | | |
| Jan 2019-Feb 2019 | 8.48 | 8.18 | 8.66 | 0.21 | 4.10 | 3.04 | 5.05 | 0.94 | 4.49 | 3.43 | 5.16 | 0.74 | 7.17 | 6.73 | 7.89 | 0.53 | 7.37 | 7.15 | 7.54 | 0.18 | 6.98 | 5.15 | 8.35 | 1.59 | 5.63 | 5.10 | 6.09 | 0.45 | | | |
| Feb 2019-Mar 2019 | 5.42 | 4.43 | 6.10 | 0.80 | 0.94 | 0 | 2.57 | 1.22 | 5.29 | 3.32 | 6.52 | 1.41 | 6.39 | 5.39 | 6.81 | 0.67 | 2.64 | 1.90 | 3.71 | 0.78 | 4.11 | 2.89 | 5.70 | 1.19 | 3.10 | 2.76 | 3.49 | 0.39 | | | |
| Mar 2019-Apr 2019 | 4.82 | 3.41 | 6.80 | 1.61 | 4.84 | 2.63 | 6.67 | 1.84 | 6.49 | 5.95 | 7.71 | 0.82 | 6.03 | 5.31 | 6.87 | 0.72 | 7.19 | 6.78 | 7.81 | 0.44 | 5.71 | 4.91 | 6.66 | 0.79 | 6.31 | 5.61 | 6.79 | 0.57 | | | |
| Apr 2019-May 2019 | 7.17 | 5.56 | 8.66 | 1.44 | 6.21 | 5.47 | 7.30 | 0.81 | 7.28 | 6.56 | 8.98 | 1.15 | 6.75 | 5.42 | 7.72 | 0.96 | 7.66 | 6.88 | 8.70 | 0.77 | 6.79 | 5.11 | 7.92 | 1.22 | 6.92 | 6.36 | 7.38 | 0.53 | | | |
| May 2019-June 2019 | 7.30 | 5.13 | 8.98 | 1.64 | 6.96 | 5.39 | 8.68 | 1.58 | 6.85 | 6.56 | 7.04 | 0.21 | 5.63 | 4.47 | 7.10 | 1.28 | 6.73 | 6.40 | 7.42 | 0.47 | 7.72 | 6.09 | 10.63 | 2.08 | 6.24 | 4.99 | 8.21 | 1.39 | | | |
| June 2019-July 2019 | 7.82 | 7.26 | 8.35 | 0.52 | 6.95 | 5.43 | 7.68 | 1.06 | 5.73 | 5.51 | 6.09 | 0.28 | 6.33 | 6.01 | 6.89 | 0.39 | 8.08 | 7.31 | 9.10 | 0.81 | 8.18 | 7.55 | 8.39 | 0.42 | 5.03 | 3.20 | 5.80 | 1.23 | | | |
| July 2019-Aug 2019 | 6.34 | 5.62 | 7.64 | 0.89 | 6.57 | 5.31 | 7.84 | 1.04 | 7.49 | 6.69 | 8.09 | 0.58 | 7.10 | 5.25 | 9.20 | 1.62 | 7.29 | 6.77 | 7.70 | 0.40 | 6.68 | 5.11 | 7.61 | 1.10 | 6.32 | 5.29 | 7.05 | 0.79 | | | |
| Aug 2019-Sep 2019 | 8.17 | 7.60 | 9.34 | 0.81 | 7.44 | 6.86 | 7.94 | 0.51 | 8.07 | 7.33 | 8.98 | 0.77 | 7.02 | 6.74 | 7.37 | 0.26 | 5.39 | 4.86 | 5.82 | 0.40 | 7.76 | 6.83 | 8.27 | 0.64 | 8.18 | 7.36 | 10.33 | 1.44 | | | |
| Sep 2019-Oct 2019 | 6.32 | 5.37 | 7.65 | 1.07 | 7.17 | 6.39 | 8.33 | 0.89 | 7.20 | 5.73 | 8.80 | 1.36 | 7.06 | 6.59 | 7.26 | 0.32 | 6.21 | 5.92 | 6.33 | 0.19 | 7.02 | 6.81 | 7.53 | 0.35 | 6.92 | 6.22 | 7.86 | 0.76 | | | |

Table 31. Arithmetic monthly mean, maximum and minimum mass percentage of Ce with standard deviation of sample particles from six sites outlined in Stephen F. Austin University Real Estate Foundation's STMicroelectronics carbon sequestration project and one site at the SFA Beef Farm.

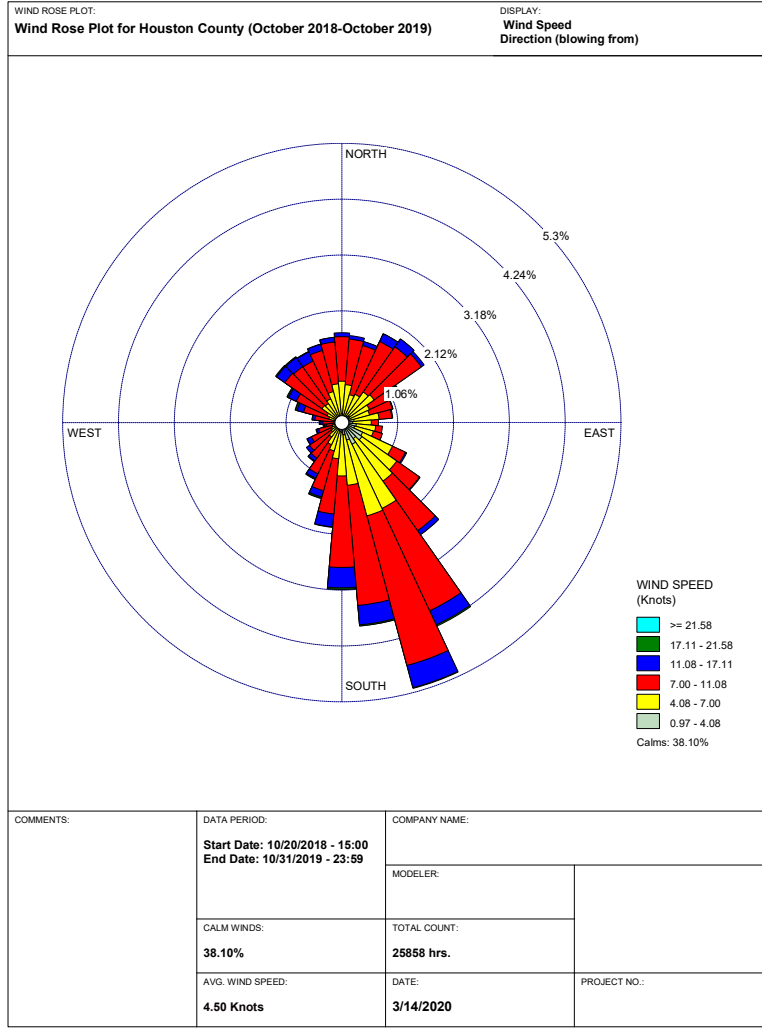
| Date Range | Property | | | | | | | | | | | | | | | | | | | | | | | | | | | |
|---------------------|--------------------|-----|------|------|--------------------|-----|-----|----|--------------------|-----|------|------|--------------------|-----|-----|----|--------------------|-----|-----|----|--------------------|-----|-----|----|-------|-----|-----|----|
| | Agriculture Center | | | | Arbor Grove | | | | Atoy | | | | Bagley Road | | | | Hilliard | | | | Maxwell | | | | Swink | | | |
| | Mass Percentage Ce | | | | Mass Percentage Ce | | | | Mass Percentage Ce | | | | Mass Percentage Ce | | | | Mass Percentage Ce | | | | Mass Percentage Ce | | | | | | | |
| | Mean | Min | Max | SD | Mean | Min | Max | SD | Mean | Min | Max | SD | Mean | Min | Max | SD | Mean | Min | Max | SD | Mean | Min | Max | SD | Mean | Min | Max | SD |
| Oct 2018-Nov 2018 | 0 | 0 | 0 | 0 | 0 | 0 | 0 | 0 | 0 | 0 | 0 | 0 | 0 | 0 | 0 | 0 | 0 | 0 | 0 | 0 | 0 | 0 | 0 | 0 | 0 | 0 | 0 | |
| Nov 2018-Dec 2018 | 0 | 0 | 0 | 0 | 0 | 0 | 0 | 0 | 0 | 0 | 0 | - | - | - | - | 0 | 0 | 0 | 0 | 0 | 0 | 0 | 0 | 0 | 0 | 0 | 0 | |
| Dec 2018-Jan 2019 | 0 | 0 | 0 | 0 | 0 | 0 | 0 | 0 | 0 | 0 | 0 | 0 | 0 | 0 | 0 | 0 | 0 | 0 | 0 | 0 | 0 | 0 | 0 | 0 | 0 | 0 | 0 | |
| Jan 2019-Feb 2019 | 0.42 | 0 | 1.66 | 0.83 | 0 | 0 | 0 | 0 | 0 | 0 | 0 | 0 | 0 | 0 | 0 | 0 | 0 | 0 | 0 | 0 | 0 | 0 | 0 | 0 | 0 | 0 | 0 | |
| Feb 2019-Mar 2019 | 0 | 0 | 0 | 0 | 0 | 0 | 0 | 0 | 0 | 0 | 0 | 0 | 0 | 0 | 0 | 0 | 0 | 0 | 0 | 0 | 0 | 0 | 0 | 0 | 0 | 0 | 0 | |
| Mar 2019-Apr 2019 | 0 | 0 | 0 | 0 | 0 | 0 | 0 | 0 | 0 | 0 | 0 | 0 | 0 | 0 | 0 | 0 | 0 | 0 | 0 | 0 | 0 | 0 | 0 | 0 | 0 | 0 | 0 | |
| Apr 2019-May 2019 | 0 | 0 | 0 | 0 | 0 | 0 | 0 | 0 | 0 | 0 | 0 | 0 | 0 | 0 | 0 | 0 | 0 | 0 | 0 | 0 | 0 | 0 | 0 | 0 | 0 | 0 | 0 | |
| May 2019-June 2019 | 0 | 0 | 0 | 0 | 0 | 0 | 0 | 0 | 0 | 0 | 0 | 0 | 0 | 0 | 0 | 0 | 0 | 0 | 0 | 0 | 0 | 0 | 0 | 0 | 0 | 0 | 0 | |
| June 2019-July 2019 | 0 | 0 | 0 | 0 | 0 | 0 | 0 | 0 | 0.67 | 0 | 2.66 | 1.33 | 0 | 0 | 0 | 0 | 0 | 0 | 0 | 0 | 0 | 0 | 0 | 0 | 0 | 0 | 0 | |
| July 2019-Aug 2019 | 0 | 0 | 0 | 0 | 0 | 0 | 0 | 0 | 0 | 0 | 0 | 0 | 0 | 0 | 0 | 0 | 0 | 0 | 0 | 0 | 0 | 0 | 0 | 0 | 0 | 0 | 0 | |
| Aug 2019-Sep 2019 | 0 | 0 | 0 | 0 | 0 | 0 | 0 | 0 | 0 | 0 | 0 | 0 | 0 | 0 | 0 | 0 | 0 | 0 | 0 | 0 | 0 | 0 | 0 | 0 | 0 | 0 | 0 | |
| Sep 2019-Oct 2019 | 0 | 0 | 0 | 0 | 0 | 0 | 0 | 0 | 0 | 0 | 0 | 0 | 0 | 0 | 0 | 0 | 0 | 0 | 0 | 0 | 0 | 0 | 0 | 0 | 0 | 0 | 0 | |



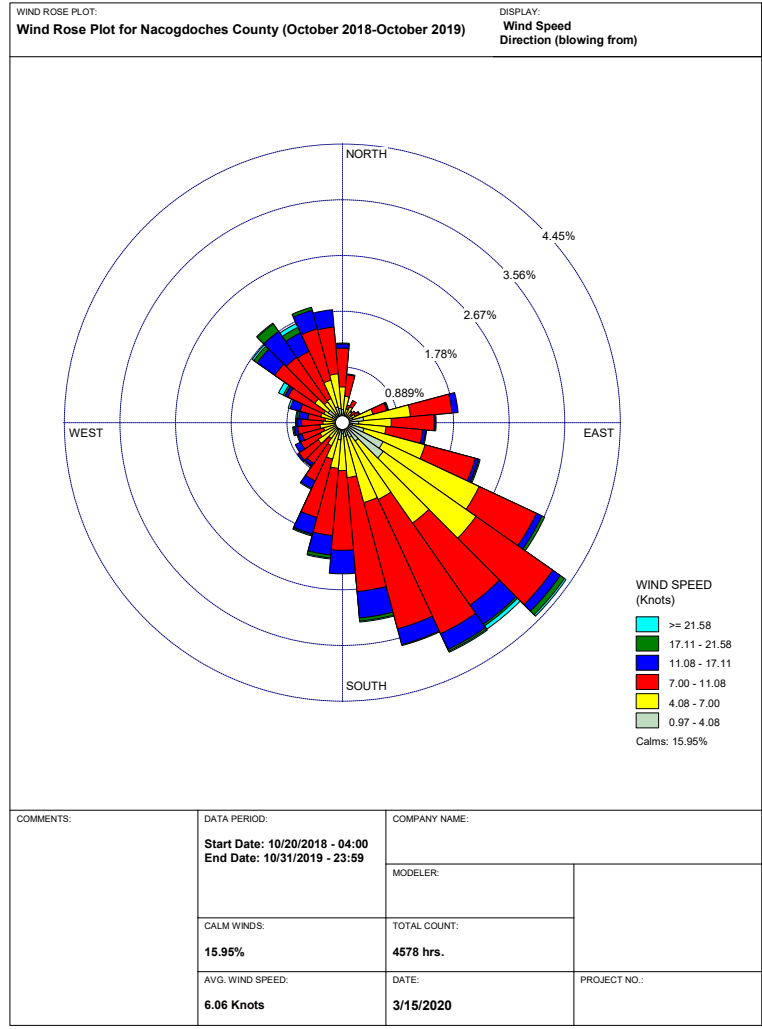
WRPLOT View - Lakes Environmental Software



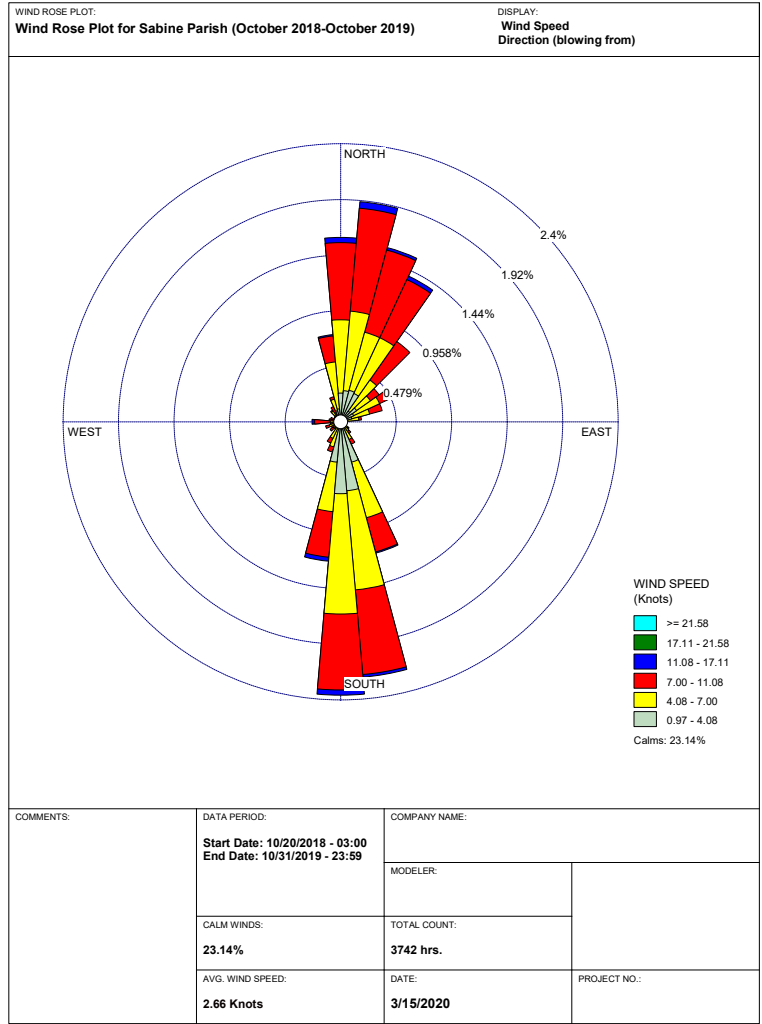
WRPLOT View - Lakes Environmental Software



WRPLOT View - Lakes Environmental Software



WRPLOT View - Lakes Environmental Software



WRPLOT View - Lakes Environmental Software

Table 32. Summary of wind data during sampling period including monthly resultant vector direction, average wind speed, and percentage of calm winds for each county. The resultant vector direction was used to determine the mean wind direction. Data was obtained from NOAA (2019). Freeware used for calculations was WRPLOT View by Lakes Environmental Software.

| County | Date Range | Resultant Vector Direction | Wind Speed | Percentage of Calm Winds |
|-------------|-----------------------|----------------------------|------------|--------------------------|
| | | Degrees | Knots | % |
| Cherokee | Oct 2018 - Nov 2018 | 6.00 | 5.77 | 12.56 |
| Cherokee | Nov 2018 - Dec 2018 | 309.00 | 6.37 | 15.60 |
| Cherokee | Dec 2018 - Jan 2019 | 341.00 | 6.73 | 11.34 |
| Cherokee | Jan 2019 - Feb 2019 | 77.00 | 6.98 | 12.74 |
| Cherokee | Feb 2019 - Mar 2019 | 35.00 | 6.12 | 13.20 |
| Cherokee | Mar 2019 - Apr 2019 | 129.00 | 6.94 | 10.10 |
| Cherokee | Apr 2019 - May 2019 | 154.00 | 6.16 | 16.24 |
| Cherokee | May 2019 - June 2019 | 162.00 | 5.69 | 19.19 |
| Cherokee | June 2019 - July 2019 | 185.00 | 5.53 | 13.59 |
| Cherokee | July 2019 - Aug 2019 | 155.00 | 5.25 | 4.86 |
| Cherokee | Aug 2019 - Sep 2019 | 115.00 | 4.47 | 23.16 |
| Cherokee | Sep 2019 - Oct 2019 | 127.00 | 5.35 | 16.39 |
| Houston | Oct 2018 - Nov 2018 | 0 | 4.68 | 36.82 |
| Houston | Nov 2018 - Dec 2018 | 354.00 | 5.08 | 34.01 |
| Houston | Dec 2018 - Jan 2019 | 357.00 | 5.48 | 28.45 |
| Houston | Jan 2019 - Feb 2019 | 14.00 | 5.84 | 28.75 |
| Houston | Feb 2019 - Mar 2019 | 16.00 | 5.17 | 29.61 |
| Houston | Mar 2019 - Apr 2019 | 25.00 | 5.48 | 31.56 |
| Houston | Apr 2019 - May 2019 | 49.00 | 4.82 | 37.70 |
| Houston | May 2019 - June 2019 | 20.00 | 3.98 | 48.98 |
| Houston | June 2019 - July 2019 | 15.00 | 3.74 | 43.83 |
| Houston | July 2019 - Aug 2019 | 13.00 | 3.49 | 34.74 |
| Houston | Aug 2019 - Sep 2019 | 23.00 | 2.83 | 55.07 |
| Houston | Sep 2019 - Oct 2019 | 33.00 | 3.55 | 46.15 |
| Nacogdoches | Oct 2018 - Nov 2018 | 357.00 | 3.07 | 33.14 |
| Nacogdoches | Nov 2018 - Dec 2018 | 11.00 | 3.00 | 40.63 |
| Nacogdoches | Dec 2018 - Jan 2019 | 149.00 | 6.30 | 13.87 |
| Nacogdoches | Jan 2019 - Feb 2019 | 114.00 | 7.13 | 10.86 |
| Nacogdoches | Feb 2019 - Mar 2019 | 32.00 | 6.79 | 11.96 |
| Nacogdoches | Mar 2019 - Apr 2019 | 76.00 | 7.08 | 14.74 |
| Nacogdoches | Apr 2019 - May 2019 | 121.00 | 6.97 | 11.14 |
| Nacogdoches | May 2019 - June 2019 | 154.00 | 7.75 | 8.07 |
| Nacogdoches | June 2019 - July 2019 | 172.00 | 5.43 | 17.59 |
| Nacogdoches | July 2019 - Aug 2019 | 262.00 | 4.79 | 19.09 |
| Nacogdoches | Aug 2019 - Sep 2019 | 109.00 | 5.58 | 7.00 |
| Nacogdoches | Sep 2019 - Oct 2019 | 99.00 | 5.26 | 15.10 |
| Sabine | Oct 2018 - Nov 2018 | 6.00 | 3.55 | 18.48 |
| Sabine | Nov 2018 - Dec 2018 | 14.00 | 2.97 | 20.34 |
| Sabine | Dec 2018 - Jan 2019 | 8.00 | 3.09 | 22.01 |
| Sabine | Jan 2019 - Feb 2019 | 18.00 | 3.92 | 15.18 |
| Sabine | Feb 2019 - Mar 2019 | 8.00 | 2.71 | 25.34 |
| Sabine | Mar 2019 - Apr 2019 | 10.00 | 3.11 | 17.96 |
| Sabine | Apr 2019 - May 2019 | 4.00 | 2.48 | 20.86 |
| Sabine | May 2019 - June 2019 | 359.00 | 1.82 | 28.21 |
| Sabine | June 2019 - July 2019 | 5.00 | 2.75 | 22.93 |
| Sabine | July 2019 - Aug 2019 | 2.00 | 1.48 | 32.89 |
| Sabine | Aug 2019 - Sep 2019 | 3.00 | 0.99 | 31.51 |
| Sabine | Sep 2019 - Oct 2019 | 4.00 | 33.96 | 1.82 |

Table 33. Arithmetic mean of Si, C, Ba, Na, Al, Ca, K and Fe in kg/ha sampled across seven sites over a twelve-month period. Four subsamples were collected per sample. One sample was collected per site per month. Six of the seven sampling sites are in Stephen F. Austin University Real Estate Foundation's STMicroelectronics carbon sequestration project and one sampling site is located at SFA's Beef Farm.

| Date Range | Monthly Deposition | | | | | | | |
|---------------------|--------------------|----------|----------|----------|----------|----------|----------|----------|
| | kg/ha | | | | | | | |
| | Si | C | Ba | Na | Al | Ca | K | Fe |
| Oct 2018-Nov 2018 | 0.997113 | 0.141208 | 0.167388 | 0.147598 | 0.078158 | 0.042053 | 0.084312 | 0.147598 |
| Nov 2018-Dec 2018 | 1.036932 | 0.271198 | 0.119299 | 0.155829 | 0.074215 | 0.009479 | 0.070747 | 0.155829 |
| Dec 2018-Jan 2019 | 0.574288 | 0.056519 | 0.10188 | 0.087447 | 0.04141 | 0.002183 | 0.042086 | 0.087447 |
| Jan 2019-Feb 2019 | 1.448665 | 0.275098 | 0.257494 | 0.218145 | 0.127712 | 0.069033 | 0.139447 | 0.218145 |
| Feb 2019-Mar 2019 | 0.619648 | 0.687149 | 0.11043 | 0.112407 | 0.064757 | 0.028525 | 0.066936 | 0.112407 |
| Mar 2019-Apr 2019 | 0.648771 | 0.225579 | 0.112044 | 0.110179 | 0.057766 | 0.026473 | 0.063386 | 0.110179 |
| Apr 2019-May 2019 | 0.22626 | 0.037828 | 0.037991 | 0.037937 | 0.01835 | 0.007402 | 0.022479 | 0.037937 |
| May 2019-June 2019 | 0.368774 | 0.04412 | 0.050949 | 0.060923 | 0.023247 | 0.005841 | 0.032259 | 0.060923 |
| June 2019-July 2019 | 0.359389 | 0.048138 | 0.054815 | 0.056628 | 0.026589 | 0.010716 | 0.030993 | 0.056628 |
| July 2019-Aug 2019 | 0.545223 | 0.101954 | 0.088 | 0.085863 | 0.043407 | 0.005783 | 0.041486 | 0.085863 |
| Aug 2019-Sep 2019 | 0.193931 | 0.026213 | 0.040697 | 0.03301 | 0.015709 | 0.011374 | 0.019015 | 0.03301 |
| Sep 2019-Oct 2019 | 1.539277 | 0.377279 | 0.298437 | 0.361934 | 0.167587 | 0.095775 | 0.171442 | 0.361934 |

VITA

In 2013, Sarah Caton graduated from McKinney North High School in McKinney, TX. While obtaining her undergraduate degree in modern languages, she worked as a student instructor at Stephen F. Austin's State University's AARC department. During the last two years of her undergraduate studies, she discovered her passion for environmental science and decided to take leveling courses to qualify for graduate school admittance in the environmental science department. After obtaining her undergraduate degree in 2017, she began her graduate research the following Fall semester and worked as a teaching assistant for two years. Sarah received her Master of Science degree in December, 2020.

Permanent Address: 419 E College St,
Nacogdoches, TX 75962

Style Manual Designation:
Soil Science Society of America

This thesis was typed by Sarah A. Caton